CONTAMINANT TRANSPORT IN NATURAL SEDIMENTS: INFLUENCE OF SOIL ORGANIC MATTER AND FE/AL-OXYHYDROXIDES ON HEAVY METALS (CU, ZN) AND NANOPARTICLES (TITANIUM DIOXIDE)

By © Leanne Fisher-Power

A Thesis submitted to the School of Graduate Studies in partial fulfillment of the requirements for the degree of

Master of Science

Department of Earth Sciences

Memorial University of Newfoundland

May 2018

St. John's, Newfoundland and Labrador

Abstract

Contaminant transport in subsurface environments may be significantly influenced by contents of aquifer sediments, such as soil organic matter (SOM) and Fe/Al-oxyhydroxides, though their effects are not fully known. This thesis systematically explored the influences of SOM and Fe/Al-oxyhydroxides on two common groundwater contaminants, engineered nanoparticles (titanium dioxide $nTiO_2$) and heavy metals (Cu and Zn), in two projects using the same natural sediment. Project 1 found dissolved SOM enhanced $nTiO_2$ transport by adsorbing onto $nTiO_2$ surface and stabilizing it in suspension, whereas solid SOM and Fe/Al-oxyhydroxides reduced transport by attracting $nTiO_2$ when surface charges were opposite. In project 2, Cu adsorption was strongly dependent on SOM and Fe/Al-oxyhydroxide content, with lesser effects for Zn. Depleted SOM decreased adsorption when pH was <6.5, whereas depleted Fe/Al-oxyhydroxides decreased adsorption when pH was >6.5. Both projects contributed to knowledge of the roles of SOM and Fe/Al-oxyhydroxides in governing contaminant transport in natural sediments.

Acknowledgments

First and foremost, I would like to thank my supervisor Dr. Tao Cheng for providing endless encouragement, knowledge, and enthusiasm as my undergraduate and graduate supervisor. It has been a pleasure to be your student, I have learned so much.

My sincerest gratitude to Dr. Abigail Steel for taking the time to serve on my Master's committee and provide valuable advice for improvements. My thanks to Dr. Penny Morrill for her mentorship.

Credit goes to Robert Bazeley for collecting the sediment used in this study, as well as to Jon Petter Gustafsson; for creating the Visual MINTEQ software, and answering inquiries. I'd also like to thank Dr. Valerie Booth for generously allowing the use of her Zetasizer, as well Gagandeep Sandhu for assistance with measurements. Thanks to Dr. Michael Katz for providing use of the BET machinery and Mason Lawrence for helping with SSA measurements.

I am grateful for the Memorial CREAIT staff that helped me with various analyses, including Pam King and Inês Nobre Silva for ICP-MS, David Grant and Dylan Goudie for SEM-MLA, Jamie Warren for DOC, Alison Pye for organic carbon, and Wanda Alyward for XRD.

My appreciation extends to the staff of the Earth Sciences Department, including Michelle Miskell, Keir Hiscock, Robbie Hicks, Diane Guzzwell, Danyelle Drodge, and Jane O'Neill.

Special thanks to Emily Cumming, who brightened each day as my office buddy, as well as Zhong Tang, Yuhong Zhou, Zahra Rastghalam, Yang Wu, and Kazuhito Mizutani for providing assistance and company in the lab.

My gratitude to Memorial University of Newfoundland for providing personal financial support through the School of Graduate Studies Fellowship. I am also thankful for receiving the Chevron Canada Limited Rising Star Award (2017-2018), Buchans Scholarship Fund of ASARCO Incorporated (2015-2016 & 2016-2017), William H. and Bertha Baird Memorial Scholarship (2016-2017), and NSERC Undergraduate Student Research Award (2015-2016).

I gratefully acknowledge funding from the Natural Sciences and Engineering Research Council of Canada's Discovery Grant (No. 402815-2012) and the Canada Foundation of Innovation's Leaders Opportunity Fund (No. 31836) which supported these projects. I also am thankful for funding from AGU and MUN that gave me the opportunity to present my research at the December 2017 AGU Fall Meeting in New Orleans.

Finally, I'd like to thank friends and family for their endless support.

Table of Contents

List of Tables

Supplementary Tables

List of Figures

Supplementary Figures

List of Abbreviations and Symbols

µm- micrometer

µg/L- microgram per liter

Al- aluminum

Al_2O_3- aluminum oxide

AOD- ammonium oxalate under darkness

atm- atmospheres

$BaCl_2$- barium chloride

C/C_0- ratio of recovered concentration to concentration in the influent

Ca- calcium

CCME- Canadian Council of Ministers of the Environment

cm- centimeter

Cu- copper

DCB- dithionite citrate bicarbonate

DLVO theory- theory by Derjaguin, Landau, Verwey, and Overbeek explaining stability of colloids

DOC- dissolved organic carbon

DOM- dissolved organic matter

ENP- engineered nanoparticle

Fe- iron

g- gram

g/cm^3- grams per centimeter cubed

H_2O_2- hydrogen peroxide

HCl- hydrochloric acid

HDD- hydrodynamic diameter

HNO_3- nitric acid

k_D- distribution coefficient

kg- kilogram

k_{so}- solubility constant

log- natural logarithm

m^2/g- meters squared per gram

Mg- magnesium

mg/g- milligrams per gram

mg/kg- milligrams per kilogram

mg/L- milligrams per liter

mg/mL- milligrams per milliliter

mL- milliliter

mL/min- milliliters per minute

mm- millimeter

mol/L- moles per liter

mV- millivolts

NaCl- sodium chloride

NaOH- sodium hydroxide

n_d- number of data points

n_p- number of adjustable parameters

$nTiO_2$- nanoscale titanium dioxide

PZC- point of zero charge

RMSE- root mean square error

rpm- revolutions per minute

SI- supporting information

SOC- soil organic carbon

SOM- soil organic matter

SSA- specific surface area

SSOM- solid soil organic matter

XRD- X-ray diffraction

Zn- Zinc

ZP- zeta potential

List of Appendices

Chapter 1. Introduction and Overview

1.1 Environmental context

Groundwater is a valuable resource that many rely on for drinking water and irrigation, which may become contaminated as a consequence of anthropogenic activities. Polluted groundwater can be very difficult and expensive to remediate, as well as negatively impact human and ecosystem health. In natural subsurface environments, groundwater contaminants may travel through aquifer sediments with heterogeneous compositions, with little attention paid to their influence. Soil organic matter (SOM) and metal oxyhydroxides (such as Fe and Al) are ubiquitous in natural sediments, and are known to influence the transport of contaminants. Nonetheless, the overall effect of SOM and Fe/Al-oxyhydroxides coexisting and competing in one system has not received much attention, and their influence is poorly understood.

This thesis investigated how two different types of groundwater contaminants travelled through a natural sediment and were affected by SOM and Fe/Al-oxyhydroxides. In the first project, the influence of SOM and Fe/Al oxyhydroxides on nanoparticle transport was studied, using titanium dioxide nanoparticles and column experiments. The second project also studied the effect of SOM and Fe/Al-oxyhydroxides, but this time on heavy metal (Cu and Zn) adsorption using batch experiments. The results of this research will help fill knowledge gaps on groundwater contaminant interactions in natural subsurface environments and may be useful in developing remediation and reduction strategies.

1.2 Nanoparticle transport review

Nanoparticles are traditionally defined as having at least one dimension between 1 and 100 nanometers; and due to their small size, have an especially high surface area to volume ratio giving them unique properties and transport characteristics (Frimmel and Niessner, 2010; Masciangioli and Zhang, 2003; Navarro et al., 2008). Nanotechnology is a rapidly expanding research area as engineered nanoparticles (ENPs) are being produced and used in increasing volumes in a broad array of applications (Nowack and Bucheli, 2007; Wiesner et al., 2006). Titanium dioxide engineered nanoparticles ($nTiO_2$) are among the most commonly used ENPs, and can be found in sunscreens, cosmetics, surface coatings, plastics, and many other every day applications (Weir et al., 2012). The widespread use of ENPs consequentially means that ENPs are being released to the environment in unprecedented and unknown quantities, with ecotoxicological effects not receiving adequate attention (Nowack and Bucheli, 2007; Wiesner et al., 2006).

Studies have found toxic effects in animals (Bermudez et al., 2004; Federici et al., 2007; Long et al., 2006; Reeves et al., 2008) as well as increased bioavailability of heavy metals linked to $nTiO_2$ (Fang et al., 2011; Rosenfeldt et al., 2014; Sun et al., 2009; Wang et al., 2011). It is therefore crucial to elucidate the transport behavior of ENPs in the natural environment in order to understand the potential risks. ENP transport is dependent on whether the ENPs tend to be dispersed (stable in suspension), aggregated and sedimented, or physicochemically removed by a porous medium, and a lack of knowledge exists on this subject (French et al., 2009). Retention within sediments immobilize ENPs, whereas stable ENPs can travel in aqueous systems, facilitate the

transport of other contaminants, and remain bioavailable to organisms (McCarthy and Zachara, 1989). The mechanisms and influences on ENP stability and transport are complex a combination of properties of the ENPs and the porous medium, water chemistry, and flow rates (McCarthy and Zachara, 1989). Surface potential is a dominant control on ENP stability, ultimately influenced by ENP and porous medium properties, solution pH, as well as electrolyte composition and concentration (Frimmel and Niessner, 2010).

ENP transport is hindered through two mechanisms; physical filtration, where the ENP is larger than the pore space and becomes trapped; and physiochemical removal, where the ENP is either aggregated and sedimented out of suspension or attached to the porous medium (Nowack and Bucheli, 2007). DLVO theory; named after scientists Boris Derjaguin, Lev Landau, Evert Verwey, and Theodoor Overbeek; describes particle interactions as a function of van der Waals and electrical double layer forces under various environmental conditions, and can be used to predict ENP stability and transport (Derjaguin and Landau, 1941; Verwey and Overbeek, 1948). DLVO theory is dependent on the zeta potential (ZP) and point of zero charge (PZC) of ENPs and porous medium. ZP is a measure of the electric potential of a particle including the electric double layer, therefore representing the potential difference between the particle (with adsorbed components) and the aqueous medium, and is an important influence on ENP stability and aggregation (Hunter, 1981). A substance's PZC is the pH at which the ZP for a substance is zero, and determines whether a substance will have positive, negative, or neutral surface charges at certain pH (Hunter, 1981). The PZC charge for $nTiO_2$ is ~6.2-

6.8, meaning that in natural waters the surface charge on $nTiO_2$ may be either positive or negative, and therefore the stability and transport of $nTiO_2$ can change rapidly with changes in environmental conditions (Loosli et al., 2013; Parks, 1965; Schmidt and Vogelsberger, 2009; Yang et al., 2007).

Studies have found that ZP is the dominant control on ENP stability, which is ultimately influenced by ENP and porous medium properties, solution pH, as well as electrolyte composition and concentration (Frimmel and Niessner, 2010). Dunphy Guzman et al. (2006) found that over 80% of $nTiO_2$ was stable as 10-200 nm aggregates over the pH range of 1-12, except for close to the PZC for $nTiO_2$, where larger aggregates formed and sedimented due to reduced electrostatic repulsion. An increase in ionic strength compresses the electrical double layer, therefore decreasing electrostatic repulsion between two like charged objects, allowing ENPs to more likely aggregate (Akaighe et al., 2012; Bekhit et al., 2006; Navarro et al., 2008). Ion valence has been found to influence ENP stability as well, with divalent electrolytes promoting aggregation and retention more readily than monovalent electrolytes (Akaighe et al., 2012; Chen et al., 2011; French et al., 2009). In addition, ENP size influences their stability, as aggregation and aggregate size decreases with increase in particle size (Chen et al., 2015).

A common way to study ENP transport is laboratory column experiments, which are designed to simulate groundwater flow through saturated porous media (Cai et al., 2014; Chen et al., 2015; Fang et al., 2009; Kretzschmar et al., 1997; Morales et al., 2011; Wang et al., 2015; Zhuang et al., 2003). Most of these experiments use a well-defined porous

media, often quartz sand, in order to clearly distinguish ENP transport behavior under different conditions such as solution pH, ionic strength, and presence of aqueous species. However, the environmental extrapolation of results from these studies may be limited, due to the fact that natural systems are far more heterogeneous in composition and properties in comparison to quartz sand, which may strongly affect ENP transport (Nowack and Bucheli, 2007). Sediment properties including composition, surface charges, and surface area are known to strongly influence the transport of ENPs (Furman et al., 2013; Jung et al., 2014; Lin et al., 2011). Common ubiquitous components of natural sediment that may influence ENP transport include SOM and metal oxyhydroxides.

SOM is expected to have a complex effect on ENP transport, as SOM is composed of both solid organic matter (SSOM) and dissolved organic matter (DOM). Little attention has been paid to SSOM-ENP interactions, but it is intuitive to hypothesize that negatively charged SSOM (Philippe and Schaumann, 2014) may attract positively charged ENPs and remove them from the aqueous phase, whereas negatively charged DOM is known to enhance ENP stability through adsorbing onto the ENP surface and altering surface charges through steric repulsion (Erhayem and Sohn, 2014; Keller et al., 2010; Loosli et al., 2013; Wu and Cheng, 2016). The overall effect of SOM in natural sediments on ENP transport is poorly studied and understood.

Metal oxyhydroxides (such as Fe and Al) also have a complicated effect on ENP transport, as heterogeneous surface charges in natural sediment arise in part by metal oxide components. For example, quartz is typically negatively charged in environmental

conditions with a PZC around pH 2-3, iron (hydr)oxides have a PZC in the range of 8.1-8.5, and aluminum (hydr)oxides have a PZC of around 9.4 (Huang, 1995). This means that at variable pH, a heterogeneous natural sediment will have an array of positive and negative surface charges, which will cause varying components to have different interactions with ENPs. It is evident that both SOM and Fe/Al-oxyhydroxides have importance influence on ENP stability and transport, though the net effect on from both components coexisting in one heterogeneous system is unclear.

The objective of Chapter 2 was to reduce knowledge gaps on ENP transport in natural systems by determining the influence of individual sediment components (SOM and Fe/Al-oxyhydroxides) on $nTiO_2$ mobility. A natural sediment was chemically treated to remove specific components and systematic laboratory column experiments were performed to determine the influence of each porous medium on $nTiO_2$ transport. The results from Chapter 2 will expand on existing knowledge on ENP transport and help clarify the applicability of extrapolating laboratory column experiments results using homogenous porous media to the natural environment.

1.3 Heavy metal adsorption review

Heavy metals are loosely defined as metallic elements with high atomic weights or density, often associated with environmental contamination (Duffus, 2002). Ranging from commonly to rarely occurring in nature, many heavy metals are economically desirable and mined for use in everyday products. The increasing demand for products made using metals has led to their widespread extraction and inevitable release into the environment (Landner and Reuther, 2005). Anthropogenic processes, including mining,

fertilizers, dyes, sewage, production of consumer goods, and transportation can generate and release heavy metals into the natural environment, where they may enter and pollute groundwater (Landner and Reuther, 2005).

Small amounts of some metals, such as iron, zinc, and copper, are essential for biological processes, but toxic in higher concentrations (Singh et al., 2011). Because these metals are required for biological processes, uptake pathways naturally exist in organisms, and can lead to uptake in toxic concentrations (Landner and Reuther, 2005). Metals may be hyper-accumulated in plants (Nazemi, 2012; Tang et al., 2009), and transfer to other organisms via food chains. Exposure to certain heavy metals has been linked to adverse health effects in humans and other organisms, including disrupting vital functions, carcinogenesis, and death (Lin et al., 2013; Park et al., 2004; Singh et al., 2011).

Two common metal contaminants are copper (Cu) and zinc (Zn). Cu is a good conductor of electricity, commonly used for making wires, tubing, and alloys (Landner and Reuther, 2005). Though Cu exists in naturally in the environment from the weathering of Cu-bearing rock, anthropogenic processes in aquatic environments account for 33-60% of Cu input (Demayo and Taylor, 1981). Canadian Council of Ministers of the Environment (CCME) water quality guidelines for the protection of aquatic life recommends a maximum of 2 µg/L Cu, though Canadian surface waters average 5 µg/L Cu (Canadian Council of Ministers of the Environment, 2008). Higher concentrations of Cu in the environment are related to anthropogenic sources (McNeely et al., 1979). Zn is often used for galvanizing, production of tires, and alloys, due to its relatively good

resistance to corrosion (Landner and Reuther, 2005). Zn also exists naturally in the environment due to the weathering of Zn-bearing rock, with a large range of typical Canadian surface water concentrations, from < 1 to 100 µg/L (Demayo and Taylor, 1981), though CCME guidelines for the protection of aquatic life suggest a maximum of 30 µg/L (Canadian Council of Ministers of the Environment, 2008). In waters surrounding mining areas, concentrations of Cu and Zn 10-1000 times greater than average can be found, due to contamination from mine tailings (Canadian Council of Ministers of the Environment, 2008). Newfoundland and Labrador provincial regulations state it is prohibited to exceed a maximum discharge of 0.3 mg/L Cu and 0.5 mg/L Zn into any body of water, often problematic for abandoned mines (Environmental Control Water and Sewage Regulations under the Water Resources Act (O.C. 2003-231)).

In natural subsurface environments, heavy metal transport is dependent on whether they tend to remain in stable in aqueous suspension or if they are removed from the aqueous phase (Landner and Reuther, 2005). Adsorption occurs when molecules, ions, or small particles are bound to a solid at its surface, and tends to decrease the bioavailability of contaminants (not to be confused with absorption, in which a substance is dissolved into the bulk of another, not at the surface). Aqueous heavy metals may be adsorbed to sediments, a key control on their fate and transport, as well as a potential abundant and inexpensive remediation option (Cao et al., 2004; Wang and Mulligan, 2006). Heavy metal adsorption is known to be influenced by many factors, which makes predicting heavy metal adsorption very complex.

The most commonly studied influences on adsorption are water chemistry conditions, such as pH, ionic strength, and dissolved species (Sauve et al., 2000; Wang and Mulligan, 2006). In general, heavy metal adsorption increases with increase in pH (Sauve et al., 2000), conversely, the solubility of heavy metals typically decreases with increase in pH (Tack et al., 1996). Adsorptive capacity tends to decrease with increase in ionic strength (James and Macnaughton, 1977). Dissolved species, such as multivalent cations, may provide competition against heavy metals for adsorptive sites in sediment, and therefore may suppress heavy metal adsorption (Fisher-Power et al., 2016; Mizutani et al., 2017; Tipping et al., 2002; Vulava et al., 2000). Sediment composition has also been found to strongly influence adsorption, however, less research is available on how sediment and its heterogeneous components affect adsorption. SOM and metal oxyhydroxides (such and Fe and Al) are ubiquitous in natural sediments and have been found to be key components for adsorbing heavy metals (e.g.; Shi et al., 2013; Bradl, 2004; Li et al., 2014).

Metal oxyhydroxides have large surface areas per unit mass and heterogeneous surface charges, and therefore have many surfaces sites available for adsorption (Bradl, 2004; Shi et al., 2013). Amorphous oxyhydroxides have adsorption capacity about 10 higher than aged oxides, again a result of increased surface area (Shuman, 1977). Research has shown that Fe and Al are the dominant metal oxyhydroxides with respect to heavy metal adsorption (Shi et al., 2013). It has been reported that Fe/Al-oxyhydroxides are the dominant adsorbing phase when pH > 6.5 (Agbenin and Olojo, 2004; Fisher-Power et al., 2016; Shi et al., 2013), and many natural waters exist in this range.

SOM is another important sediment component with respect to heavy metal adsorption. SOM has a high affinity for heavy metal cations because it carries negative charges under most environmental conditions (Yuan et al., 2014). SOM is expected to have a complex effect on heavy metal adsorption, as SOM may exist either as DOM or as SSOM. Research has indicated that SSOM tends to adsorb aqueous heavy metals and remove them from the aqueous phase, whereas DOM may form stable complexes with heavy metals and keep them in the aqueous phase (Agbenin and Olojo, 2004; McBride et al., 1997; Pérez-Novo et al., 2008; Wang and Mulligan, 2006). It has been reported that SSOM is the dominant heavy metal adsorbent in natural sediment when pH <6.5, and therefore SSOM is very important for heavy metal adsorption in acidic and near neutral waters (Agbenin and Olojo, 2004; Fisher-Power et al., 2016; Shi et al., 2013). The overall effect of SOM on heavy metal adsorption is little-known, presumably a function of the relative affinities of DOM and SSOM for heavy metals under various environmental conditions. Furthermore, SOM and Fe/Al-oxyhydroxides often occur together in variable concentrations in natural sediments, and their effects when coexisting and competing in one system are poorly documented and understood.

A common way to study heavy metal adsorption is laboratory batch experiments. In these experiments, a substrate is mixed with contaminant under various water chemistry conditions to determine their influence at equilibrium (Dişli, 2010). Due to the strong influence of pH on heavy metal adsorption, pH edge experiments are adsorption experiments conducted over a range of pH values to investigate heavy metal adsorption as a function of pH. The applicability of these experiments to natural environments is of

question, because the experiments commonly use a much lower solid to solution ratio than found in natural subsurface environments (Mizutani et al., 2017) and the substrate may not be representative of the heterogeneity of natural aquifer sediments.

Heavy metal adsorption may be predicted using adsorption models. Classic adsorption models, such as linear, Langmuir, and Freundlich isotherms are commonly used calculations (Jeppu and Clement, 2012; Oiffer et al., 2009; Williams et al., 2003). A limitation of these models is that they do not consider the influence of water chemistry conditions and sediment composition, and are therefore not always applicable under varying environmental conditions (Jeppu and Clement, 2012). Advances in research and technology have led to the development of surface complexation models (SCMs), which use digital software to compute chemical speciation of many species at once under a wide range of conditions (Bonten et al., 2011). SCMs utilize extensive databases and can incorporate many factors that classic adsorption models do not. Visual MINTEQ (Gustafsson, 2010) is a SCM software available for free download commonly used in adsorption research. The user can input water chemistry conditions, such as pH, ionic strength, dissolved species, and temperature; as well as solid phases like SOM and Fe/Al-oxyhydroxides to predict heavy metal adsorption and speciation under environmental conditions.

The objective of Chapter 3 was to further understanding of heavy metal adsorption in the natural environment by determining the influence of individual sediment components (SOM and Fe/Al-oxyhydroxides) on Cu and Zn adsorption. A natural sediment was chemically treated to remove either SOM, Fe/Al-oxyhydroxides, or

both, used in systematic batch adsorption experiments, and modelled using SCM software. The results from Chapter 3 will add to the literature of heavy metal adsorption in the natural environments and help clarify the individual and synergistic influences of SOM and Fe/Al-oxyhydroxides on heavy metal adsorption.

1.4 Thesis purpose and objectives

Although nanoparticle transport and heavy metal adsorption are heavily researched topics, there is a knowledge gap on the individual and synergistic influences from SOM and Fe/Al-oxyhydroxides in natural sediment. Due to the heterogeneous and complex nature of sediments, it is difficult to attribute adsorption phenomena to a single factor, and difficulties arise in experimental methods and analytical techniques (Lewis and Sjöstrom, 2010). SOM and Fe/Al-oxyhydroxides are often artificially added to a well-defined simulated sediment material to investigate their influence (e.g., Cheng et al., 2004; Han et al., 2014; Tong et al., 2011; Wang et al., 2012; Wu and Cheng, 2016). These experiments are convenient and provide useful information about how SOM or Fe/Al-oxyhydroxides may influence contaminant transport; however, they may not accurately represent the processes which occur in natural complex sediments (Nowack and Bucheli, 2007). A better understanding of the individual and synergistic influences of SOM and Fe/Al-oxyhydroxides in natural sediment is necessary for evaluating contaminant transport in the environment.

Limited ENP transport studies have been conducted using natural sediment as the porous medium, leaving a lack of knowledge of how ENPs interact in the natural environment under the influence of heterogeneous soil components (Nowack and

Bucheli, 2007). A study by Fang et al. (2011) studied the stability of $nTiO_2$ suspensions in natural soil and found that the stability was positively correlated with dissolved organic carbon and clay content, and negatively correlated with ionic strength, pH, and ZP. Few other studies use natural sediments to study ENP facilitated transport of contaminants (Grolimund et al., 1996; Grolimund and Borkovec, 2005; Wang et al., 2015; Zhuang et al., 2003), but to my knowledge, no current studies systematically remove individual sediment components to determine their influence ENP transport.

A number of heavy metal adsorption studies have used natural sediment as the adsorbent (e.g., Arias et al., 2006; Cerqueira et al., 2011; Fan et al., 2013; Shi et al., 2013), however, the individual contributions of SOM and Fe/Al-oxyhydroxides are not commonly investigated. Agbenin and Olojo (2004) chemically treated a sediment to remove either SOM or Fe/Al-oxyhydroxides, and reported that removing SOM reduced the distribution coefficient for Cu 40 times, but for Zn only by half; whereas removal of amorphous metal oxides reduced the Cu and Zn distribution coefficients 100 and 20 times, respectively. Although this study provided insight into the influences of SOM and Fe/Al-oxyhydroxides on Cu and Zn adsorption to natural sediment, it had a few limitations. The sediments were not characterized after the treatment processes in Agbenin and Olojo's 2004 study, and the removal efficiency of the SOM and Fe/Al-oxyhydroxides was not reported. The interpretation of their results assumed SOM and Fe/Al-oxyhydroxides were independent of one another in the sediment, and each component had been 100% removed by the treatment processes while no other properties changed, though this was unlikely the case. Characterization of the sediment after

treatment would provide useful insights into the interpretation of their results. In addition, to my knowledge, no adsorption experiments have been performed on sediment treated to deplete both SOM and Fe/Al-oxyhydroxides, leaving a lack of knowledge about their synergistic influence.

This research intended to explore the individual and synergistic influences of SOM and Fe/Al-oxyhydroxides on the transport of two different types of groundwater contaminants. To do this, two projects were completed; the first investigating $nTiO_2$ transport as influenced by SOM and Fe/Al-oxyhydroxides (Chapter 2), and the second on Cu and Zn adsorption (Chapter 3). In both projects, the same natural sediment was chemically treated to remove either SOM, Fe/Al-oxyhydroxides, or both; and used in systematic experiments to determine their individual and synergistic effects. Overall, the results from this research will help further the understanding of how SOM and Fe/Al-oxyhydroxides influence the transport of groundwater contaminants in natural subsurface environments.

1.5 Co-authorship Statement

I, Leanne Fisher-Power, am the author of this thesis. I performed the literature review, designed the project, carried out experiments, analyzed data, and prepared manuscripts under the supervision and guidance of Dr. Tao Cheng. I was the principal author on manuscripts based on Chapters 2 and 3 prepared for journal submission, co-authored by Dr. Cheng (Chapter 2 was published in Environmental Science & Technology doi:10.1021/acs.est.7b05062, and Chapter 3 will be submitted to a presently

undetermined journal). Revision of this thesis was completed by Dr. Abigail Steel, who sat on my Master's committee.

Chapter 2. Nanoscale titanium dioxide ($nTiO_2$) transport in natural sediments: Importance of soil organic matter and Fe/Al-oxyhydroxides

Abstract

Many engineered nanoparticle (ENP) transport experiments use quartz sand as the transport media; however, sediments are complex in nature, with heterogeneous compositions that may influence transport. Nanoscale titanium dioxide ($nTiO_2$) transport in water-saturated columns of quartz sand and variations of a natural sediment was studied, with the objective of understanding the influence of soil organic matter (SOM) and Fe/Al-oxyhydroxides and identifying the underlying mechanisms. Results indicated $nTiO_2$ transport was strongly influenced by pH and sediment composition. When influent pH=5, $nTiO_2$ transport was low, as positively-charged $nTiO_2$ was attracted to negatively-charged minerals and SOM. $nTiO_2$ transport was slightly enhanced in sediments with sufficient SOM concentrations due to leached dissolved organic matter (DOM), which adsorbed onto $nTiO_2$ surface, reversing zeta potential to negative. When influent pH=9, $nTiO_2$ transport was generally high since negatively-charged medium repelled negatively-charged $nTiO_2$. However, in sediments with SOM or amorphous Fe/Al-oxyhydroxides depleted, transport was low due to pH buffering by the sediments causing attraction between $nTiO_2$ and crystalline Fe-oxyhydroxides. This was counteracted by DOM adsorbing to $nTiO_2$, stabilizing it in suspension. Our research demonstrates the importance of SOM and Fe/Al-oxyhydroxides in governing ENP transport in natural sediments.

2.1 Introduction

The widespread use of engineered nanoparticles (ENPs) has led to their release into the environment with limited knowledge about their transport and associated risks. A common way to study ENP transport is laboratory column experiments designed to simulate groundwater flow through saturated porous media (Cai et al., 2014; Chen et al., 2011, 2015; Fang et al., 2009; Kretzschmar et al., 1997; Morales et al., 2011; Wang et al., 2015; Zhuang et al., 2003). Most of these experiments use well-defined porous media, often quartz sand, in order to distinguish the influence of water chemistry (pH, ionic strength, cations and anions, etc.) on ENP transport. Due to technical difficulties in experiments (Lewis and Sjöstrom, 2010), a limited number of studies have been conducted to investigate ENP transport in natural sediments, which are far more complicated compared to quartz sand. Sediment properties including composition, surface charge, and surface area are known to influence the transport of ENPs (Cornelis et al., 2013; Furman et al., 2013; Jung et al., 2014; Lin et al., 2011). Fang et al. (2011) studied the stability of $nTiO_2$ suspensions in natural soil and found that stability was positively correlated to dissolved organic carbon (DOC) and clay content, but negatively correlated to ionic strength, pH, and zeta potential (ZP). Sun et al. (2015) demonstrated that zinc oxide nanoparticles were highly mobile in quartz sand columns under a various water chemistry conditions, but much less mobile in soil columns due to heterogeneous ZPs, blocking, and straining. Other studies have used natural sediments to study ENP facilitated transport of contaminants (Grolimund et al., 1996; Grolimund and Borkovec, 2005; Wang et al., 2015; Zhuang et al., 2003). Though these studies contribute useful

information of ENP transport in natural sediment, the roles of specific sediment components and associated mechanisms have not fully been identified, leaving a knowledge gap regarding ENP interaction with heterogeneous soil components (Nowack and Bucheli, 2007; Sun et al., 2015).

Common ubiquitous components of natural sediment that may influence transport include soil organic matter (SOM) and metal oxyhydroxides (Fe and Al). SOM is composed of both solid soil organic matter (SSOM) and dissolved organic matter (DOM) (Grillo et al., 2015). While a large number of studies have shown that DOM enhances ENP stability and transport through adsorbing onto the ENP surface and altering surface charges through steric repulsion (Chen et al., 2012; Erhayem and Sohn, 2014; Keller et al., 2010; Loosli et al., 2013; Wu and Cheng, 2016), little attention has been paid to SSOM-ENP interactions. It is intuitive to hypothesize that negatively-charged SSOM (Philippe and Schaumann, 2014) may attract positively-charged ENPs and remove them from the aqueous phase. Moreover, partial dissolution of SSOM releases DOM that may interact with ENPs. The overall effect of SOM (both solid and dissolved) in natural sediments on ENP transport is complicated and poorly understood.

Metal oxyhydroxides have a complex effect on ENP transport, as heterogeneous surface charges in natural sediments arise in part by metal oxide components. For example, quartz is negatively-charged in environmental conditions with a point of zero charge (PZC) around pH 2-3, Fe-oxyhydroxides have a PZC in the range of 8.1-8.5, and Al-oxyhydroxides have a PZC around 9.4 (Huang, 1995). At variable pH, a complicated natural sediment will have an array of positive and negative surface charges, which will

cause varying components to have different interactions with ENPs. Johnson et al. (1996) found increasing the percentage of Fe-oxyhydroxide coated surfaces increased deposition of silica microspheres, and Cornelis et al. (2013) found extractable Al in sediments was correlated with increasing attachment efficiency of silver ENPs. Numerous other studies demonstrate the importance of Fe-oxide coating on quartz sand in ENP transport (Han et al., 2014; Wang et al., 2012); however, coatings on quartz sand are artificial and may not behave the same as Fe-oxide coatings in natural sediments. Additionally, SOM and Fe/Al-oxyhydroxides often co-exist in natural sediments, therefore, research is needed to understand not only their individual effect, but also their synergistic effect when both are present in one heterogeneous system.

The objective of this study was to examine the influence of SOM and Fe/Al-oxyhydroxides on ENP transport in a natural sediment and identify the underlying mechanisms. A natural sediment was separated into portions, treated to deplete specific components (Fe/Al-oxyhydroxides, SOM, or both), and used in systematic laboratory column experiments to determine the influence of sediment component(s) on ENP transport using nanoscale titanium dioxide ($nTiO_2$) as a representative ENP. By comparing $nTiO_2$ breakthrough curves and changes in water chemistry and particle property in different column experiments, mechanisms of how SOM and Fe/Al-oxyhydroxides influence particles retention and transport were proposed.

2.2 Materials and methods

2.2.1 Transport media

The sediment was a diamicton from central Newfoundland, Canada; used and characterized in previous work (Fisher-Power et al., 2016; Mizutani et al., 2017). This sediment was chosen as an example of aquifer materials as found in natural environments. It was glacial in origin, mainly composed of plagioclase (36%), quartz (31%), alkali feldspar (13%), and a variety of other silicates (Figure S1 panel A, SI). The sediment also contained important minor components including SOM as well as crystalline and amorphous metal oxyhydroxides. Before being used in any experiments, the sediment was air dried, sieved to less than 2 mm, and homogenized to avoid settling. The sediment was separated into four representative portions: to be (1) untreated, (2) treated to deplete SOM using hydrogen peroxide (H_2O_2) based on a procedure by Jackson (1958), (3) treated to deplete amorphous metal oxyhydroxides using a modified ammonium oxalate under darkness (AOD) method, and (4) treated to deplete both SOM and metal oxyhydroxides using AOD extraction followed by H_2O_2 extraction. Details of the treatment processes are described in the Supporting Information (SI).

After processing, each sediment was characterized to elucidate their properties and differences resulting from the treatments. Modal mineralogy from X-ray diffraction (XRD), pH, grain size distribution, and ZP were determined; as well as the quantification of extractable Fe and Al oxides; soil organic carbon (SOC) (used to represent SOM); and leachable DOC (used to represent leachable DOM). Select characterizations of the untreated sediment were completed previously (Fisher-Power et al., 2016; Mizutani et al.,

2017), and additional characterizations were completed in this study, with detailed procedures in the SI.

Additionally, quartz sand (0.252-0.355 mm diameter) from Univar Canada was used as control porous media, as $nTiO_2$ transport in pure quartz columns is well documented. To remove impurities, the sand was soaked in 0.1 mol/L NaOH for 24 hours, followed by 24 hours in 0.1 mol/L HCl, and rinsed with deionized water until the absorbance of the water mixed with sand was zero.

2.2.2 Column experiments

To determine the influence of the natural sediment and individual sediment components on $nTiO_2$ transport, systematic column experiments were conducted using quartz sand and each variation of the sediment as the transport medium (summary of experimental conditions in Table S1, SI). Sediments were packed into a column at a 1:4 sediment to quartz sand mass ratio, based on practical considerations (maintaining sufficient hydraulic conductivity and ensuring particulates were low as to not clog column stoppers). The sediments and quartz sand were mixed uniformly by shaking the dry material before packing and mixing while packing the saturated columns.

A Kimble Kontes Chromaflex ® chromatography column (2.5 cm inner diameter and 15 cm length) made of borosilicate glass was used to hold the transport medium. The column was fitted with 20 μm high-density polyethylene bed supports on each end and configured vertically, with Cole-Parmer Masterflex ® Tygon 0.8 mm tubing connected to either side. For each experiment, the column was packed with sediment and/or quartz sand, and $nTiO_2$-free 1 mM NaCl background solution adjusted to pH 5 or 9 (typical pH

range of groundwater chosen above and below the PZC of $nTiO_2$). Small volumes of background solution followed by porous media were added incrementally until the entire column was full, tapping and packing to remove air bubbles and ensure uniform packing. The volume of background solution added to saturate the column and dry mass of porous media used was recorded, allowing for calculations of porosity and bulk density.

Aeroxide® P25 titanium (IV) oxide powder from Arcos Organics with minimum 99.5% purity was used to prepare the $nTiO_2$ suspensions. Previous analysis determined the powder was 90% anatase and 10% rutile (Wu and Cheng, 2016). For all experiments, 50 mg/L $nTiO_2$ suspensions were prepared in 1 mM NaCl in nanopure water and sonicated by Branson Digital Sonifier® (Crystal Electronics) at 200W, 30% amplitude, for 30 minutes. The pH of $nTiO_2$ suspensions were adjusted to pH 5 or 9 after sonication using small volumes of 1.0 mol/L NaOH or HCl solution.

Prior to $nTiO_2$ injection, 1 mM NaCl background solution with pH 5 or 9 (to match the pH of the influent suspensions) was injected for approximately 16 hours at a rate of 1 mL/min using a Masterflex® peristaltic pump from Cole-Parmer to ensure that electrical conductivity, light absorbance, and pH of the effluent became stable. 50 mg/L $nTiO_2$ suspension was then injected for 7 pore volumes before influent was switched back to $nTiO_2$-free background solution. The column experiments were completed when no $nTiO_2$ was detectable in the effluent.

During particle injection and elution stages, effluent samples were collected using a Spectrum® Labs C-F2 Fraction Collector and monitored for pH and electrical

conductivity. Light absorbance of the samples were analyzed by a Thermo Scientific GENESYS™ 10S UV-Vis Spectrophotometer at wavelength 368 nm, and $nTiO_2$ concentration was determined using a calibration curve generated by diluting the 50 mg/L $nTiO_2$ suspension. At the midpoint of $nTiO_2$ injection (~3.5 pore volumes) effluent samples were collected for ZP and hydrodynamic diameter (HDD) analysis by a Malvern Nano ZS Zetasizer. DOC concentration of column effluents was analyzed by an OI Analytical Aurora 1030 Total Organic Carbon Analyzer. $nTiO_2$ recovery in each experiment was calculated as the ratio of the sum of $nTiO_2$ mass in the effluent samples and the total injected $nTiO_2$ mass. Influent pH was checked over time (adjusting as necessary to keep stable at pH 5 or 9), and light absorbance of influent suspensions was monitored to ensure particle stability. All column experiments were conducted in triplicate.

2.3 Results and Discussion

2.3.1 Sediment properties

The treatment processes were successful in removing their target components (Fe/Al-oxyhydroxides, SOM, or both) (Figure 1) while generally preserving the sediment's other properties (Table S2, SI). Fe/Al-oxyhydroxide concentrations varied according to sediment treatment, with the greatest amounts in the untreated sediment (Figure 1a and 1b). Processing by AOD and AOD-H_2O_2 to deplete metals was 96-97% effective in removing AOD extractable Al and 81-88% effective for Fe; however, treatment by H_2O_2 for organic depletion also removed 42 and 62% Al and Fe respectively (Figure 1a). This was due to degradation and removal of Fe/Al-oxyhydroxides naturally

associated with organic matter in the sediment during the H_2O_2 procedure (Tipping et al., 2002; Yang et al., 2013). Dithionite-citrate-bicarbonate (DCB) extractable Fe was less affected by the treatment processes, as it includes some crystalline Fe (not extractable by AOD) in addition to amorphous Fe (Mehra, 1958), with 74-75% removal for AOD and AOD-H_2O_2 treated sediments and 48% for H_2O_2 treated sediment (Figure 1b). Again, Fe depletion for the H_2O_2 treated sediment was a result of Fe-oxyhydroxides associated with SOM being removed. SOC concentration in the sediments also changed according to treatment type (Figure 1c). Treatments that targeted SOM (H_2O_2 and AOD-H_2O_2) removed most of the sediment's original SOC, reducing by 90-94%; however, the AOD treatment (which targeted metal oxyhydroxides) also removed a substantial percentage (79%) of SOC (Figure 1c). This was a result of leaching and degradation of SOC associated with Fe/Al-oxyhydroxides in the sediment, which were consequently removed during the treatment process (Fisher-Power et al., 2016; Tipping et al., 2002; Yang et al., 2013).

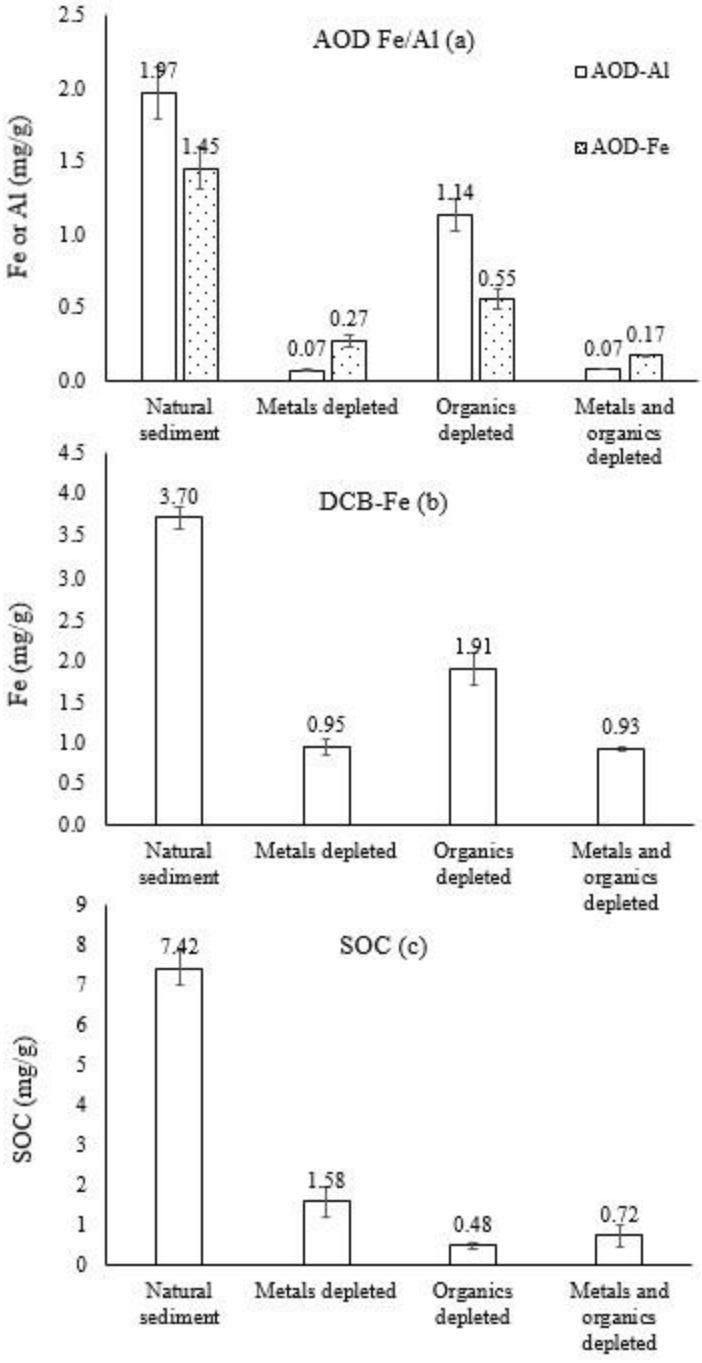

Figure 1. Proportions of Al, Fe, and SOC in the sediments.

2.3.2 $nTiO_2$ transport

$nTiO_2$ breakthrough curves were determined a function of pH and porous medium in the column experiments (Figure 2; Figure S2, SI with error bars). Effluent $nTiO_2$ concentrations were low for all experiments with influent pH 5; and typically much higher for experiments with influent pH 9 (Figure 2). Columns containing only quartz sand had 0% recovery of $nTiO_2$ for experiments with influent pH 5 (Figure 2a); whereas almost all of the injected $nTiO_2$ (96%) was recovered for experiments with influent pH 9 (Figure 2b). Breakthrough patterns for the sediments at influent pH 5 varied according to sediment type (Figure 2a), with the untreated sediment having the highest effluent recovery (~3.6%). AOD treated sediment had significant but low $nTiO_2$ recovery (~1%) at influent pH 5, while H_2O_2 and AOD-H_2O_2 treated sediments had zero or near zero $nTiO_2$ recovery, similar to the quartz sand (Figure 2a).

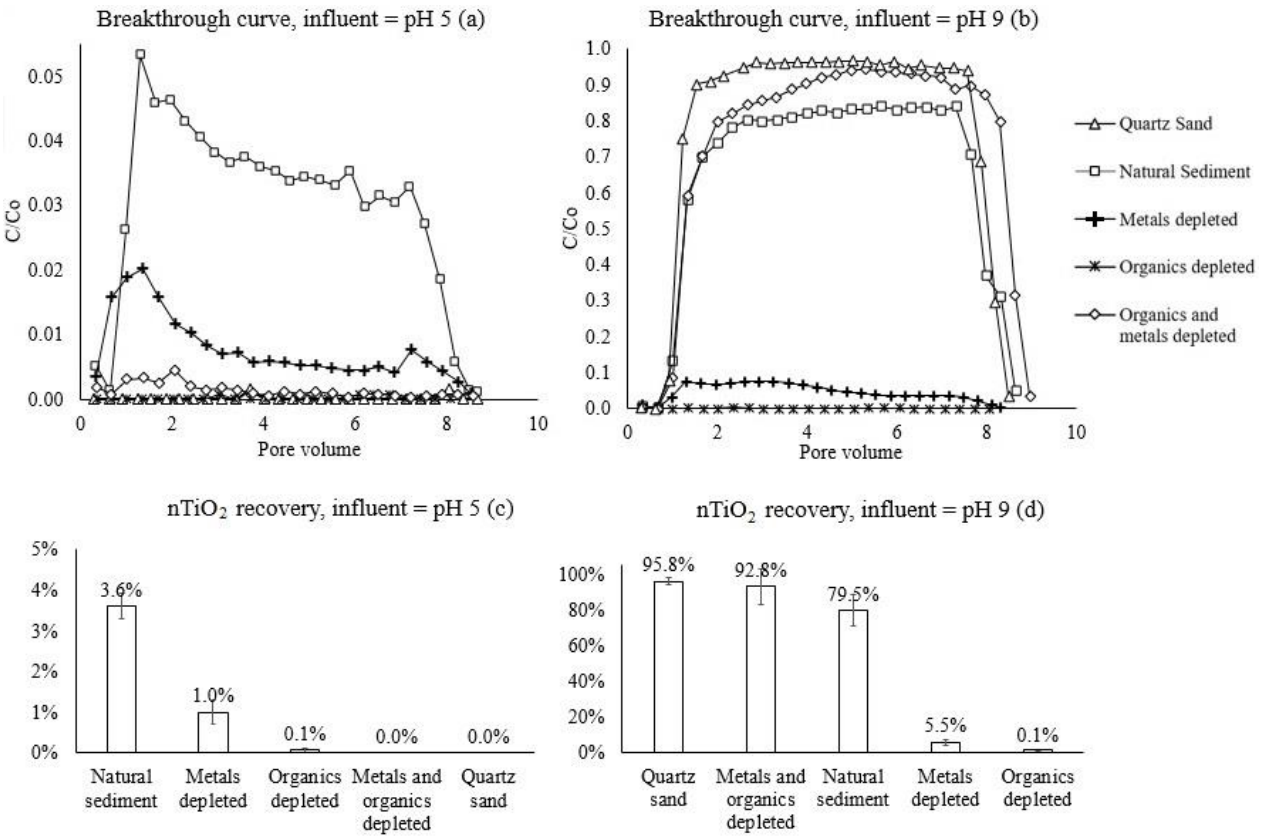

Figure 2. $nTiO_2$ breakthrough curves for experiments with influent pH 5 and 9. C/C_0 is the ratio of recovered $nTiO_2$ concentration to $nTiO_2$ concentration in the influent.

$nTiO_2$ transport was also dependent on sediment type for the pH 9 influent experiments (Figure 2b). Two of the sediments had high $nTiO_2$ recovery; the AOD-H_2O_2 treated sediment with ~93%, and the untreated natural sediment with ~80%. In contrast, low recovery of $nTiO_2$ was observed for the AOD and H_2O_2 treated sediments; the AOD treated sediment had ~6% recovery, whereas no $nTiO_2$ was recovered from the H_2O_2 treated sediment (Figure 2b). Blocking shapes (characteristic of deposited $nTiO_2$ preventing further deposition as collector surfaces become covered (Johnson et al., 1996; Johnson and Elimelech, 1995; Liu et al., 1995; Song and Elimelech, 1993)) were observed for the untreated sediment and for the AOD-H_2O_2 treated sediment to a greater

extent, as less deposition sites were available due to the AOD and H_2O_2 treatment processes.

Despite changes in Fe/Al-oxyhydroxide and SOC concentrations, XRD spectra showed that mineralogy of each treated sediment did not greatly differ from the untreated sediment, indicating that bulk mineralogy was not significantly affected by the treatment processes (Figure S1, SI). The pH of the sediments was not strongly influenced by the treatments (ranging from 5.74 to 5.86 for the untreated, AOD treated, and H_2O_2 treated sediments) except for the AOD-H_2O_2 treated sediment which increased to 6.35 (Table S2, SI). Grain size distribution changed slightly for the AOD and AOD-H_2O_2 treated sediments; the treated sediments had a higher proportion of sand-sized particles but lower proportion of clay and silt relative to the untreated sediment (Table S2, SI). A larger change was observed for the H_2O_2 treated sediment grain size distribution, as the proportion of sand size particles increased and fine particles decreased (Table S2, SI), presumably due to the breakdown and loss of fine particles during treatment.

The influence of physical properties of the porous medium also needed to be considered. Quartz sand columns had porosity of 40%, whereas porosity of mixed sediment and sand columns was slightly less (36-37%) due to grain size variation (Table S2, SI). Similarly, bulk density was 1.73 g/cm^3 for quartz sand, and slightly greater for treated sediments (1.77-1.83 g/cm^3) (Table S2, SI). Although quartz sand has smoother surfaces, larger mean grain size and pore diameters, and reduced specific surface area (SSA) relative to sediment, which may enhance nTiO_2 transport, quartz was a major mineral phase of each of the sediments (Figure S1, SI), and extra quartz sand was added

to each of the sediments at a consistent ratio, allowing for focus on the influence of varying SOM and Fe/Al-oxyhydroxide content.

2.3.3 Zeta potential of $nTiO_2$ and sediments

The zero recovery of $nTiO_2$ in quartz sand at pH 5 and nearly 100% recovery at pH 9 can be explained by comparing the ZP of $nTiO_2$ and quartz at pH 5 and 9 (Figure 3). At pH 5, $nTiO_2$ was positively-charged and quartz sand had negative ZP (Figure 3), leading to electrostatic attraction and zero recovery in column effluents (Figure 2a). Conversely, at pH 9 $nTiO_2$ was negatively-charged as was quartz sand (Figure 3), and therefore electrostatic repulsion occurred, leading to nearly 100% recovery (Figure 2b). This logic also partially explained $nTiO_2$ transport behavior in the sediments; however, it disagrees with some of the experimental results. As expected, positive $nTiO_2$ at pH 5 was attracted to the untreated, AOD treated, and AOD- H_2O_2 treated sediments with negative ZPs (Figure 3), accounting for the low recoveries (Figure 2a); and negative $nTiO_2$ at pH 9 was repelled by the untreated and AOD-H_2O_2 treated sediments with negative ZPs (Figure 3), agreeing with the high recoveries (Figure 2b). In contrast, the H_2O_2 treated sediment at pH 5 had a positive ZP suggesting it should repel positive $nTiO_2$ (Figure 3), however, no $nTiO_2$ was recovered from the H_2O_2 treated sediment columns at pH 5 (Figure 2a). Additionally, the negative ZP of the AOD and H_2O_2 treated sediments at pH 9 suggested that negatively-charged $nTiO_2$ should be repelled, leading to high recovery (Figure 3), however, low $nTiO_2$ recovery was observed in these experiments (Figure 2b). A limitation of the sediment ZP measurement was that it may not be representative of all the surface sites in the sediment, tending to disproportionally favor certain components.

For example, amorphous Al and Fe, clays, and DOM were more likely to be mobilized and represented by these measurements in comparison to larger solid sites that existed in the sediment, such as quartz and other minerals. The H_2O_2 treated sediment leached a higher proportion of positively-charged Fe/Al-oxyhydroxides relative to negatively-charged DOM due to SOM depletion, accounting for the reported positive ZP at pH 5. Despite this positive ZP, the H_2O_2 treated sediment also contained negatively-charged quartz and other minerals which were less represented by the ZP measurement, and attracted $nTiO_2$ accounting for the nil recovery.

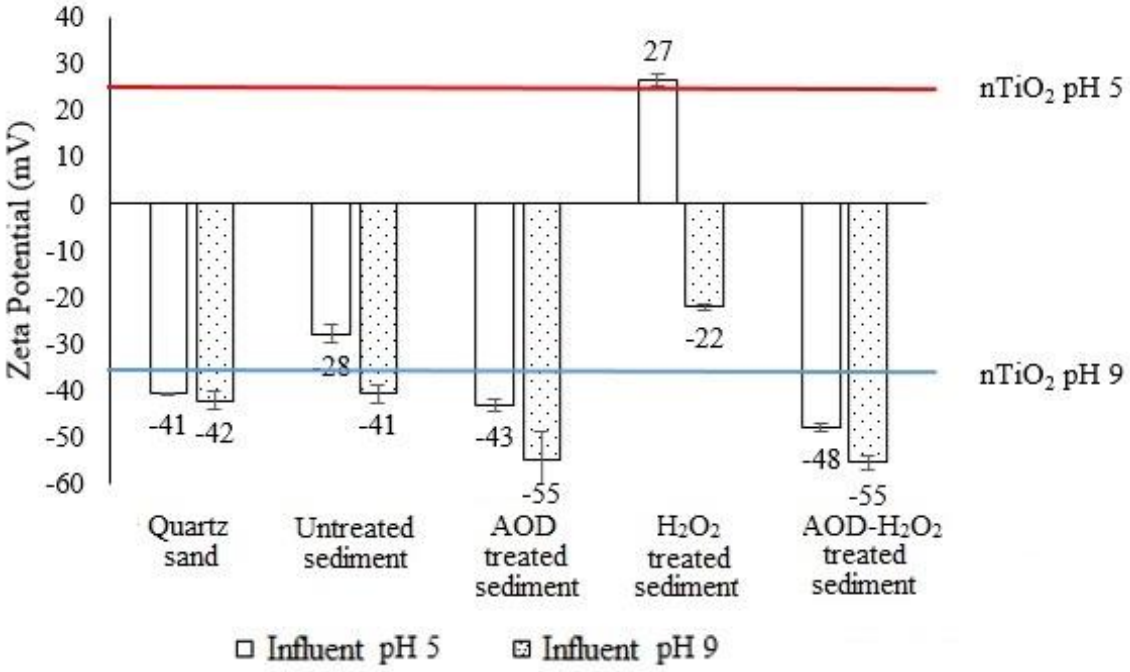

Figure 3. Zeta potential of quartz sand, sediments, and $nTiO_2$ at pH 5 and 9. Zeta potential of quartz sand determined previously by Wu and Cheng (2016).

2.3.4 $nTiO_2$ transport mechanisms

Discrepancies in predicted and observed $nTiO_2$ transport based upon ZPs indicated that individual sediment component ZPs under experimental pH conditions needed to be considered. Although effluent pH remained approximately constant during each experiment (Figure S3, SI), pH of the column effluents varied from the influent pH of 5 or 9 as the porous media buffered suspension pH as it travelled through the column, which could have large effects on ZP and therefore $nTiO_2$ transport (Figure 4a). Xu et al. (2012) reported pH buffering by acidic soils was correlated to cation exchange capacity and deprotonation of SOM, consistent with the sediment used in this study. Effluent pH was buffered closer to the natural pH of each sediment (Table S2, SI), and was similar for experiments at both 5 and 9, slightly higher for pH 9 influents (Figure 4a). pH buffering by the sediments in the pH 9 experiments was stronger than in the pH 5 experiments, as the sediments were naturally acidic (Table S2, SI).

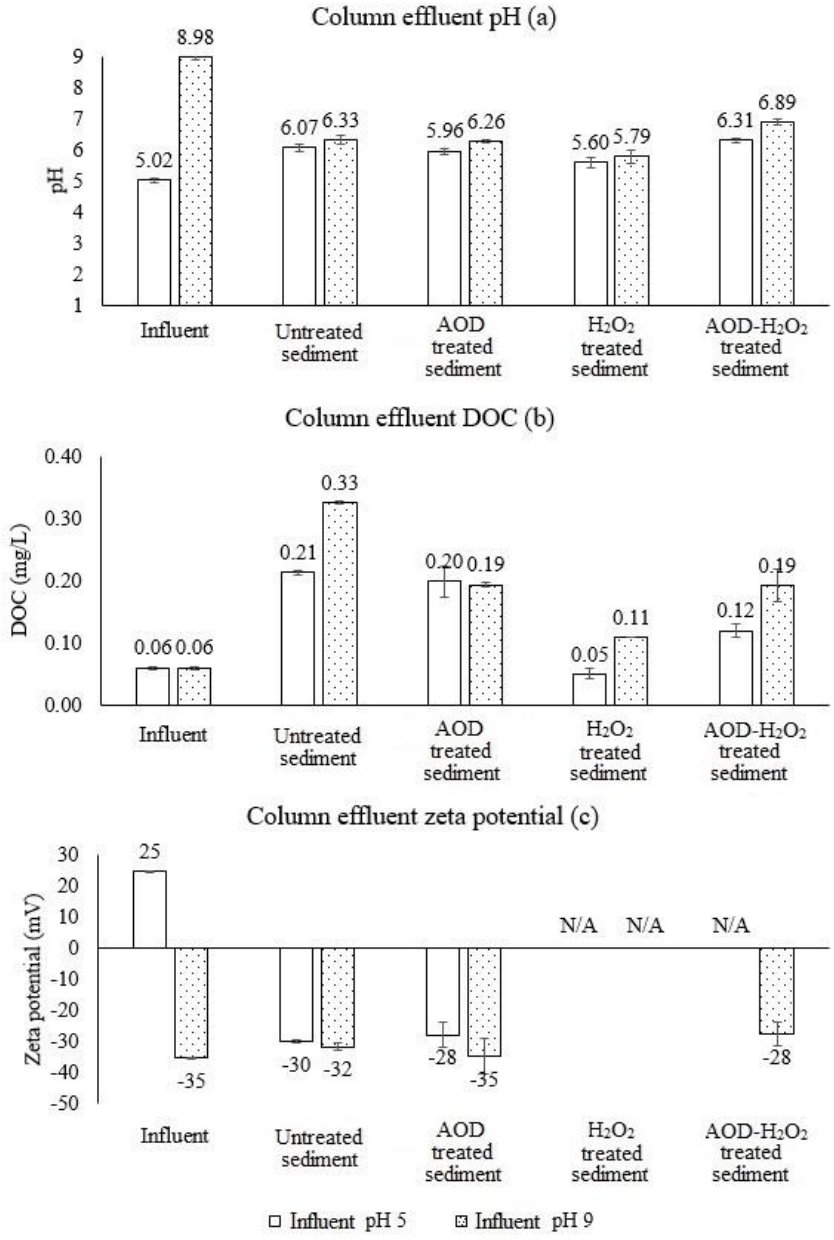

Figure 4. Column effluent pH, DOC, and zeta potential for each experiment.

Differences in influent and effluent pH indicated that pH of the pore water changed along the column length, and consequently influenced ZP of $nTiO_2$ and sediment

components and therefore the nature of their electrostatic interactions. At either end of the column existed two pH end members: the influent, with pH adjusted to 5 or 9; and the effluent, with pH influenced by the transport media. To determine zones of theoretical attractive or repulsive electrostatic interactions between $nTiO_2$ and various sediment components, pH of each column influent and effluent was plotted (pH 5 influent experiments at the top, and pH 9 at the bottom) along with charges of representative sediment components and $nTiO_2$ (positive or negative, based on each component's PZC) in Figure 5. Quartz was selected to represent the bulk minerals in the sediment, because the majority of minerals had strongly negative ZP under the pH range of our experiments (Mikanovic et al., 2006; Prasanphan and Nuntiya, 2006; Salopek et al., 1992). Fe oxide was representative of the metal oxyhydroxides in the sediment, due to its variable ZP with changing pH; whereas the major constituent of SOM, humic substances, was chosen for SOM. Although a wide range of PZC values have been reported for $nTiO_2$ (Kosmulski, 2002), 6.2 represents an average previously determined for $nTiO_2$ under the same water chemistry conditions (Loosli et al., 2013). If the true PZC of $nTiO_2$ is slightly higher or lower than 6.2, and the line in Figure 5 is shifted slightly, the explanation of results remains the same due to the range of charges experienced for each component along column length.

ENP transport may also be influenced by changes in ionic strength, composition, and valence; alterations in pore space and geometry; as well as sediment colloids and clays (e.g., Akaighe et al., 2012; Chen et al., 2011a; French et al., 2009; Frimmel and Niessner, 2010; Tang and Cheng, 2018; Zhou et al., 2012). In the interpretation of our results, we

assumed that changes in each of these factors among the different sediment types were negligible, and therefore only changes in pH and SOM and Fe/Al-oxyhydroxide concentrations were responsible for the observed $nTiO_2$ transport behavior.

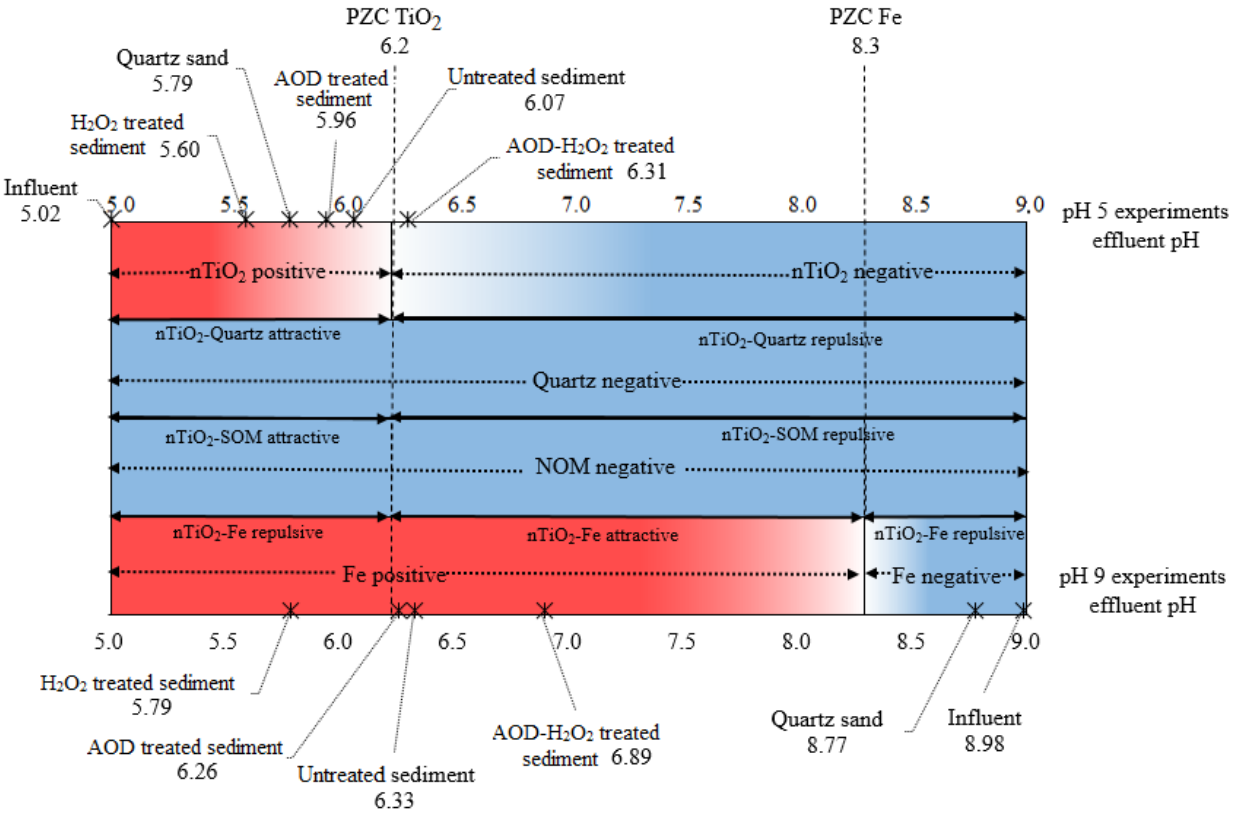

Figure 5. Column effluent pH and ranges of positive or negative surface potentials for nTiO2, Quartz, SOM, and Fe oxides based on previously determined PZC (quartz and Fe oxide (Huang, 1995), nTiO2 (Loosli et al., 2015; Parks, 1965), SOM (Philippe and Schaumann, 2014)).

For the pH 5 influent experiments, column effluent pH remained within a range where $nTiO_2$ was expected to be positively-charged, except for the AOD-H_2O_2 treated sediment, with effluent pH 6.31 (Figure 5). Although the AOD-H_2O_2 treated sediment column effluent pH was above the PZC of $nTiO_2$ (and any $nTiO_2$ that eluded the column

was expected to be negatively-charged), no $nTiO_2$ was detected in the column effluent because attraction to quartz and other minerals near the influent site caused retention of all of the $nTiO_2$ in the column (before the pH was buffered above the PZC of $nTiO_2$). Homoaggregation and straining was also possible under these conditions, however, the rate of aggregation in pore spaces occurs at much slower rates than deposition (Solovitch et al., 2010). In all of the sediments, quartz and other negatively-charged minerals were a major component, accounting for the low recovery of $nTiO_2$ for the pH 5 influent suspensions as attractive forces were expected, and $nTiO_2$ was retained in the column. Repulsive forces existed between $nTiO_2$ and Fe oxides in this pH range; however, the Fe oxides were in much lower concentration relative to the minerals in the sediment, and were unlikely to cause repulsion under these conditions.

Like quartz, forces between $nTiO_2$ and SOM were also attractive under these conditions, therefore in sediments with sufficient SOM concentrations, $nTiO_2$ was also attracted to SOM in the sediment. The SOM existed as either SSOM or leached as DOM; although SSOM may have attracted $nTiO_2$ and removed it from pore water, DOM is known to facilitate the transport of ENPs. Wu and Cheng (2016) found that DOM, in concentrations as low as 0.13 mg/L, prevented $nTiO_2$ attachment to quartz sand by adsorbing onto $nTiO_2$ surfaces, thereby modifying $nTiO_2$'s surface charge from positive to negative, and stabilizing it in suspension. Similar results have been reported indicating that DOM can play a major role in enhancing ENP transport (Chen et al., 2012; Loosli et al., 2013). In our experiments, the untreated and AOD treated sediments, which had not undergone the H_2O_2 organic degradation process, contained the greatest concentrations of

SOC (Figure 1) and were the only experiments with $nTiO_2$ recovered in the column effluent (Figure 2a), as DOM leached from these sediments, attached to $nTiO_2$ surface, and facilitated its transport. The highest concentrations of leached DOC in column effluents from the pH 5 experiments came from the untreated and AOD treated sediment (~ 0.20 mg/L) (Figure 4b), correlated with greatest $nTiO_2$ recovery (Figure 2a), whereas the quartz sand, H_2O_2, and AOD-H_2O_2 treated sediments had lower leached DOC concentrations (Figure 4b), and therefore facilitation did not occur, and all of the injected $nTiO_2$ was retained (Figure 2a).

Although ZP of influent $nTiO_2$ was positive at pH 5, effluent samples from the untreated and AOD treated sediments had negative ZP, -28 to -30 mV (Figure 4c), correlated to DOM adsorption onto $nTiO_2$ reversing its surface charge to negative. Effluent ZP was not measured for the H_2O_2 and AOD-H_2O_2 treated sediments in the pH 5 experiments due to no $nTiO_2$ being detected in column effluents, correlated with lower DOC concentrations. Decreasing $nTiO_2$ recovery with time was observed for the untreated and AOD treated sediments (Figure 2a), consistent with ripening behavior; where $nTiO_2$ already deposited in the column attracted the $nTiO_2$ with reversed charges, providing further evidence that DOM had adsorbed onto $nTiO_2$ in these experiments (Chen et al., 2012; Gentile and Fidalgo de Cortalezzi, 2016; Liu et al., 1995). HDD of all the column effluents with $nTiO_2$ recovered was smaller than that of the influent (Figure S4, SI), indicating that aggregation was not occurring.

In summary, two competing processes were responsible for $nTiO_2$ behavior in the pH 5 experiments; the attachment of positively-charged $nTiO_2$ to SOM, quartz sand, and

other negatively-charged minerals, removing it from the pore water, versus the attraction of leached DOM to $nTiO_2$, which reversed the ZP of $nTiO_2$ and facilitated transport. The majority of $nTiO_2$ was retained in the column (>95%), indicating that attachment was the dominant process, whereas DOM influenced a small percentage. Physical differences between sediment and quartz sand (sediment with smaller pore sizes, rougher surfaces, greater SSA) suggested that quartz sand columns would yield greater transport of $nTiO_2$, however, our results indicated enhanced transport was dependent on surface charges and leached DOM.

pH buffering of influent suspensions by the sediments was much stronger in the pH 9 experiments, and a larger range of pH was experienced along the column lengths than in the pH 5 experiments (Figure 5). Within this range, as pH decreased from 9, ZP of $nTiO_2$ changed from negative, to near neutral, and positive when pH was below its PZC ~6.2 (Loosli et al., 2015; Parks, 1965). Additionally, surface charges on Fe oxides changed from negative to positive when pH was below their PZC of ~8.3 (Huang, 1995), whereas SOM and quartz remained negative across the whole range (Figure 5). These large changes in pH and ZPs of $nTiO_2$ and Fe oxides indicated that electrostatic forces between $nTiO_2$ and various sediment components were variable along the column lengths, leading to complex $nTiO_2$ transport behavior.

The effluent pH of the quartz sand experiments at influent pH 9 (8.77) was not strongly buffered along the length of the column, and with negative surface potentials on both $nTiO_2$ and quartz at this pH, repulsive electrostatic forces were expected (Figure 5). This was consistent with nearly 100% $nTiO_2$ recovery observed in quartz sand columns at

pH 9 (Figure 2b). Like quartz sand, the AOD-H_2O_2 sediment had low concentrations of SOC and Fe/Al-oxyhydroxides (Figure 1), leaving a composition of mainly negatively-charged minerals, and therefore negatively-charged $nTiO_2$ was repelled and eluded from the AOD-H_2O_2 sediment columns as well (Figure 2b). High recovery (93%) for the AOD-H_2O_2 treated sediment alike the quartz sand confirmed that $nTiO_2$ homoaggregation and straining was not a major factor in our experiments at this pH; and observed differences for the pH 9 experiments should be due to changes in Fe/Al-oxyhydroxides and SOM concentrations.

About 80% of injected $nTiO_2$ was recovered in untreated natural sediment column effluent (Figure 2b). This high recovery was attributable to electrostatic repulsion between $nTiO_2$ and transport medium. Across the entire pH range of the untreated sediment column, $nTiO_2$ carried negative charges and was repelled by like-charged SOM, quartz, and other minerals (Figure 5). Although anticipated electrostatic forces between $nTiO_2$ and SOM were repulsive at pH 9 (Figure 5), a fraction of DOM may adsorb onto $nTiO_2$ surfaces even at this high pH; and the magnitude of DOM adsorption would increase with decreasing pH along the column length (Wu and Cheng, 2016). It was therefore possible that in our experiments some of the leached DOM adsorbed onto $nTiO_2$, facilitating transport and contributing to high $nTiO_2$ recovery. This process became more important as pore water pH decreased along the column, which lowered energy barriers for DOM adsorption onto $nTiO_2$. The effluent pH (6.33) was very close to the PZC of $nTiO_2$, and therefore ZP was expected to be near zero. However, effluent ZP was found strongly negative at -32 mV (Figure 4c), indicating that $nTiO_2$ eluding the

column could be covered by negatively-charged DOM. Effluent DOC of the untreated sediment column with pH 9 influent was found at 0.33 mg/L, the highest of all of the experiments (Figure 4b), confirming that DOM could have a strong effect on $nTiO_2$.

To explain the 20% of $nTiO_2$ retained in the untreated sediment, two mechanisms were considered; attraction by Fe/Al-oxyhydroxides and the influence of surface roughness. Despite electrostatic forces between $nTiO_2$ and Fe oxides being repulsive at the pH 9 influent site, as the suspension travelled through the column and was buffered by the sediment, it passed the PZC of Fe oxides, and Fe oxides became increasingly important away from the influent site as electrostatic forces became attractive and some of the $nTiO_2$ was attached to oxides surfaces and removed from suspension (Figure 5). Additionally, although pH ranges of 9 to 6.2 for SOM and 9 to 8.3 for Fe oxides suggested repulsive electrostatic forces with $nTiO_2$ (Figure 5), SSOM and metal oxides have irregular rough surfaces which are known to drastically reduce interaction energies between ENPs and porous media, and therefore these sites may have attracted some of the $nTiO_2$ (Bayat et al., 2015; Shen et al., 2011; Wu and Cheng, 2016). Bayat et al. (2015) found rough surface of dolomite grains accounted for 10% Al_2O_3 ENP deposition under unfavorable conditions, whereas Wu and Cheng (2016) reported that up to 15% of $nTiO_2$ was deposited onto Fe oxide coating of quartz sand under unfavorable electrostatics at pH 9. Surfaces on Fe/Al-oxyhydroxides and SSOM within sediments are rough in nature (Li et al., 2017; Wu and Cheng, 2016), and therefore may have similarly led to increased deposition of $nTiO_2$ even under unfavoured conditions. Repulsive forces between $nTiO_2$ and quartz/minerals/SSOM and DOM facilitation were the dominant

processes governing $nTiO_2$ transport in the untreated sediment, counteracted by attraction to Fe/Al-oxyhydroxides and rough surfaces.

In contrast to the other pH 9 experiments with high $nTiO_2$ mobility, no $nTiO_2$ was recovered from the H_2O_2 treated sediment column (Figure 2b). Buffered pH and complex competing interactions between $nTiO_2$ and varying proportions of Fe/Al-oxyhydroxides and SOC accounted for the low recovery. The H_2O_2 treated sediment had its SOC and therefore DOC depleted (Figure 1c), and most likely retained all the injected $nTiO_2$ in the buffered pH range of 8.3 to 6.2, where attractive electrostatic forces existed between $nTiO_2$ and Fe oxides (Figure 5). AOD-Al, AOD-Fe and DCB-Fe were relatively high for the H_2O_2 treated sediment compared to the other treatments (except the untreated sediment) (Figure 1), whereas SOC was depleted and DOC concentrations in the column effluent were low (Figure 4b), therefore deposition of all the injected $nTiO_2$ within the H_2O_2 treated sediment was most likely due to Fe/Al-oxyhydroxides playing an important role in attracting $nTiO_2$ in the absence of SOM (Cornelis et al., 2013; Johnson et al., 1996).

For the AOD treated sediment column effluent, 6% of the injected $nTiO_2$ was recovered, higher than nil recovery by the H_2O_2 treated sediment, but much lower than the other sediments. The reason for low $nTiO_2$ recovery for the AOD treated sediment was similar to that of the H_2O_2 treated sediment; DCB-Fe strongly attracted $nTiO_2$ under reduced SOM/DOM concentrations once pH was buffered below the PZC of Fe oxides. Even though AOD-Al and Fe were depleted by the AOD treatment process, DCB-Fe was still 26% of the original sediment's (Figure 1a and 1b). Additionally, AOD treatment

reduced SOC by 79% (Figure 1c), which reduced DOM concentration in the pore water of the column, evidenced by lower DOC concentration in the column effluent (0.19 mg/L, 57% relative to the untreated sediment) (Figure 4b). The $nTiO_2$ that did elute the column (6%) was strongly negatively-charged (-35 mV) at pH 6.26 (Figure 4c), indicating that DOM had attached to and stabilized this small fraction of $nTiO_2$. However, the DOM covered $nTiO_2$ would have also been attracted to positively-charged DCB-Fe, limiting the facilitation of $nTiO_2$ transport by DOM.

The pH 9 experiments revealed $nTiO_2$ transport was influenced by pH buffering by the sediments, which could cause electrostatic forces to change from repulsive to attractive when charges on $nTiO_2$ and Fe reversed at their PZC. Quartz and other negatively-charged minerals always repulsed $nTiO_2$ under these conditions, whereas Fe/Al-oxyhydroxides and rough surfaces led to $nTiO_2$ attachment. Additionally, leached DOM may facilitate $nTiO_2$ transport. Comparable $nTiO_2$ transport in quartz sand and AOD-H_2O_2 treated sediment columns indicated variation in physical properties (such as pore size, grain roughness, and SSA) were not responsible for the differences in $nTiO_2$ transport behavior, whereas varying concentrations SOM and Fe/Al-oxyhydroxides had substantial effects, emphasizing their important influence on ENP transport.

2.3.5 Environmental implications

ENPs in natural subsurface environments may travel through sediments with complex compositions including SOM and Fe/Al-oxyhydroxides, though their influence is little-known. Results of our column experiments demonstrated that SOM and Fe/Al-oxyhydroxides could have big influence on $nTiO_2$ retention and transport, even though

they were only minor components (< 1% by mass) in the sediment. pH was a key factor that determined the role of SOM and Fe/Al-oxyhydroxides, since pH strongly influenced ZP of $nTiO_2$ and Fe/Al-oxyhydroxides, and therefore interactions of $nTiO_2$ with various components in the sediment. Leached DOM, even at low concentrations, may considerably promote transport by adsorbing to and reversing ZP of $nTiO_2$. Differences in $nTiO_2$ transport in quartz sand and natural sediment columns emphasize the necessity of considering influences of SOM and Fe/Al-oxyhydroxides when evaluating ENP transport in natural sediments.

2.4 References

Akaighe, N., Depner, S.W., Banerjee, S., Sharma, V.K., Sohn, M., 2012. The effects of monovalent and divalent cations on the stability of silver nanoparticles formed from direct reduction of silver ions by Suwannee River humic acid / natural organic matter. Sci. Total Environ. 441, 277–289. doi:10.1016/j.scitotenv.2012.09.055

Bayat, A.E., Junin, R., Shamshirband, S., Tong Chong, W., 2015. Transport and retention of engineered Al2O3, TiO2, and SiO2 nanoparticles through various sedimentary rocks. Sci. Rep. 5, 14264. doi:10.1038/srep14264

Cai, L., Tong, M., Wang, X., Kim, H., 2014. Influence of Clay Particles on the Transport and Retention of Titanium Dioxide Nanoparticles in Quartz Sand. Environ. Sci. Technol. 48, 7323–7332. doi:dx.doi.org/10.1021/es5019652

Chen, G., Liu, X., Su, C., 2012. Distinct effects of humic acid on transport and retention of TiO2 rutile nanoparticles in saturated sand columns. Environ. Sci. Technol. 46, 7142–7150. doi:10.1021/es204010g

Chen, G., Liu, X., Su, C., 2011a. Transport and retention of TiO2 rutile nanoparticles in saturated porous media under low-ionic-strength conditions: Measurements and mechanisms. Langmuir 27, 5393–5402. doi:10.1021/la200251v

Chen, G., Liu, X., Su, C., 2011b. Transport and retention of TiO2 rutile nanoparticles in saturated porous media under low-ionic-strength conditions: Measurements and mechanisms. Langmuir 27, 5393–5402. doi:10.1021/la200251v

Chen, M., Xu, N., Cao, X., Zhou, K., Chen, Z., Wang, Y., Liu, C., 2015. Facilitated transport of anatase titanium dioxides nanoparticles in the presence of phosphate in saturated sands. J. Colloid Interface Sci. 451, 134–143. doi:10.1016/j.jcis.2015.04.010

Cornelis, G., Pang, L., Doolette, C., Kirby, J.K., McLaughlin, M.J., 2013. Transport of silver nanoparticles in saturated columns of natural soils. Sci. Total Environ. 463–464, 120–130. doi:10.1016/j.scitotenv.2013.05.089

Erhayem, M., Sohn, M., 2014. Stability studies for titanium dioxide nanoparticles upon adsorption of Suwannee River humic and fulvic acids and natural organic matter. Sci. Total Environ. 468–469, 249–257. doi:10.1016/j.scitotenv.2013.08.038

Fang, J., Shan, X., Wen, B., Lin, J., Owens, G., 2009. Stability of titania nanoparticles in soil suspensions and transport in saturated homogeneous soil columns. Environ. Pollut. 157, 1101–1109. doi:10.1016/j.envpol.2008.11.006

Fang, J., Shan, X., Wen, B., Lin, J., Owens, G., Zhou, S., 2011. Transport of copper as affected by titania nanoparticles in soil columns. Environ. Pollut. 159, 1248–1256. doi:10.1016/j.envpol.2011.01.039

Fisher-Power, L.M., Cheng, T., Rastghalam, Z.S., 2016. Cu and Zn adsorption to a heterogeneous natural sediment: Influence of leached cations and natural organic matter. Chemosphere 144, 1973–1979. doi:10.1016/j.chemosphere.2015.10.109

French, R.A., Jacobson, A.R., Kim, B., Isley, S.L., Penn, L., Baveye, P.C., 2009. Influence of ionic strength, pH, and cation valence on aggregation kinetics of titanium dioxide nanoparticles. Environ. Sci. Technol. 43, 1354–1359. doi:10.1021/es802628n

Frimmel, F., Niessner, R., 2010. Nanoparticles in the Water Cycle. Springer, Heidelberg. doi:10.1007/s13398-014-0173-7.2

Furman, O., Usenko, S., Lau, B.L.T., 2013. Relative importance of the humic and fulvic fractions of natural organic matter in the aggregation and deposition of silver nanoparticles. Environ. Sci. Technol. 47, 1349–1356. doi:10.1021/es303275g

Gentile, G.J., Fidalgo de Cortalezzi, M.M., 2016. Enhanced retention of bacteria by TiO2 nanoparticles in saturated porous media. J. Contam. Hydrol. 191, 66–75. doi:10.1016/j.jconhyd.2016.05.004

Grillo, R., Rosa, A.H., Fraceto, L.F., 2015. Chemosphere Engineered nanoparticles and organic matter : A review of the state-of-the-art. Chemosphere 119, 608–619. doi:10.1016/j.chemosphere.2014.07.049

Grolimund, D., Borkovec, M., 2005. Colloid-facilitated transport of strongly sorbing contaminants in natural porous media: Mathematical modeling and laboratory column experiments. Environ. Sci. Technol. 39, 6378–6386. doi:10.1021/es050207y

Grolimund, D., Borkovec, M., Barmettler, K., Sticher, H., 1996. Colloid-facilitated transport of strongly sorbing contaminants in natural porous media: A laboratory column study. Environ. Sci. Technol. 30, 3118–3123. doi:10.1021/es960246x

Han, P., Wang, X., Cai, L., Tong, M., Kim, H., 2014. Transport and retention behaviors of titanium dioxide nanoparticles in iron oxide-coated quartz sand: Effects of pH, ionic strength, and humic acid. Colloids Surfaces A Physicochem. Eng. Asp. 454, 119–127. doi:10.1016/j.colsurfa.2014.04.020

Huang, P., 1995. Environmental Impacts of Soil Component Interactions: Metals, Other Inorganics, and Microbial Activities. CRC Press, Saskatoon.

Jackson, M.L., 1958. Soil Chemical Analysis. Prentice-Hall Inc., Englewood Cliffs, NJ.

Johnson, P.R., Elimelech, M., 1995. Dynamics of Colloid Deposition in Porous Media : Blocking Based on Random Sequential Adsorption. Langmuir 801–812.

Johnson, P.R., Sun, N., Elimelech, M., 1996. Colloid Transport in Geochemically Heterogeneous Porous Media : Modeling and Measurements Colloid Transport in

Geochemically Heterogeneous Porous Media : Modeling and Measurements. Environ. Sci. Technol. 30, 3284–3293. doi:10.1021/es960053

Jung, B., O'Carroll, D., Sleep, B., 2014. The influence of humic acid and clay content on the transport of polymer-coated iron nanoparticles through sand. Sci. Total Environ. 496, 155–64. doi:10.1016/j.scitotenv.2014.06.075

Keller, A., Wang, H., Zhou, D., Lenihan, H., Cherr, G., Cardinale, B., Miller, R., Ji, Z., 2010. Stability and Aggregation of Metal Oxide Nanoparticles in Natural Aqueous Matrices. Environ. Sci. Technol. 44, 1962–1967.

Kosmulski, M., 2002. The significance of the difference in the point of zero charge between rutile and anatase. Adv. Colloid Interface Sci. 99, 255–264.

Kretzschmar, R., Barmettler, K., Grolimund, D., Yan, Y., Borkovec, M., Sticher, H., 1997. Experimental determination of colloid deposition rates and collision efficiencies in natural porous media. Water Resour. Res. 33, 1129. doi:10.1029/97WR00298

Lewis, J., Sjöstrom, J., 2010. Optimizing the experimental design of soil columns in saturated and unsaturated transport experiments. J. Contam. Hydrol. 115, 1–13. doi:10.1016/j.jconhyd.2010.04.001

Li, Y., Qu, G., Zhang, L., Wang, T., Sun, Q., Liang, D., Hu, S., 2017. Humic acid removal from micro-polluted source water using gas phase surface discharge plasma at different grounding modes. Sep. Purif. Technol. 180, 36–43. doi:10.1016/j.seppur.2017.02.046

Lin, S., Cheng, Y., Bobcombe, Y., L. Jones, K., Liu, J., Wiesner, M.R., 2011. Deposition of silver nanoparticles in geochemically heterogeneous porous media: Predicting affinity from surface composition analysis. Environ. Sci. Technol. 45, 5209–5215. doi:10.1021/es2002327

Liu, D., Johnson, P.R., Elimelech, M., 1995. Colloid Deposition Dynamics in Flow-Through Porous Media: Role of Electrolyte Concentration. Environ. Sci. Technol. 29, 2963–2973. doi:10.1021/es00012a012

Loosli, F., Le Coustumer, P., Stoll, S., 2015. Effect of electrolyte valency, alginate concentration and pH on engineered TiO2 nanoparticle stability in aqueous solution. Sci. Total Environ. 535, 1–7. doi:10.1016/j.scitotenv.2015.02.037

Loosli, F., Le Coustumer, P., Stoll, S., 2013. TiO2 nanoparticles aggregation and disaggregation in presence of alginate and Suwannee River humic acids. pH and concentration effects on nanoparticle stability. Water Res. 47, 6052–6063. doi:10.1016/j.watres.2013.07.021

Mehra, O.P., 1958. Iron Oxide Removal from Soils and Clays by a Dithionite-Citrate System Buffered with Sodium Bicarbonate. Clays Clay Miner. 7, 317–327. doi:10.1346/CCMN.1958.0070122

Mikanovic, N., Khayat, K., Pagé, M., Jolicoeur, C., 2006. Aqueous CaCO3 dispersions as reference systems for early-age cementitious materials. Colloids Surfaces A Physicochem. Eng. Asp. 291, 202–211. doi:10.1016/j.colsurfa.2006.06.042

Mizutani, K., Fisher-Power, L.M., Shi, Z., Cheng, T., 2017. Cu and Zn adsorption to a terrestrial sediment: Influence of solid-to-solution ratio. Chemosphere 175, 341–349. doi:10.1016/j.chemosphere.2017.02.069

Morales, V.L., Zhang, W., Gao, B., Lion, L.W., Bisogni, J.J., McDonough, B. a., Steenhuis, T.S., 2011. Impact of dissolved organic matter on colloid transport in the vadose zone: Deterministic approximation of transport deposition coefficients from polymeric coating characteristics. Water Res. 45, 1691–1701. doi:10.1016/j.watres.2010.10.030

Nowack, B., Bucheli, T.D., 2007. Occurrence , behavior and effects of nanoparticles in the environment. Environ. Pollut. 150, 5–22. doi:10.1016/j.envpol.2007.06.006

Parks, A., 1965. The Isoelectric Points of Solid Oxides, Solid Hydroxides, and Aqueous Hydroxo Complex Systems. Chem. Rev. 65, 177–198.

Philippe, A., Schaumann, G.E., 2014. Interactions of Dissolved Organic Matter with Natural and Engineered Inorganic Colloids : A Review. Environ. Sci. Technol. 48, 8946–8962. doi:dx.doi.org/10.1021/es502342r

Prasanphan, S., Nuntiya, A., 2006. Electrokinetic Properties of Kaolins, Sodium Feldspar and Quartz. Chiang Mai J. Sci. 33, 183–190.

Salopek, B., Krasic, D., Filipovic, S., 1992. Measurement and application of zeta-potential. Rud. Zb. 4, 147–151.

Shen, C.Y., Li, B.G., Wang, C., Huang, Y.F., Jin, Y., 2011. Surface Roughness Effect on Deposition of Nano- and Micro-Sized Colloids in Saturated Columns at Different Solution Ionic Strengths. Vadose Zo. J. 10, 1071–1081. doi:Doi 10.2136/Vzj2011.0011

Solovitch, N., Labille, J., Rose, J., Chaurand, P., Borschneck, D., Wiesner, M.R., Bottero, J.-Y., 2010. Concurrent Aggregation and Deposition of TiO2 Nanoparticles in a Sandy Porous Media. Environ. Sci. Technol. 44, 4897–4902.

Song, L., Elimelech, M., 1993. Dynamics of colloid deposition in porous media: Modeling the role of retained particles. Colloids Surfaces A Physicochem. Eng. Asp. 73, 49–63. doi:10.1016/0927-7757(93)80006-Z

Sun, P., Shijirbaatar, A., Fang, J., Owens, G., Lin, D., Zhang, K., 2015. Distinguishable Transport Behavior of Zinc Oxide Nanoparticles in Silica Sand and Soil Columns. Sci. Total Environ. 505, 189–198. doi:10.1016/j.scitotenv.2014.09.095

Tang, Z., Cheng, T., 2018. Stability and aggregation of nanoscale titanium dioxide particle (nTiO2): Effect of cation valence, humic acid, and clay colloids. Chemosphere 192, 51–58. doi:10.1016/j.chemosphere.2017.10.105

Tipping, E., Rey-Castro, C., Bryan, S.E., Hamilton-Taylor, J., 2002. Al(III) and Fe(III) binding by humic substances in freshwaters, and implications for trace metal speciation. Geochim. Cosmochim. Acta 66, 3211–3224. doi:10.1016/S0016-7037(02)00930-4

Wang, D., Bradford, S.A., Harvey, R.W., Gao, B., Cang, L., Zhou, D., 2012. Humic acid facilitates the transport of ARS-labeled hydroxyapatite nanoparticles in iron

oxyhydroxide-coated sand. Environ. Sci. Technol. 46, 2738–2745. doi:10.1021/es203784u

Wang, Q., Cheng, T., Wu, Y., 2015. Distinct Roles of Illite Colloid and Humic Acid in Mediating Arsenate Transport in Water-Saturated Sand Columns. Water. Air. Soil Pollut. 226, 1–15. doi:10.1007/s11270-015-2413-7

Wu, Y., Cheng, T., 2016. Stability of nTiO2 particles and their attachment to sand : Effects of humic acid at different pH. Sci. Total Environ. 541, 579–589. doi:http://dx.doi.org/10.1016/j.scitotenv.2015.09.116 0048-9697

Yang, Y., Saiers, J.E., Barnett, M.O., 2013. Impact of interactions between natural organic matter and metal oxides on the desorption kinetics of uranium from heterogeneous colloidal suspensions. Environ. Sci. Technol. 47, 2661–2669. doi:10.1021/es304013r

Zhou, D., Abdel-fattah, A.I., Keller, A. a, 2012. Clay particles destabilize engineered nanoparticles in aqueous environments. Environ. Sci. Technol. 46, 7520–7526.

Zhuang, J., Flury, M., Jin, Y., 2003. Colloid-Facilitated Cs Transport through Water-Saturated Hanford Sediment and Ottawa Sand. Environ. Sci. Technol. 37, 4905–4911. doi:10.1021/es0264504

Chapter 3. Cu and Zn adsorption to natural sediment: Importance of soil organic matter and Fe/Al-oxyhydroxides

Abstract

Adsorption of heavy metals in subsurface environments is highly dependent on the composition of the soil and sediment. The importance of soil organic matter (SOM) and Fe/Al-oxyhydroxides in natural sediments on heavy metal adsorption has been previously identified; however, their individual and synergistic effects have not been fully examined. In this study, a natural sediment was treated to remove either SOM, Fe/Al-oxyhydroxides, or both, and used in Cu and Zn batch adsorption experiments in the pH range of 3−8, with the objective of examining the influence of SOM and Fe/Al-oxyhydroxides. Two methods of incorporating leached cations (predicted by calculation and by actual measurements) in surface complexation models were examined to determine the performance of each in predicting Cu and Zn adsorption. Experimental results showed that Cu and Zn adsorption was dependent on pH and sediment composition. Similar trends were observed for both Cu and Zn, but were more significant for Cu, indicating that Cu adsorption was more susceptible to changes in sediment composition than Zn. Cu adsorption was significantly reduced as a result of organic matter depletion when pH was <6.5, whereas when Fe/Al-oxyhydroxides were depleted, adsorption was greatly impeded when pH >6.5. Removal of both SOM and Fe/Al-oxyhydroxides caused the largest decrease in adsorption across the entire pH range. Surface complexation models using measured leached cation concentrations generally better simulated Cu and Zn adsorption than models using calculated cation

concentrations. The models also suggested that the adsorptive sites in the treated sediments were not efficient for adsorbing Cu due to degradation, but still adequate for Zn. Our results emphasize the important influence of SOM and Fe/Al-oxyhydroxides on heavy metal adsorption and the necessity of considering their effect when modelling heavy metal transport in natural environments.

3.1 Introduction

Adsorption of heavy metals by natural sediments has important implications to the fate and transport of contaminants in subsurface environments. In natural environments, sediments are complex and contain soil organic matter (SOM) and metal oxyhydroxides in varying concentrations (Bradl, 2004). Although the importance SOM and metal oxyhydroxides in heavy metal adsorption has been documented (e.g., Agbenin and Olojo, 2004; Fisher-Power et al., 2016; Mizutani et al., 2017; Pérez-Novo et al., 2008; Shi et al., 2013), many adsorption models do not consider composition of the aquifer material, which may lead to inaccurate predictions. A further complication is that natural sediments leach multivalent cations and dissolved organic matter (DOM) which have been found to strongly influence adsorption (Cappuyns and Swennen, 2008; Fisher-Power et al., 2016; Lumsdon, 2004; Shi et al., 2013, 2007; Xu et al., 2009). The effects of all of these components coexisting and competing in one system are unclear. Thus, information about the influence of each component on heavy metal adsorption is essential for understanding the mechanisms of heavy metal adsorption in the environment.

SOM has a complex effect on heavy metal adsorption, as it may exist either in the dissolved or solid phase. McBride et al. (1997) noted that solid SOM (SSOM) limited

metal solubility, whereas DOM promoted metal solubility. Many other researchers have similarly reported that SSOM tends to adsorb aqueous heavy metals and remove them from the aqueous phase, while DOM may form stable aqueous complexes with heavy metals (Agbenin and Olojo, 2004; Pérez-Novo et al., 2008; Wang and Mulligan, 2006). The overall effect of SOM in natural sediments, both solid and dissolved, is poorly reported, and presumably a function of the affinity of each for heavy metals. Pérez-Novo et al. (2008) performed Cu and Zn adsorption experiments on sediments before and after treatment to remove SOM, and found Cu adsorption was greatly reduced, whereas Zn adsorption was also reduced but to a lesser extent, suggesting that overall SOM tends to promote metal sorption rather than decrease it.

Amorphous Fe and Al oxyhydroxides have large surface areas per unit mass, and therefore have many surface functional sites available for adsorption (Shi et al., 2013; Wang et al., 2013). The adsorption capacity of amorphous oxides was previously found about 10 times higher than that of aged oxides, linked to increased cation exchange capacity and surface area (Shuman, 1977). In addition, Fe/Al-oxyhydroxides have heterogeneous surface charges and complexes which may act as adsorptive sites (Bradl, 2004; Wang et al., 2013). Fe/Al-oxyhydroxides were found as the dominant adsorbing phase for Cu and Zn when pH was > 6.5, whereas SOM was more important when pH < 6.5 (Fisher-Power et al., 2016). SOM and Fe/Al-oxyhydroxides often co-exist in natural sediments, and their synergistic effects on heavy metal adsorption are poorly documented. Agbenin and Olojo (2004) reported that removing SOM from soil reduced the distribution coefficient for Cu 40 times, but only by half for Zn; whereas removal of

amorphous metal oxides reduced the distribution coefficient for Cu 100 times and 20 times for Zn. Research expanding on these ideas and findings would help to increase knowledge of heavy metal adsorption in heterogeneous natural sediments.

In a previous study (Fisher-Power et al., 2016), laboratory batch experiments and surface complexation modelling was used to investigate Cu and Zn adsorption to a natural sediment, focusing on the influence of leached multivalent cations and DOM. The study found that leached cations substantially decreased Cu and Zn adsorption due to competition for adsorptive sites, whereas DOM decreased Cu adsorption due to the formation of aqueous Cu-DOM complexes. In a follow up investigation (Mizutani et al., 2017), additional adsorption experiments were performed on the same sediment to examine the influence of solid to solution ratio (SSR) on Cu and Zn adsorption. In the current study, we focused on the individual and synergistic influence of SOM and Fe/Al-oxyhydroxides on Cu and Zn adsorption to the same natural sediment to help understand how these sediment components influence heavy metal adsorption in the natural environment. The natural sediment was separated into four portions, one of which was unmodified, and the others treated to deplete SOM, Fe/Al-oxyhydroxides, or both. Each of the sediments were characterized and used in batch Cu and Zn adsorption experiments to determine the effects of SOM and Fe/Al-oxyhydroxides on Cu and Zn adsorption. In addition, two methods of incorporating competitive leached cations (Ca, Mg, Fe, and Al; predicted by calculation and by actual measurement) were implemented in chemical speciation software Visual MINTEQ (Gustafsson, 2010) to determine the performance of each in predicting Cu and Zn adsorption.

3.2 Materials and Methods

3.2.1 Sediment collection, treatment, and characterization

The sediment in this study was used and characterized in its untreated form in previous adsorption research (Fisher-Power et al., 2016; Mizutani et al., 2017). Additional characterization was completed in this study to elucidate the properties of the treated sediments relative to the untreated sediment. The sediment was considered a diamicton, collected from Gullbridge, central Newfoundland, Canada. It was sieved to remove fragments greater than 2 mm, air dried, and stored in the laboratory in a sealed bucket, mixing well before use. Mineralogy was previously determined (Fisher-Power et al., 2016) as dominantly plagioclase (36%), quartz (31%), alkali feldspar (13%), with a variety of other silicates (Figure S5, Supporting Information (SI)). The sediment was separated into four portions: (1) untreated; (2) treated using hydrogen peroxide (H_2O_2) based on a procedure by Jackson (1958) to deplete SOM; (3) treated using a modified ammonium oxalate under darkness (AOD) method (McKeague and Day, 1966) to deplete amorphous Fe/Al-oxyhydroxides; and (4) treated to deplete both SOM and Fe/Al-oxyhydroxides (AOD procedure followed by H_2O_2 procedure). The treatment processes are described in detail in the Supporting Information (SI).

After the treatment procedures, each portion of the sediment was characterized to determine their properties and differences relative to the untreated sediment. Modal mineralogy of crushed sediments was analyzed by Rigaku Ultima IV X-ray diffraction (XRD). Amorphous Fe and Al oxides were quantified by acid ammonium extraction under darkness (McKeague and Day, 1966), whereas dithionite-citrate-bicarbonate

(DCB) extraction (Mehra, 1958) quantified total extractable Fe (amorphous + some crystalline). The amount of soil organic carbon (SOC) was found by elemental combustion analysis using a Carlo Erba NA1500 Series II Elemental Analyzer. Sediment pH was found after mixing 1 gram of sediment in 5 mL nanopure water for 30 minutes. The grain size distribution and percentage of clay, silt, and sand were determined by a Horiba LA-950 Laser Particle Size Analyzer. Exchangeable Ca and Mg concentrations were determined using $BaCl_2$ extraction (Hendershot and Duquette, 1986), and concentrations of originally sorbed Cu and Zn using 0.1 M HNO_3 extraction.

3.2.2 Adsorption experiments

pH adsorption edge experiments were conducted using each of the four sediment types to determine how Cu and Zn adsorption is influenced by pH and sediment composition. In a 50 mL polypropylene centrifuge tube, 1 g of sediment was mixed with 40 mL of 0.01 mol/L $NaNO_3$ prepared in nanopure water and spiked with 3125 µg/L Cu and 3125 µg/L Zn. Blank samples were also prepared but excluded sediment as a control. The samples were mixed for 48 hours on a VWR orbital shaker (Model 5000) at 300 rpm. The pH of each sample was adjusted initially and over the shaking period by adding small volumes of 0.1 mol/L HNO_3 or NaOH to achieve the range of 3-8. After the 48 hours of mixing the samples were centrifuged, the final pH was measured, and the supernatant was separated and filtered through 0.22 µm membrane filters. Filtrates were analyzed by a HP 4500 Plus ICP-MS for Cu and Zn concentrations and an OI Analytical Aurora 1030 TOC Analyzer for dissolved organic carbon (DOC). All experiments were performed at room temperature (22 °C). The difference between the total available Cu

and Zn (originally adsorbed and spiked) and the aqueous Cu and Zn in the filtrates determined the amount of Cu and Zn adsorbed to the sediment. The distribution coefficient (log k_D) was calculated using Equation 1.

$$\log k_D = \log \frac{C^*}{C} \quad (1)$$

where C^*(mg/g) and C (mg/mL) are the adsorbed and aqueous concentrations of Cu or Zn at adsorption equilibrium, respectively.

3.2.3 Surface complexation modelling

Cu and Zn adsorption to each sediment was simulated using the component additivity approach in Visual MINTEQ (version 3.1) (Gustafsson, 2010). This approach assumes that sorbents do not interact with each other, all sorbent surfaces are available for adsorption, and only single solute-sorbent complexes are formed (Alessi and Fein, 2010). Input parameters included pH, temperature, partial pressure of CO_2 ($10^{-3.5}$ atm), and total concentrations of Na, NO_3^-, Cu, and Zn. Measured DOC concentrations were input as well as the amount of organic carbon in the solid phase (the active fraction of SOC with respect to metal binding was set at 0.8; and SOC concentration was converted to SOM concentration assuming 50% of the SOM mass is SOC; as determined previously (Fisher-Power et al., 2016)). The Stockholm Humic Model (Gustafsson, 2001) was used to model adsorption and complexation by SSOM and DOM. Pre-defined adsorption models were used for calculating adsorption to Fe/Al-oxyhydroxides including models for goethite (1-pK three plane CD-MUSIC Model (Weng et al., 2001), input as the difference between DCB-Fe and AOD-Fe), ferrihydrite (4-site 1-pK three plane CD-

MUSIC model (Gustafsson et al., 2011), input as AOD-Fe), and gibbsite (Gibbsite-DLM 2-pK diffuse layer model (Karamalidis and Dzombak, 2010), input as AOD-Fe). Clays were modelled using a fixed charged site, assuming a cation exchange capacity of 0.1 equivalent kg^{-1} (Shi et al., 2013).

Two different methods were used to incorporate leached cations, with all other parameters consistent, to evaluate the performance of each method. In the first method, leached cation concentrations (Fe, Al, Ca, and Mg) were input based upon commonly used calculations, whereas experimentally determined concentrations were used in the second method. For the first method, leached Ca and Mg were calculated in Visual MINTEQ by inputting total $BaCl_2$ extractable Ca and Mg concentrations and allowing the software to predict speciation. Al^{3+} activity was calculated by a linear regression model based on the solubility of Al hydroxide when pH > 5.5 (with solubility constant log K_{so} = 8.3 as suggested by Visual MINTEQ for $Al(OH)_3$ in soils), and a linear regression model between Al^{3+} activity and pH when pH < 5.5 as determined by Shi et al. (2013). Fe^{3+} activity was calculated using a linear regression model based on the solubility of Fe^{3+} hydroxides by assuming solubility control by $Fe(OH)_3$ (with solubility constant log K_{so} = 2.7 as suggested by Visual MINTEQ for aged ferrihydrite). For the second method, Ca and Mg concentrations and Al and Fe activities were input based upon previously well characterized cation leaching from the untreated sediment under the same conditions (Mizutani et al., 2017). Generally, Ca and Mg concentrations as well as Al and Fe activities were underestimated by the first method relative to the second method (Figure

6). To compare the performance of each method, the root mean square error (RMSE) between experimental and modelled results was calculated for each (Equations 2 and 3).

$$\text{RMSE (\% adsorption vs. pH)} = \sqrt{\frac{1}{n_d - n_p} \sum \left(\frac{\%\ adsorbed\ experimental - \%\ adsorbed\ model}{100\ \%} \right)^2} \quad (2)$$

$$\text{RMSE (log } k_D \text{ vs. pH)} = \sqrt{\frac{1}{n_d - n_p} \sum (\log k_D\ (experimental) - \log k_D (model))^2} \quad (3)$$

where n_d is the number of data points and n_p is the number of adjustable parameters.

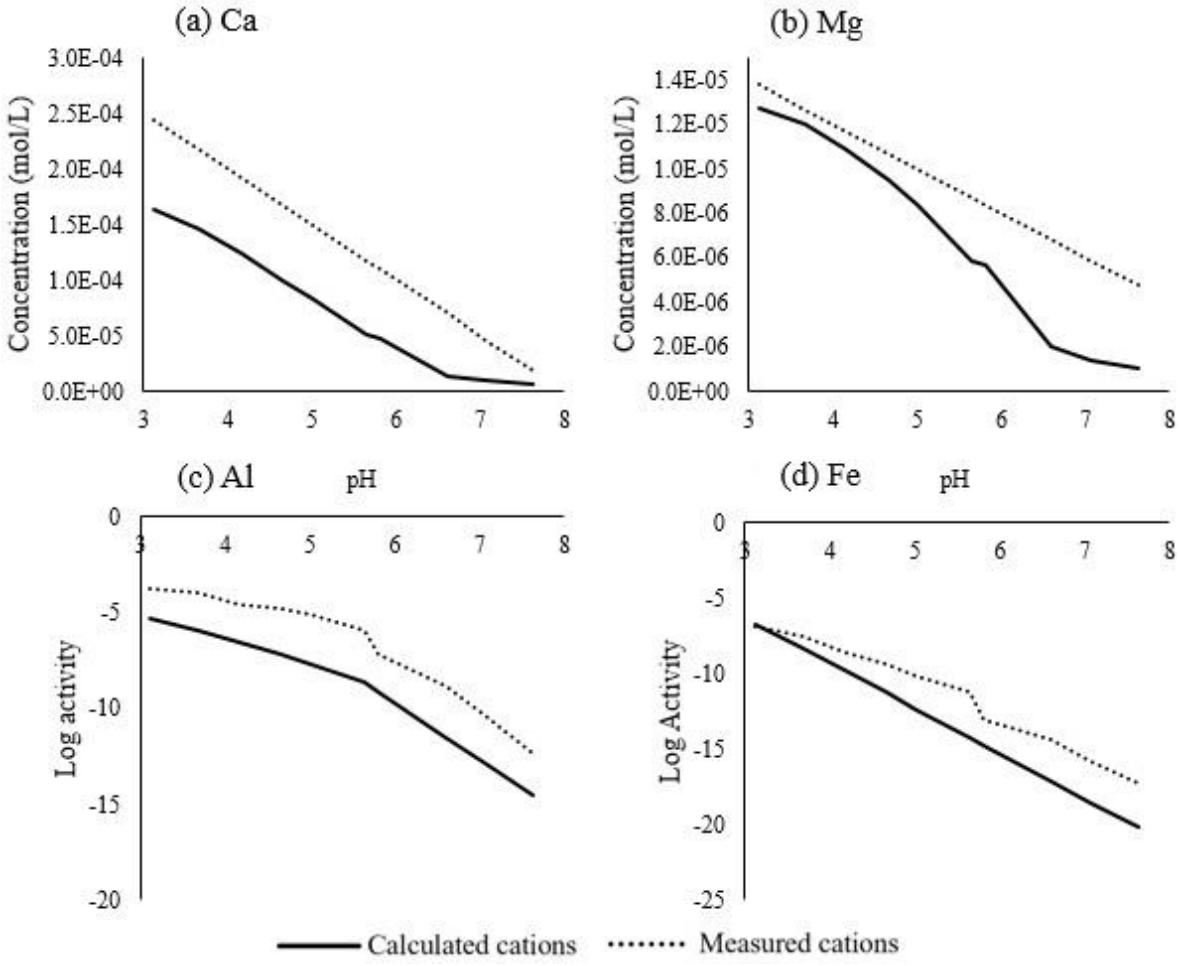

Figure 6. Comparison of leached Ca/Mg concentrations and Al/Fe activities for the untreated sediment, either calculated or determined from measurements by Mizutani et al. (2017), used in separate Visual MINTEQ models.

3.3 Results and Discussion

3.3.1 Changes in sediment properties

As a result of the AOD and H_2O_2 treatment processes, targeted components (Fe/Al-oxyhydroxides for AOD and SOM for H_2O_2) were greatly depleted relative to the untreated sediment (Figure 7). Amorphous Fe was reduced by 73-80% when the sediment

had undergone the AOD and AOD-H_2O_2 treatment processes, whereas amorphous Al was reduced by 95% (Figure 7a). Although amorphous Al was not targeted by the H_2O_2 procedure, the H_2O_2 treated sediment was 35% depleted in amorphous Al, presumably due to Al associated with SOM in the sediment being removed during the H_2O_2 treatment process (Tipping et al., 2002; Yang et al., 2013). Amorphous Fe seemed enriched in the H_2O_2 sediment relative to the untreated sediment (Figure 7a); however, the standard deviation of both measurements overlapped, so it is likely that amorphous Fe was not significantly affected by the H_2O_2 procedure. DCB extractable Fe, which includes both amorphous and some crystalline Fe, was less affected by the AOD and AOD-H_2O_2 treatment processes, with 60-62% removal (Figure 7b). Similar to AOD-Fe, the H_2O_2 treatment did not significantly effect DCB-Fe (Figure 7b). SOC content also varied according to treatment type, with 84-90% removal from the H_2O_2 and AOD- H_2O_2 treated sediments, and 61% removal for the AOD treatment (Figure 7c). Although the AOD treatment did not target SOC, the large SOC depletion was a result of the leaching and degradation of SOC associated with amorphous Fe/Al-oxyhydroxides in the sediment during treatment (Fisher-Power et al., 2016; Tipping et al., 2002; Yang et al., 2013).

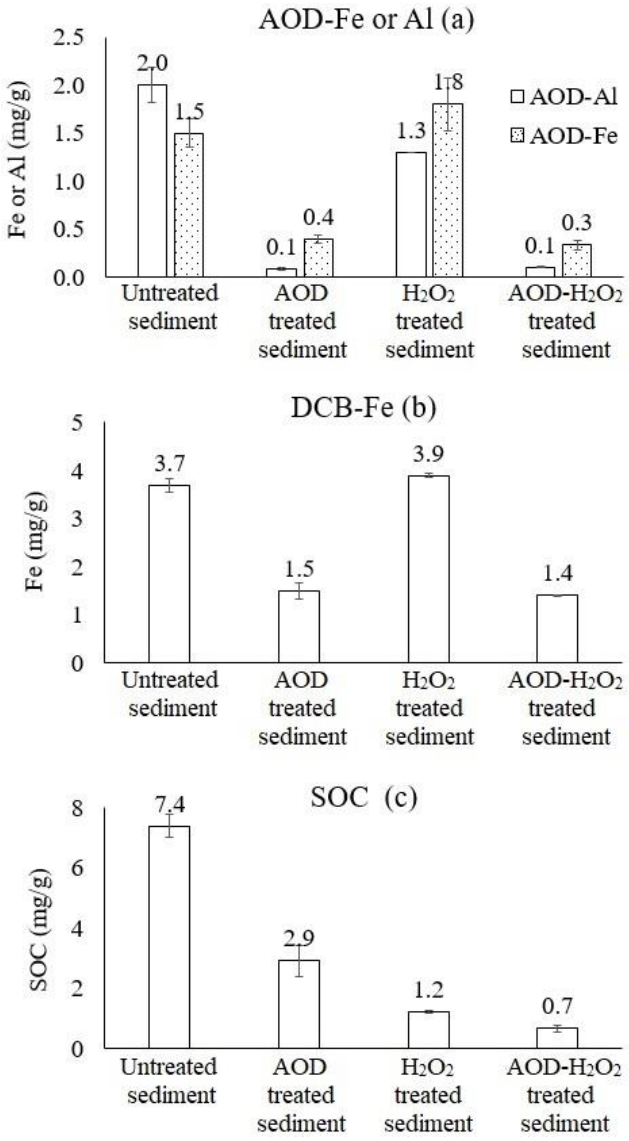

Figure 7. Proportions of AOD-Al and Fe, DCB-Fe, and SOC in the sediments.

XRD spectra of each sediment indicated that although large changes occurred in Fe/Al-oxyhydroxide and SOC concentrations in the treated sediments, mineralogy remained generally unchanged (Figure S5, SI). Grain size distributions were largely unaffected (Figure S6, SI), with a greater proportion of clay sized particles in the H_2O_2

and AOD-H_2O_2 treated sediments due to the breakdown of particles during the H_2O_2 treatment process (Table S3, SI). pH of the sediments varied from 5.07-6.30 (Table S3, SI) presumably caused by variations in SOM and Fe/Al-oxyhydroxide content (Xu et al., 2012). Concentrations of exchangeable Ca and Mg varied due to the treatment processes (Table S3, SI) (a result of the degradation and removal of Fe/Al-oxyhydroxides and SOM); however, Ca and Mg leaching is mainly controlled by cation exchange capacity (Fisher-Power et al., 2016; Hendershot and Duquette, 1986), therefore each variation of the sediment would have leached similar concentrations of Ca and Mg under the experimental conditions. The originally sorbed Cu and Zn concentrations varied with sediment treatment as well (Table S3, SI); the AOD and AOD-H_2O_2 treated sediment had all of its extractable Cu removed, indicating that the AOD process was also effective in removing Cu ions. The same was not true for Cu in the H_2O_2 treatment, in which extractable Cu increased, indicating that more Cu was readily desorbed due to the degradation of SOM sites in the sediment. An increase in extractable Zn was observed for all treated sediments (Table S3, SI), a result of the degradation of Fe/Al-oxyhydroxides and SOM in the sediment in which Zn would typically more strongly adsorb.

Leached DOC concentrations from each sediment in the batch experiments indicated that DOM leaching was dependent on pH and sediment type (Figure 8). At pH < 5.5, the untreated, AOD treated, and H_2O_2 treated sediments had similar leached DOC concentrations (5-10 mg/L), with gradual decrease with increasing pH for 3 to 5.5. After minimum concentrations in the mid pH range 5.5 to 6, the untreated sediment had a large increase in leached DOC, up to 25 mg/L, as pH approached 8. This was consistent with

our previous adsorption experiments, where DOC release was the greatest at high pH due to the deprotonation of SOM (Fisher-Power et al., 2016; Mizutani et al., 2017). The same, however, was not observed for AOD and H_2O_2 treated sediments, as DOC leaching increased from pH 6 to 8 only slightly, indicating that excess DOC had been removed during the treatment processes. This was consistent with the removal of SOC from the sediments as indicated in Figure 7c. The AOD-H_2O_2 treated sediment had the lowest leached DOC concentrations consistently across the pH range, never more than 3.5 mg/L, indicating that undergoing both sediment treatment processes removed much of the leachable DOC from the sediments.

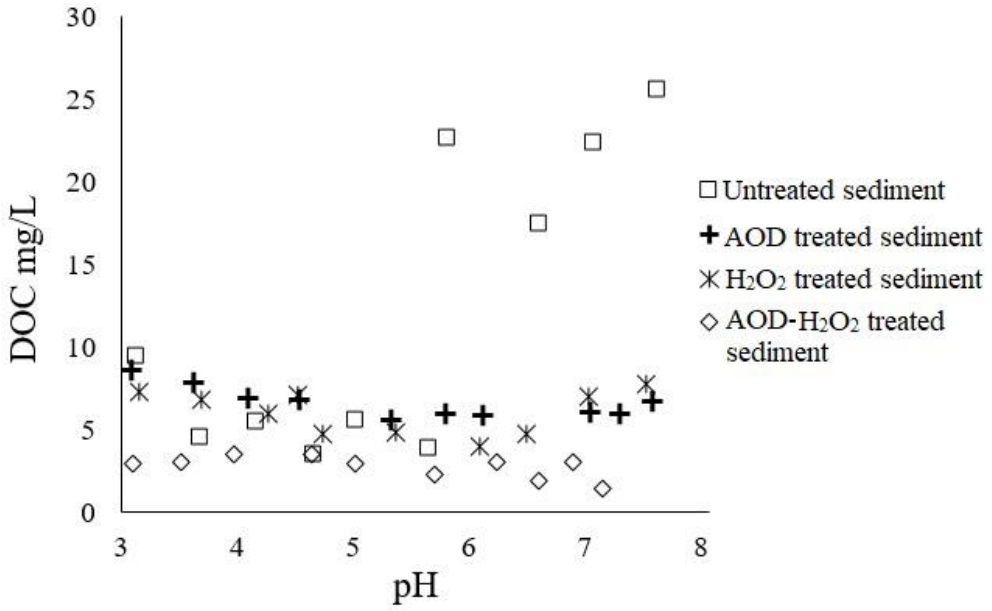

Figure 8. Concentrations of DOC leached from each sediment during the adsorption experiments.

3.3.2 Adsorption experiment results

Adsorption of Cu and Zn was dependent on pH and sediment type (Figure 9). For all the experiments, Cu adsorption was greater than Zn adsorption, and adsorption of both Cu and Zn increased with increasing pH. This was consistent with numerous reports of preferential adsorption of Cu over Zn in competitive circumstances (Agbenin and Olojo, 2004; Elliott et al., 1986; Fisher-Power et al., 2016; Gomes et al., 2001; Pérez-Novo et al., 2008). The untreated sediment generally adsorbed the most Cu and Zn, with greater differences in adsorption for the treated sediments observed for Cu than Zn. At pH 3 for the untreated sediment, Cu adsorption was at its minimum around 40%. A sharp edge occurred for Cu between pH 4 to 5, where adsorption increased from around 45 to 90% adsorbed. Cu adsorption continued to rise from pH 5-6 where it reached a maximum around 95%, however, adsorption decreased to 87% as pH increased to 8. This decrease and the overall trend was more distinct in the log k_D data (Figure 9b). Zn adsorption was very low at pH 3 (<5%), and rose gradually from pH 4 to 7 up to 87% where it reached a stable plateau as pH increased to 8 (Figure 9c). The log k_D data for Zn emphasized these trends, and unlike the Cu data, no decrease in adsorption was observed for Zn after a maximum was reached (Figure 9d). Similar adsorption edge behavior was observed for Cu and Zn adsorption to a savanna alfisol by Agbenin and Olojo (2004), and in previous work (Mizutani et al., 2017), identical adsorption experiments were conducted on the untreated sediment and the results from both were found to be the same (Figure S7, SI).

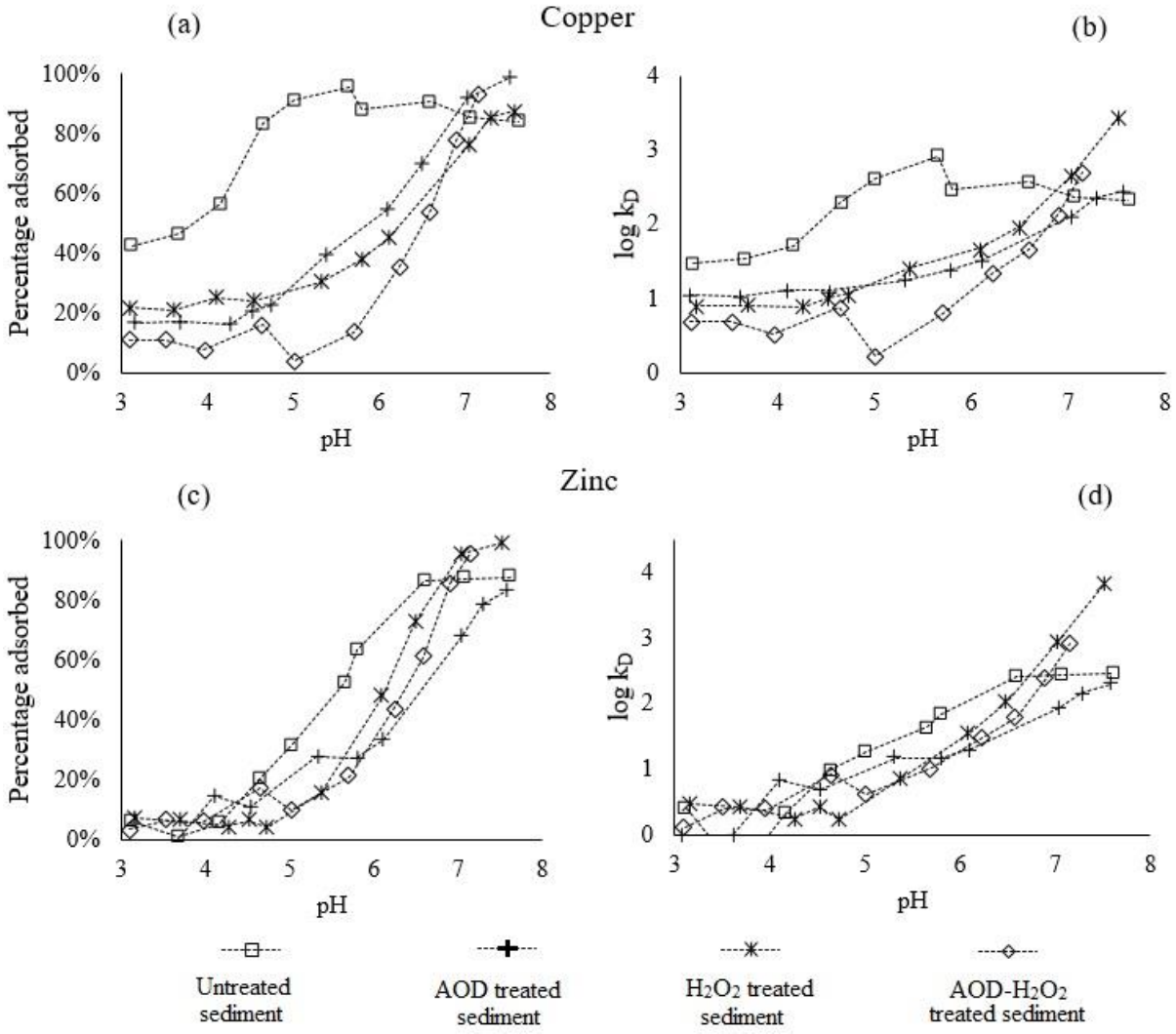

Figure 9. Experimentally determined Cu (a and b) and Zn (c and d) percentage adsorbed (a and c) and log k_D (b and d) for each sediment in the 3-8 pH range.

We previously determined that at pH < 6.5, SSOM was the dominant adsorbent for Cu and Zn, whereas Fe/Al-oxyhydroxides were more important when pH was > 6.5 (Fisher-Power et al., 2016; Mizutani et al., 2017). Additionally, leached cations suppressed Cu and Zn adsorption, most influentially at low pH (< 6) where greater leached concentrations provided more competition for adsorptive sites in the sediment

(Fisher-Power et al., 2016; Mizutani et al., 2017). Leached DOM tended to decrease Cu adsorption when pH was > 6, due to the formation of aqueous Cu-DOM complexes at high DOC concentrations (Fisher-Power et al., 2016; Mizutani et al., 2017), which was consistent with the results of this study where Cu adsorption decreased after pH 6, but Zn was unaffected. It has been widely reported that Cu has a greater affinity for SSOM and DOM than Zn, also consistent with our experimental observations (e.g., Agbenin and Olojo, 2004; McBride et al., 1997; Pérez-Novo et al., 2008).

The treated sediments typically had reduced adsorption relative to the untreated sediment, to a much greater extent for Cu than Zn (Figure 9). The sediment treated by AOD, which had amorphous Fe/Al-oxyhydroxides depleted, adsorbed much less Cu at pH range 3-7. Cu adsorption was reduced from 40% in the untreated sediment to 16% in the AOD treated sediment at pH 3, and reduced up to 55% in the mid pH range 4-6. For the AOD treated sediment adsorption maximum of Cu did not occur to until pH 8, rather than by pH 5 in the untreated sediment. Additionally, there was no decrease in Cu adsorption at pH > 6 as seen in the untreated sediment, as leached DOC concentrations were much lower for the AOD treated sediment (Figure 8). Zn adsorption was less effected by the AOD treatment, and was similarly low for the AOD treated sediment as it was for the untreated sediment at pH 3-5, but reduced in comparison from pH 5-7. In this range, Fe/Al-oxyhydroxides become more and more important in adsorbing Zn, and their removal led to the observed decrease. The overall decreases in Cu and Zn adsorption for the AOD treated sediment were attributable to depleted Fe/Al-oxyhydroxides in the higher pH range 6-8 (where metal oxyhydroxides are the dominant adsorbent), but also

due to reduced SSOM concentrations that occurred during the AOD process in low pH range 3-6 (Figure 7c).

Interestingly, the sediment treated by H_2O_2 to deplete organics had similar reduction of Cu adsorption as the AOD treated sediment (Figure 9 a and b). This indicated that much of the sediment's SSOM active in Cu adsorption was removed not only by the H_2O_2 process (which targeted SOM), but also by the AOD process (Figure 7b). Though the reduction in Cu adsorption was explained by SSOM depletion for the lower pH range > 6.5 for the H_2O_2 treated sediment, adsorption maximum was not reached until pH 7.5, where Fe/Al-oxyhydroxides were likely the main adsorbing phase. In the H_2O_2 treated sediment, significant concentrations of amorphous Al were removed (Figure 7a), accounting for this reduction in Cu adsorption from pH 6.5 to 7.5. This again demonstrated that the treatment processes were not independent of one another, and removing either Fe/Al-oxyhydroxides or SOM from the sediment consequently caused reduction in the other as well, leading to large effects on adsorption. Zn adsorption was similar for the AOD and H_2O_2 treated sediments from pH 3-6, but thereafter Zn adsorption was greater for the H_2O_2 treated sediment and similar to the untreated sediment, as lesser proportions of Fe/Al-oxyhydroxides were removed, and therefore were available as adsorptive sites. In previous studies where natural sediment was treated by H_2O_2 to remove organic matter, Cu was greatly affected by the removal of SOM in comparison to Zn (Agbenin and Olojo, 2004; Pérez-Novo et al., 2008), consistent with our results.

The AOD-H_2O_2 treated sediment, which had both Fe/Al-oxyhydroxides and SOM depleted, had the lowest Cu and Zn adsorption of all the sediments, but reached the same maximum adsorption values at pH 8. This was a result of the removal of adsorptive sites on SSOM and Fe/Al-oxyhydroxides due to undergoing both treated processes, and therefore having the greatest proportions of Fe/Al-oxyhydroxide and SOM removed (Figure 7). Again, Cu adsorption was more affected by these changes, reduced up to 75% from pH 3-7 in comparison to the untreated sediment, whereas Zn was only reduced up to 30% from pH 5-7.

A sediment was also treated to either deplete SOM by H_2O_2 treatment or metal oxyhydroxides by AOD treatment in a similar study, and it was reported that removing SOM reduced the distribution coefficient for Cu 40 times, but for Zn only by half; whereas removal of amorphous metal oxides reduced Cu distribution coefficient 100 times and 20 times for Zn (Agbenin and Olojo, 2004). We did not observe a much larger decrease in Cu and Zn adsorption when our sediment was treated by AOD in comparison to H_2O_2, indicating SSOM was of a relatively greater importance than the metal oxyhydroxides in our sediment compared to theirs. A limitation of their study was that the treated sediments were not characterized, and therefore the removal efficiency of SOM and Fe/Al-oxyhydroxides was not reported. It is also unclear if the treatment processes were independent of one another or if any other properties of the sediment changed. The results of Agbenin and Olojo (2004) suggested that the processes were independent of one another, with metal oxyhydroxide removal causing the greatest reduction, different from our results.

In another study, Coston et al. (1995) found that some of the natural coatings of amorphous and crystalline Fe and Al on quartz grains in a sediment were resistant to chemical extraction processes, and coating thicknesses were reduced by chemical treatments rather than complete removal. This suggests that a portion of the Fe/Al-oxyhydroxides in our sediment were not depleted by the AOD treatment process (evident in Figure 7), and therefore still contributed to Cu and Zn adsorption. They found that Pb adsorption (similar to that of Cu) was decreased when grains with Fe and Al coatings were magnetically separated, but Zn adsorption was unaffected, suggesting that Fe/Al-oxyhydroxides concentrations are not as sensitive for Zn adsorption as Cu and Pb (Coston et al., 1995). Other studies have documented that Cu was selectively adsorbed to Fe/Al-oxyhydroxides over Zn, and Zn was instead dominantly adsorbed to SSOM (Forbes et al., 1976; Grimme, 1968; Kinniburgh et al., 1976; McKenzie, 1980; Peng et al., 2018). Although Zn adsorption was not as affected by Fe/Al-oxyhydroxide depletion as Cu in our experiments, Zn adsorption was still significantly decreased, different than Coston et al. (1995) observed. This could possibly be linked to the simultaneous reduction of SSOM by the AOD treatment process, which may be responsible for the reduced Zn adsorption; as Coston et al. (1995)'s sediment did not contain significant organics. It also is possible SSOM compensated for depleted Fe/Al-oxyhydroxide concentrations in our sediment by playing a more important role in Cu and Zn adsorption.

3.3.3 Modelling results

Model simulated adsorption was strongly impacted by the method used to estimate cation concentration (Figure 10 for Cu, Figure 11 for Zn). Large discrepancies were observed between the two methods, as well as each method and the experimental results. RMSE values for each method are displayed in Table 1, with lower values indicating a better model fit to experimental data. Generally, using measured ion concentrations provided a better fit than using calculated concentrations, however there were some exceptions. For the untreated sediment, Cu and Zn adsorption was modelled much better by using measured concentrations (Table 1). Cu adsorption to the untreated sediment was over predicted in the pH range 3.5-5 using calculated cation concentrations, and adsorption maximum was predicted to occur at pH 4, whereas the experimental data suggested the maximum did not occur until pH 5 (Figure 10 a and b). This was a result of under-prediction of leached cation concentrations by the calculations, and therefore under prediction of the magnitude of competition for adsorptive sites. Using measured cation concentrations provided better fit to the Cu experimental data for the untreated sediment. Both models predicted a plateau after pH 5.5, consistent with experimental results, however, the model with calculated ions more accurately predicted the decrease in Cu adsorption due to DOM complexation. This is consistent with our previous study, where increased cation concentrations led to increased Cu adsorption, as a result of greater competition for binding sites on DOM rather than sites in the solid phase (Fisher-Power et al., 2016). Zn adsorption was also over-predicted from pH 3.5-6 by the model using calculated cation concentrations for the untreated sediment, again due to under-prediction

of cation concentrations (Figure 11, a and b). In contrast, using the model with measured concentrations under-predicted the experimental measured adsorption of Zn from pH 4-6, indicating that the model over-predicted the magnitude of competition against Zn for adsorptive sites in the sediment.

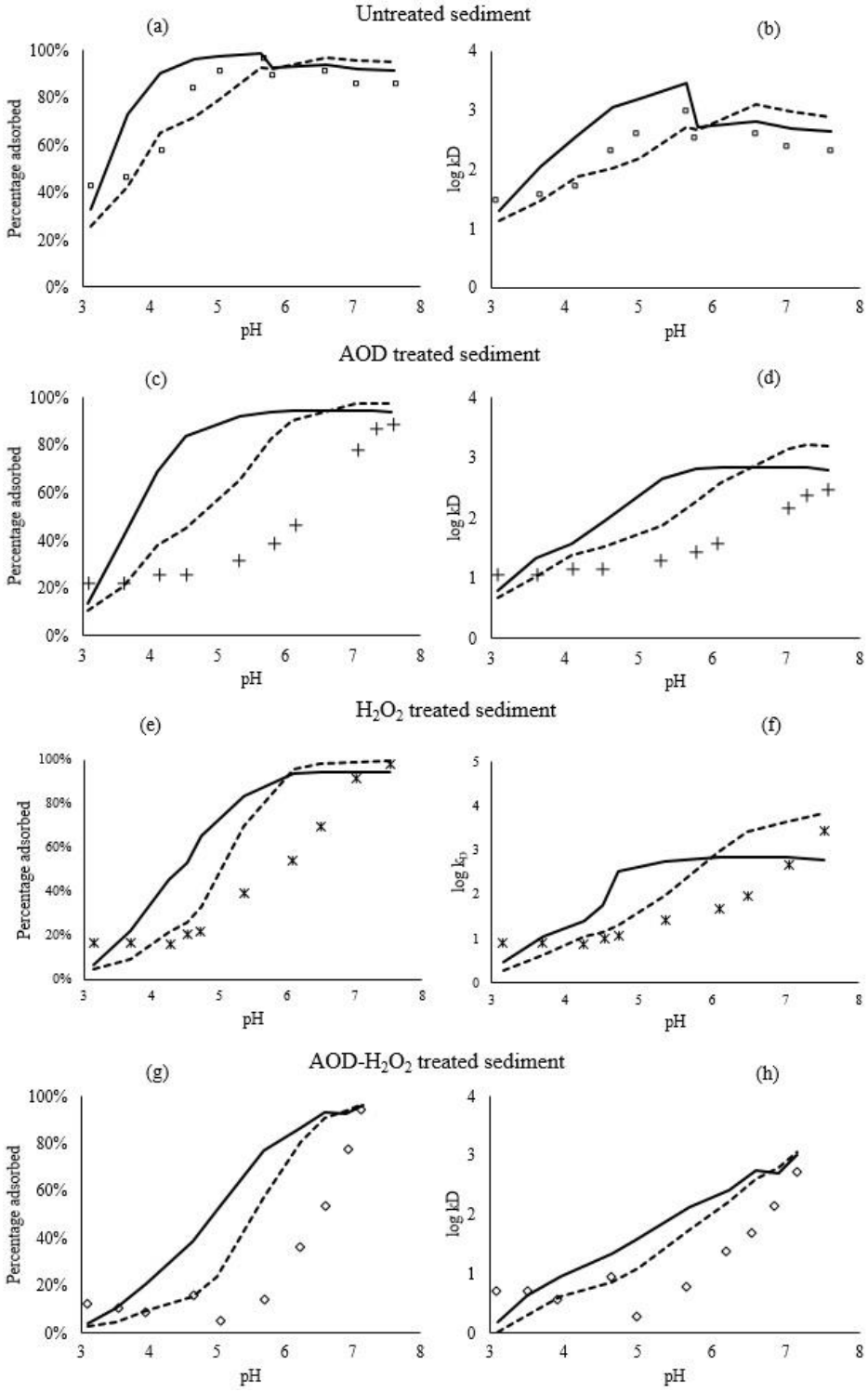

Figure 10. Visual MINTEQ calculated Cu adsorption for each sediment in the 3-8 pH range. Symbols are experimental results, solid lines represent the model with calculated cations, and dashed lines represent the model with measured cations.

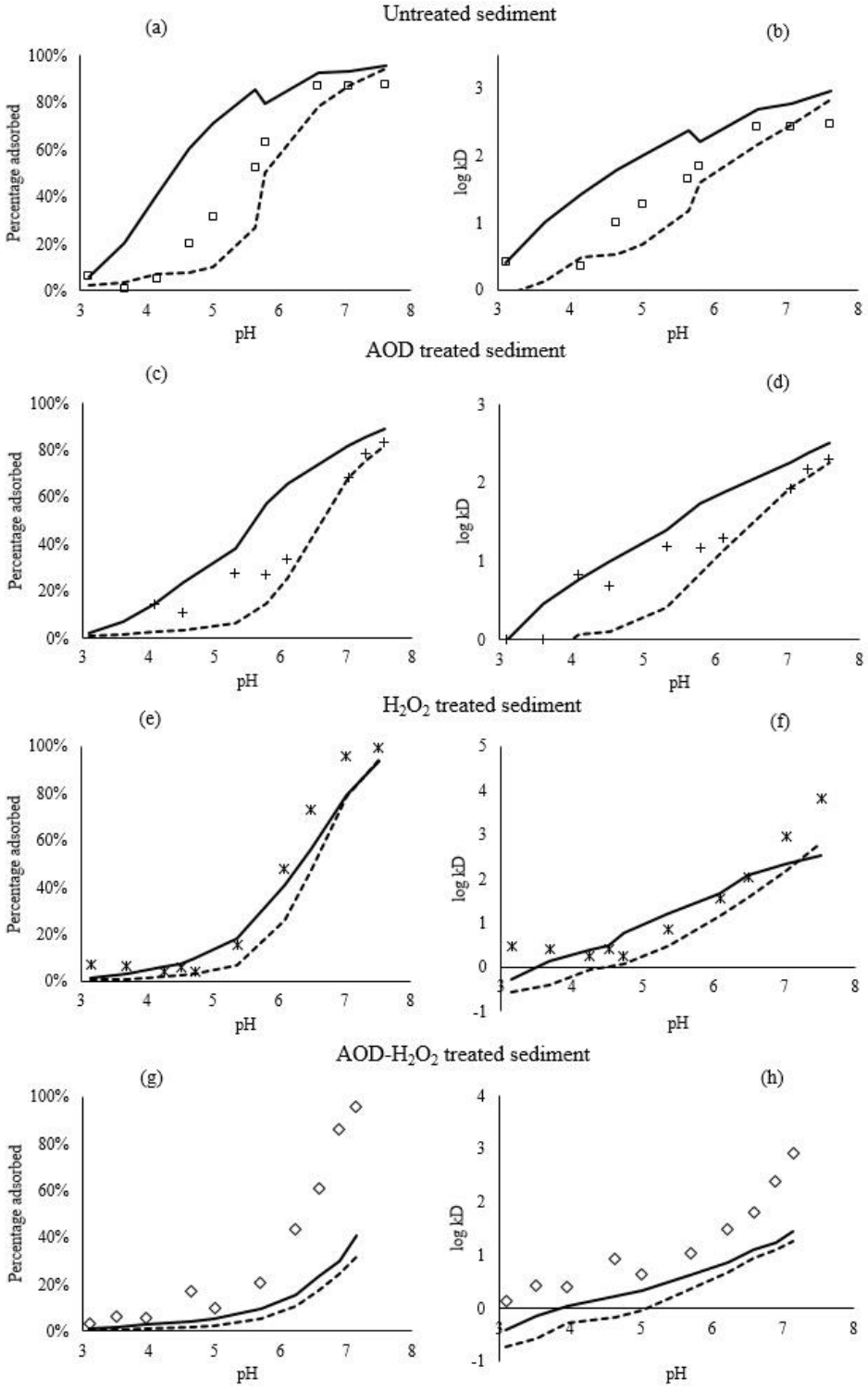

Figure 11. Visual MINTEQ calculated Zn adsorption for each sediment in the 3-8 pH range. Symbols are experimental results, solid lines represent the model with calculated cations, and dashed lines represent the model with measured cations.

Table 1. A comparison of calculated RMSEs between each model (either using measured or calculated cations) and experimental data for Cu and Zn adsorption. Lower values indicate a more appropriate model fit of the data.

	Copper				Zinc			
	% Adsorbed		Log k_D		% Adsorbed		Log k_D	
	Measured cations	Modelled cations	Measured cations	Modelled cations	Measured cations	Modelled cations	Measured cations	Modelled cations
Untreated sediment	0.10	0.17	1.45	2.52	0.13	0.15	1.81	5.94
AOD treated sediment	0.27	0.42	5.04	7.71	0.10	0.17	1.96	1.19
H_2O_2 treated sediment	0.21	0.30	5.77	7.44	0.13	0.09	4.19	3.16
AOD-H_2O_2 treated sediment	0.26	0.36	4.39	6.92	0.35	0.31	9.95	5.82

Model predicted Cu adsorption to the AOD treated sediment for both methods was less accurate, with strong over-prediction from pH 3.5-7 (Figure 10, c and d); to a greater extent for the calculated cations model (Table 1). This over-prediction indicated that Visual MINTEQ over-estimated the capability of adsorptive sites on SSOM in the lower pH range and Fe/Al-oxyhydroxides in the higher range, indicating that the AOD process removed many of the active sites on SSOM and Fe/Al-oxyhydroxides for Cu binding. This also suggested that some of the SSOM and Fe/Al-oxyhydroxides in the AOD treated sediment were not efficient as the SSOM and Fe/Al-oxyhydroxides in the untreated sediment in adsorbing Cu, likely because the treatment process changed their properties. Zn adsorption, which was less affected by the AOD treatment, was predicted similarly as it was for the untreated sediment; slightly over-predicted when modelled cations were

used, and slightly under-predicted when measured cations were used (Figure 11, c and d). This was again probably due to the calculations under predicting leached cation concentrations, whereas Visual MINTEQ over-predicted the magnitude of competition from the measured cations. Similar RMSE values were reported for the two methods (Table 1).

Similar to the AOD treated sediment, Cu adsorption for the H_2O_2 treated sediment was largely over-predicted by using calculated cation concentrations from pH 4-7, and by using measured cation concentrations from pH 5-7 (Figure 10, e and f). The over-prediction was again likely due to the model's over-prediction of the capability of the adsorptive sites on SSOM and Fe/Al-oxyhydroxides remaining in the H_2O_2 treated sediment, further suggesting that the properties of the SSOM and Fe/Al-oxyhydroxides were changed and they were not as effective as those in the untreated sediment for Cu adsorption. Conversely, model predicted Zn adsorption was reasonably accurate for the H_2O_2 treated sediment using either the calculated or measured cation concentrations (Figure 11, e and f). In this case, the model calculated cation concentrations matched the experimental data well (Table 1), with some under prediction from pH 6-8, whereas the measured cations data had stronger under-prediction from pH 5-8. The under-prediction in both methods indicated that Zn more readily adsorbed to SSOM and Fe/Al-oxyhydroxides than anticipated by the models, possibly again due to over-prediction of competitive cations for adsorption sites.

When both SOM and Fe/Al-oxyhydroxides were depleted, as in the AOD-H_2O_2 treated sediment, both methods over-predicted Cu adsorption, whereas both models

under-predicted Zn adsorption (Figures 10 and 11, g and h). Cu adsorption was more strongly over-predicted using calculated cation concentrations and for a greater pH range (3.5-7) in comparison to the model using measured cation concentrations (pH 5-7) (Figure 10, g and h). These discrepancies were a result of under-estimated cation concentrations using the calculated cation concentrations as well as over-estimation of the adsorption capability of the remaining Fe/Al-oxyhydroxide sites. The AOD-H_2O_2 sediment had undergone processes to deplete both SOM and Fe/Al-oxyhydroxides, again suggesting that most of the reactive adsorptive sites were removed, leaving behind SSOM and Fe/Al-oxyhydroxides which were not effective for adsorbing Cu. In contrast, Zn adsorption was under-predicted for the entire pH range, to a greater extent when using the measured cation concentrations (Figure 11, g and h). Under-prediction was the greatest from pH 5-7, where Fe/Al-oxyhydroxides were important for adsorbing Zn, suggesting that the Fe/Al-oxyhydroxides remaining in the sediment were more effective for Zn adsorption than predicted by Visual MINTEQ models, and cation competition was not as important as anticipated.

For most of the cases, using measured cation concentrations provided more accurate predictions. Models were more accurate for the untreated sediment and less applicable for the treated sediments. This suggested that the inaccurate model predictions for the treated sediments arose due to altered properties of SOM and Fe/Al-oxyhydroxides as a result of the treatment processes, and the databases used which typically describe natural adsorbents were no longer suitable. In addition, the component additivity modelling approach used, which assumes that sorbents do not interact with each other, all sorbent

surfaces are available for adsorption, and only single solute-sorbent complexes are formed (Alessi and Fein, 2010) may not have been entirely valid. SOM and Fe/Al-oxyhydroxides in our sediment may have existed as coatings and have been naturally associated with one another, and therefore ternary complexes between Cu/Zn, SOM, and Fe/Al-oxyhydroxides may have formed (Bradl, 2004; Peng et al., 2018), which the models did not account for. In future work, it is recommended that a general composite modelling approach (which does not require characterization of soil components) is attempted to improve model fit.

3.3.4 Environmental implications

Heavy metals in subsurface environments may travel through sediments containing SOM and Fe/Al-oxyhydroxides. Our results indicated that Cu adsorption was strongly dependent on sediment composition, greatly reduced due to organic matter depletion at pH <6.5, and due to Fe/Al-oxyhydroxide depletion when pH >6.5, whereas Zn was less effected. Experimental observations were typically better simulated by using experimentally determined concentrations of leached cations rather than calculated cation concentrations, suggesting that the calculated concentrations could be inaccurate. The models also indicated that the SSOM and Fe/Al-oxyhydroxide adsorptive sites remaining in the treated sediments were not as effective as those in untreated sediment for Cu adsorption, suggesting changes in the properties of SSOM and Fe/Al-oxyhydroxides. However, the SSOM and Fe/Al-oxyhydroxides in the treated sediments were still effective for Zn adsorption. Results of our adsorption experiments demonstrated that SOM and Fe/Al-oxyhydroxides could have a strong influence on heavy metal adsorption,

and adsorption by natural sediments may be a potential abundant and inexpensive remediation for contaminated sites.

The SOM and Fe/Al-oxyhydroxide removal processes used in this study were not 100% efficient at extracting their targeted components and also were not independent of one another (i.e. treatment to remove SOM also depleted Fe/Al-oxyhydroxides, and vice versa). Therefore, in future work it is recommended to explore a similar but opposite approach; instead of removing SOM and Fe/Al-oxyhydroxides from sediment, SOM and Fe/Al-oxyhydroxides could be systematically added in various concentrations to a mineral matrix. This method may more clearly determine the individual and synergistic influence of SOM and Fe/Al oxyhydroxides on heavy metal adsorption. This approach may also improve model predictions as the SOM or Fe/Al-oxyhydroxides would not be degraded in this method, and therefore more accurately be described by commonly used solid phase adsorptive databases.

3.4 References

Agbenin, J.O., Olojo, L.A., 2004. Competitive adsorption of copper and zinc by a Bt horizon of a savanna Alfisol as affected by pH and selective removal of hydrous oxides and organic matter. Geoderma 119, 85–95. doi:http://dx.doi.org/10.1016/S0016-7061(03)00242-8

Alessi, D.S., Fein, J.B., 2010. Cadmium adsorption to mixtures of soil components: Testing the component additivity approach. Chem. Geol. 270, 186–195. doi:10.1016/j.chemgeo.2009.11.016

Bradl, H.B., 2004. Adsorption of heavy metal ions on soils and soils constituents. J. Colloid Interface Sci. 277, 1–18. doi:10.1016/j.jcis.2004.04.005

Cappuyns, V., Swennen, R., 2008. The use of leaching tests to study the potential mobilization of heavy metals from soils and sediments: A comparison. Water. Air. Soil Pollut. 191, 95–111. doi:10.1007/s11270-007-9609-4

Coston, J.A., Fuller, C.C., Davis, J.A., 1995. Pb2+ and Zn2+ adsorption by a natural aluminum-and iron-bearing surface coating on an aquifer sand. Geochim. Cosmochim. Acta 59, 3535–3547. doi:10.1016/0016-7037(95)00231-N

Elliott, H., Liberati, M., Huang, C., 1986. Competitive Adsorption of Heavy Metals by Soils. J. Environ. Qual. 15, 214–219. doi:doi:10.2134/jeq1986.00472425001500030002x

Fisher-Power, L.M., Cheng, T., Rastghalam, Z.S., 2016. Cu and Zn adsorption to a heterogeneous natural sediment: Influence of leached cations and natural organic matter. Chemosphere 144, 1973–1979. doi:10.1016/j.chemosphere.2015.10.109

Forbes, E.A., Posner, M.A., Quirk, J.P., 1976. The specific adsorption of divalent Cd, Co, Cu, Pb, and Zn on goethite. Eur. J. Soil Sci. 27, 154–166.

Gomes, P.C., Fontes, M.P.F., da Silva, A.G., de S. Mendonça, E., Netto, A.R., 2001. Selectivity Sequence and Competitive Adsorption of Heavy Metals by Brazilian Soils. Soil Sci. Soc. Am. J. 65, 1115. doi:10.2136/sssaj2001.6541115x

Grimme, H., 1968. Die Adsorption von Mn, Co, Cu und Zn durch Goethit aus verdünnten Lösungen. J. Plant Nutr. Soil Sci. 121, 58–65.

Gustafsson, J.P., 2010. Visual MINTEQ Version 3.1.

Gustafsson, J.P., 2001. Modeling the Acid–Base Properties and Metal Complexation of Humic Substances with the Stockholm Humic Model. J. Colloid Interface Sci. 244, 102–112. doi:10.1006/jcis.2001.7871

Gustafsson, J.P., Tiberg, C., Edkymish, A., Kleja, D.B., 2011. Modelling lead (II) sorption to ferrihydrite and soil organic matter. Environ. Chem. 8, 485–492. doi:10.1071/EN11025

Hendershot, W., Duquette, M., 1986. A Simple Barium Chloride Method for Determining Cation Exchange Capacity and Exchangeable Cations. Soil Sci. Soc. Am. J. 50, 605–608.

Jackson, M.L., 1958. Soil Chemical Analysis. Prentice-Hall Inc., Englewood Cliffs, NJ.

Karamalidis, A., Dzombak, D., 2010. Surface complexation modeling: Gibbsite. Wiley & Sons, New York.

Kinniburgh, D.G., Jackson, M.L., Syers, J.K., 1976. Adsorption of Alkaline Earth, Transition, and Heavy Metal Cations by Hydrous Oxide Gels of Iron and Aluminum. Soil Sci. Soc. Am. J. 40, 796–799.

Lumsdon, D.G., 2004. Partitioning of organic carbon, aluminium and cadmium between solid and solution in soils: Application of a mineral-humic particle additivity model. Eur. J. Soil Sci. 55, 271–285. doi:10.1111/j.1365-2389.2004.00599.x

McBride, M., Sauve, S., Hendershot, W., 1997. Solubility control of Cu, Zn, Cd and Pb in contaminated soils. Eur. J. Soil Sci. 48, 337–346. doi:10.1111/j.1365-2389.1997.tb00554.x

McKeague, J.A., Day, J.H., 1966. Dithionite- and Oxalate-Extractable Fe and Al as Aids in Differentiating Various Classes Of Soils. Can. J. Soil Sci. 46, 13–22. doi:10.4141/cjss66-003

McKenzie, R.M., 1980. The adsorption of lead and other heavy metals on oxides of manganese and iron. Aust. J. Soil Res. 18, 61–73.

Mehra, O.P., 1958. Iron Oxide Removal from Soils and Clays by a Dithionite-Citrate System Buffered with Sodium Bicarbonate. Clays Clay Miner. 7, 317–327. doi:10.1346/CCMN.1958.0070122

Mizutani, K., Fisher-Power, L.M., Shi, Z., Cheng, T., 2017. Cu and Zn adsorption to a terrestrial sediment: Influence of solid-to-solution ratio. Chemosphere 175, 341–349. doi:10.1016/j.chemosphere.2017.02.069

Peng, L., Liu, P., Feng, X., Wang, Z., Cheng, T., Liang, Y., Lin, Z., Shi, Z., 2018. Kinetics of heavy metal adsorption and desorption in soil: Developing a unified model based on chemical speciation. Geochim. Cosmochim. Acta 224, 282–300. doi:10.1016/j.gca.2018.01.014

Pérez-Novo, C., Pateiro-Moure, M., Osorio, F., Nóvoa-Muñoz, J.C., López-Periago, E., Arias-Estévez, M., 2008. Influence of organic matter removal on competitive and

noncompetitive adsorption of copper and zinc in acid soils. J. Colloid Interface Sci. 322, 33–40. doi:10.1016/j.jcis.2008.03.002

Shi, Z., Allen, H.E., Di Toro, D.M., Lee, S.Z., Flores Meza, D.M., Lofts, S., 2007. Predicting cadmium adsorption on soils using WHAM VI. Chemosphere 69, 605–612. doi:10.1016/j.chemosphere.2007.03.001

Shi, Z., Allen, H.E., Di Toro, D.M., Lee, S.Z., Harsh, J.B., 2013. Predicting PbII adsorption on soils: The roles of soil organic matter, cation competition and iron (hydr)oxides. Environ. Chem. 10, 465–474. doi:10.1071/EN13153

Shuman, L.M., 1977. Adsorption of Zn by Fe and Al Hydrous Oxides as Influenced by Aging and pH. Soil Sci. Soc. Am. J. 41, 703–706.

Tipping, E., Rey-Castro, C., Bryan, S.E., Hamilton-Taylor, J., 2002. Al(III) and Fe(III) binding by humic substances in freshwaters, and implications for trace metal speciation. Geochim. Cosmochim. Acta 66, 3211–3224. doi:10.1016/S0016-7037(02)00930-4

Wang, S., Mulligan, C.N., 2006. Natural attenuation processes for remediation of arsenic contaminated soils and groundwater. J. Hazard. Mater. 138, 459–470. doi:10.1016/j.jhazmat.2006.09.048

Wang, X., Liu, F., Tan, W., Li, W., Feng, X., Sparks, D.L., 2013. Characteristics of phosphate adsorption-desorption onto ferrihydrite: Comparison with well-crystalline fe (Hydr)oxides. Soil Sci. 178, 1–11. doi:10.1097/SS.0b013e31828683f8

Weng, L., Temminghoff, E.J.M., Van Riemsdijk, W.H., 2001. Contribution of individual sorbents to the control of heavy metal activity in sandy soil. Environ. Sci. Technol. 35, 4436–4443. doi:10.1021/es010085j

Xu, C., Guo, L., Dou, F., Ping, C.L., 2009. Potential DOC production from size-fractionated Arctic tundra soils. Cold Reg. Sci. Technol. 55, 141–150. doi:10.1016/j.coldregions.2008.08.001

Xu, R., Zhao, A., Yuan, J., Jiang, J., 2012. pH buffering capacity of acid soils from tropical and subtropical regions of China as influenced by incorporation of crop straw biochars. J. Soils Sediments 12, 494–502. doi:10.1007/s11368-012-0483-3

Yang, Y., Saiers, J.E., Barnett, M.O., 2013. Impact of interactions between natural organic matter and metal oxides on the desorption kinetics of uranium from heterogeneous colloidal suspensions. Environ. Sci. Technol. 47, 2661–2669. doi:10.1021/es304013r

Chapter 4. Summary

SOM and Fe/Al-oxyhydroxides in sediment have been found to have significant effects on contaminant transport, however, their individual and synergistic influence when coexisting in natural subsurface environments is little known. The goal of this thesis was to explore the influences of SOM and Fe/Al-oxyhydroxides on two different types of groundwater contaminants in two separate projects. The first project explored how ENP transport was effected by SOM and Fe/Al-oxyhydroxides, whereas the second project focused on heavy metal adsorption. In both projects, the same natural sediment was chemically treated to remove either SOM, Fe/Al-oxyhydroxides, or both; and each was used in systematic experiments to determine their individual and synergistic effects.

The effects of SOM and Fe/Al-oxyhydroxides on $nTiO_2$ transport was explored in Chapter 2 by performing column experiments. It was found that $nTiO_2$ transport was strongly influenced by SOM and Fe/Al-oxyhydroxides. In experiments with influent pH=5, positively-charged $nTiO_2$ was attracted to negatively-charged minerals and SOM, and therefore transport was near zero. Leached DOM slightly enhanced $nTiO_2$ transport by adsorbing onto $nTiO_2$ surface, reversing ZP to negative, and stabilizing it in suspension. In experiments on the untreated sediment with influent pH=9, negatively charged minerals and SOM repelled negatively-charged $nTiO_2$, and therefore transport was much higher. Despite this, when SOM or Fe/Al-oxyhydroxides were depleted, $nTiO_2$ transport was again low, a result of pH buffering by the sediments creating attractive zones between $nTiO_2$ and Fe-oxyhydroxides in the sediment column. DOM was again found to adsorb to $nTiO_2$, stabilizing it in suspension. This research emphasized the

importance influence of SOM and Fe/Al-oxyhydroxides on ENP transport natural sediments, and demonstrated how the results of laboratory experiments using quartz sand may not representative of natural subsurface environments.

Chapter 3 focused on investigating how SOM and Fe/Al-oxyhydroxides influenced Cu and Zn adsorption to the same natural sediment using batch experiments. It was found that Cu adsorption was strongly dependent on SOM and Fe/Al-oxyhydroxide content, with effects to a lesser extent for Zn adsorption. Depleted SOM resulted in decreased adsorption when pH was < 6.5, whereas depleted Fe/Al-oxyhydroxides decreased adsorption when pH was > 6.5. Depletion of both SOM and Fe/Al-oxyhydroxides decreased adsorption to the greatest extent for the entire pH range. Surface complexation models suggested that adsorptive sites remaining in the treated sediments were degraded and not as efficient for Cu adsorption, but were still suitable for Zn. The results from this research demonstrated how heavy metal adsorption could be strongly influenced by SOM and Fe/Al-oxyhydroxides, and emphasized their importance when modelling heavy metal behavior in natural subsurface environments.

Some limitations were uncovered during both projects associated to the AOD and H_2O_2 sediment treatment processes. The treatments were generally successful at depleting their targeted components in both projects; however, there were some discrepancies between the properties of the treated sediments in Chapters 2 and 3. This was due to small modifications in the treatment process, as the procedure took place at a different time for each chapter. Separate characterizations were completed in each chapter to quantify the properties of the sediments each and account for these

discrepancies in the interpretation of each chapter's results. It was also found that SOM and Fe/Al-oxyhydroxides were often naturally associated with each other in the sediment. This resulted in partial depletion of the non-targeted component during treatment, which did not fully isolate one specific component at a time. An implication of these limitations was that the SOM and Fe/Al-oxyhydroxides were not totally and independently isolated from the sediment; and therefore, the results were complicated and not strictly due to the 100% removal of either SOM and/or Fe/Al-oxyhydroxides.

In future research, it is recommended that a different approach is used to address the limitations from these projects and reveal more information about the influences of SOM and Fe/Al-oxyhydroxides on contaminant transport. Instead of chemically treating a natural sediment to remove specific components, components could be added one at a time to a control substrate (such as quartz sand) to determine their individual and synergistic effects. A caveat of this approach is that the composed sediments cannot then be considered "natural"; however, this type of study could be very useful to help isolate the individual and synergistic effects of SOM and Fe/Al-oxyhydroxides.

Overall, both chapters revealed important controls on groundwater contaminant transport in natural sediments by SOM and Fe/Al-oxyhydroxides, and demonstrated how observed transport can greatly alter from predictions that do not consider their influence. Based upon these findings, it is recommended that the influences of SOM and Fe/Al-oxyhydroxides are considered when predicting contaminant transport in natural subsurface environments, and that SOM and Fe/Al-oxyhydroxides may be explored as potential tools for groundwater contaminant remediation.

References

Agbenin, J.O., Olojo, L.A., 2004. Competitive adsorption of copper and zinc by a Bt horizon of a savanna Alfisol as affected by pH and selective removal of hydrous oxides and organic matter. Geoderma 119, 85–95. doi:http://dx.doi.org/10.1016/S0016-7061(03)00242-8

Akaighe, N., Depner, S.W., Banerjee, S., Sharma, V.K., Sohn, M., 2012. The effects of monovalent and divalent cations on the stability of silver nanoparticles formed from direct reduction of silver ions by Suwannee River humic acid / natural organic matter. Sci. Total Environ. 441, 277–289. doi:10.1016/j.scitotenv.2012.09.055

Alessi, D.S., Fein, J.B., 2010. Cadmium adsorption to mixtures of soil components: Testing the component additivity approach. Chem. Geol. 270, 186–195. doi:10.1016/j.chemgeo.2009.11.016

Arias, M., Perez-Novo, C., Lopez, E., Soto, B., 2006. Competitive adsorption and desorption of copper and zinc in acid soils. Geoderma 133, 151–159. doi:10.1016/j.geoderma.2005.07.002

Bayat, A.E., Junin, R., Shamshirband, S., Tong Chong, W., 2015. Transport and retention of engineered Al2O3, TiO2, and SiO2 nanoparticles through various sedimentary rocks. Sci. Rep. 5, 14264. doi:10.1038/srep14264

Bekhit, H.M., Hassan, A.E., Harris-Burr, R., Papelis, C., 2006. Experimental and Numerical Investigations of Effects of Silica Colloids on Transport of Strontium in Saturated Sand Columns. Environ. Sci. Technol. 40, 5402–5408.

doi:10.1021/es060333h

Bermudez, E., Mangum, J.B., Wong, B.A., Asgharian, B., Hext, P.M., Warheit, D.B., Everitt, J.I., 2004. Pulmonary responses of mice, rats, and hamsters to subchronic inhalation of ultrafine titanium dioxide particles. Toxicol. Sci. 77, 347–357. doi:10.1093/toxsci/kfh019

Bonten, L.T.C., Groenenberg, J.E., Meesenburg, H., Vries, W. De, 2011. Using advanced surface complexation models for modelling soil chemistry under forests: Solling forest , Germany. Environ. Pollut. 159, 2831–2839. doi:10.1016/j.envpol.2011.05.002

Bradl, H.B., 2004. Adsorption of heavy metal ions on soils and soils constituents. J. Colloid Interface Sci. 277, 1–18. doi:10.1016/j.jcis.2004.04.005

Cai, L., Tong, M., Wang, X., Kim, H., 2014. Influence of Clay Particles on the Transport and Retention of Titanium Dioxide Nanoparticles in Quartz Sand. Environ. Sci. Technol. 48, 7323–7332. doi:dx.doi.org/10.1021/es5019652

Canadian Council of Ministers of the Environment, 2008. Canadian Water Quality Guidlines.

Cao, X., Ma, L.Q., Rhue, D.R., Appel, C.S., 2004. Mechanisms of lead, copper, and zinc retention by phosphate rock. Environ. Pollut. 131, 435–444. doi:10.1016/j.envpol.2004.03.003

Cappuyns, V., Swennen, R., 2008. The use of leaching tests to study the potential

mobilization of heavy metals from soils and sediments: A comparison. Water. Air. Soil Pollut. 191, 95–111. doi:10.1007/s11270-007-9609-4

Cerqueira, B., Covelo, E.F., Andrade, L., Vega, F.A., 2011. The influence of soil properties on the individual and competitive sorption and desorption of Cu and Cd. Geoderma 162, 20–26. doi:10.1016/j.geoderma.2010.08.013

Chen, G., Liu, X., Su, C., 2012. Distinct effects of humic acid on transport and retention of TiO2 rutile nanoparticles in saturated sand columns. Environ. Sci. Technol. 46, 7142–7150. doi:10.1021/es204010g

Chen, G., Liu, X., Su, C., 2011. Transport and retention of TiO2 rutile nanoparticles in saturated porous media under low-ionic-strength conditions: Measurements and mechanisms. Langmuir 27, 5393–5402. doi:10.1021/la200251v

Chen, M., Xu, N., Cao, X., Zhou, K., Chen, Z., Wang, Y., Liu, C., 2015. Facilitated transport of anatase titanium dioxides nanoparticles in the presence of phosphate in saturated sands. J. Colloid Interface Sci. 451, 134–143. doi:10.1016/j.jcis.2015.04.010

Cheng, T., Barnett, M.O., Roden, E.E., Zhuang, J., 2004. Effects of phosphate on uranium(VI) adsorption to goethite-coated sand. Environ. Sci. Technol. 38, 6059–6065. doi:10.1021/es040388o

Cornelis, G., Pang, L., Doolette, C., Kirby, J.K., McLaughlin, M.J., 2013. Transport of silver nanoparticles in saturated columns of natural soils. Sci. Total Environ. 463–

464, 120–130. doi:10.1016/j.scitotenv.2013.05.089

Coston, J.A., Fuller, C.C., Davis, J.A., 1995. Pb2+ and Zn2+ adsorption by a natural aluminum-and iron-bearing surface coating on an aquifer sand. Geochim. Cosmochim. Acta 59, 3535–3547. doi:10.1016/0016-7037(95)00231-N

Demayo, A., Taylor, M.C., 1981. Guidelines for Surface Water Quality, Inorganic Chemical Substances. Water Quality Branch, Inland Waters Directorate, Environment.

Derjaguin, B., Landau, L., 1941. Theory of the stability of strongly charged lyophobic sols and of the adhesion of strongly charged particles in solutions of electrolytes. Acta Phys. Chem. 14, 633–662.

Dişli, E., 2010. Batch and Column Experiments to Support Heavy Metals (Cu, Zn, and Mn) Transport Modeling in Alluvial Sediments Between the Mogan Lake and the Eymir Lake, Gölbaşı, Ankara. Ground Water Monit. Remediat. 30, 125–139. doi:10.1111/j1745

Duffus, J.H., 2002. Heavy Metals —a Meaningless Term? Pure Appl. Chem. Natl. Represent. Z. Bardodej (Czech Repub. J. Park (Korea F. J. R. Paumgartten (Brazil 74, 793–807. doi:10.1351/pac200274050793

Dunphy Guzman, K., Finnegan, M., Banfield, J., 2006. Influence of surface potential on aggregation and transport of itiania nanoparticles. Environ. Sci. Technol. 40, 7688–7693. doi:10.1021/es060847g

Elliott, H., Liberati, M., Huang, C., 1986. Competitive Adsorption of Heavy Metals by Soils. J. Environ. Qual. 15, 214–219. doi:doi:10.2134/jeq1986.00472425001500030002x

Erhayem, M., Sohn, M., 2014. Stability studies for titanium dioxide nanoparticles upon adsorption of Suwannee River humic and fulvic acids and natural organic matter. Sci. Total Environ. 468–469, 249–257. doi:10.1016/j.scitotenv.2013.08.038

Fan, J., He, X., Wang, D., 2013. Experimental study on the effects of sediment size and porosity on contaminant adsorption/desorption and interfacial diffusion characteristics. J. Hydrodyn. Ser. B 25, 20–26. doi:10.1016/S1001-6058(13)60334-0

Fang, J., Shan, X., Wen, B., Lin, J., Owens, G., 2009. Stability of titania nanoparticles in soil suspensions and transport in saturated homogeneous soil columns. Environ. Pollut. 157, 1101–1109. doi:10.1016/j.envpol.2008.11.006

Fang, J., Shan, X., Wen, B., Lin, J., Owens, G., Zhou, S., 2011. Transport of copper as affected by titania nanoparticles in soil columns. Environ. Pollut. 159, 1248–1256. doi:10.1016/j.envpol.2011.01.039

Federici, G., Shaw, B.J., Handy, R.D., 2007. Toxicity of titanium dioxide nanoparticles to rainbow trout (Oncorhynchus mykiss): Gill injury, oxidative stress, and other physiological effects. Aquat. Toxicol. 84, 415–430. doi:10.1016/j.aquatox.2007.07.009

Fisher-Power, L.M., Cheng, T., Rastghalam, Z.S., 2016. Cu and Zn adsorption to a

heterogeneous natural sediment: Influence of leached cations and natural organic matter. Chemosphere 144, 1973–1979. doi:10.1016/j.chemosphere.2015.10.109

Forbes, E.A., Posner, M.A., Quirk, J.P., 1976. The specific adsorption of divalent Cd, Co, Cu, Pb, and Zn on goethite. Eur. J. Soil Sci. 27, 154–166.

French, R.A., Jacobson, A.R., Kim, B., Isley, S.L., Penn, L., Baveye, P.C., 2009. Influence of ionic strength, pH, and cation valence on aggregation kinetics of titanium dioxide nanoparticles. Environ. Sci. Technol. 43, 1354–1359. doi:10.1021/es802628n

Frimmel, F., Niessner, R., 2010. Nanoparticles in the Water Cycle. Springer, Heidelberg. doi:10.1007/s13398-014-0173-7.2

Furman, O., Usenko, S., Lau, B.L.T., 2013. Relative importance of the humic and fulvic fractions of natural organic matter in the aggregation and deposition of silver nanoparticles. Environ. Sci. Technol. 47, 1349–1356. doi:10.1021/es303275g

Gentile, G.J., Fidalgo de Cortalezzi, M.M., 2016. Enhanced retention of bacteria by TiO2 nanoparticles in saturated porous media. J. Contam. Hydrol. 191, 66–75. doi:10.1016/j.jconhyd.2016.05.004

Gomes, P.C., Fontes, M.P.F., da Silva, A.G., de S. Mendonça, E., Netto, A.R., 2001. Selectivity Sequence and Competitive Adsorption of Heavy Metals by Brazilian Soils. Soil Sci. Soc. Am. J. 65, 1115. doi:10.2136/sssaj2001.6541115x

Grillo, R., Rosa, A.H., Fraceto, L.F., 2015. Chemosphere Engineered nanoparticles and

organic matter : A review of the state-of-the-art. Chemosphere 119, 608–619. doi:10.1016/j.chemosphere.2014.07.049

Grimme, H., 1968. Die Adsorption von Mn, Co, Cu und Zn durch Goethit aus verdünnten Lösungen. J. Plant Nutr. Soil Sci. 121, 58–65.

Grolimund, D., Borkovec, M., 2005. Colloid-facilitated transport of strongly sorbing contaminants in natural porous media: Mathematical modeling and laboratory column experiments. Environ. Sci. Technol. 39, 6378–6386. doi:10.1021/es050207y

Grolimund, D., Borkovec, M., Barmettler, K., Sticher, H., 1996. Colloid-facilitated transport of strongly sorbing contaminants in natural porous media: A laboratory column study. Environ. Sci. Technol. 30, 3118–3123. doi:10.1021/es960246x

Gustafsson, J.P., 2010. Visual MINTEQ Version 3.1.

Gustafsson, J.P., 2001. Modeling the Acid–Base Properties and Metal Complexation of Humic Substances with the Stockholm Humic Model. J. Colloid Interface Sci. 244, 102–112. doi:10.1006/jcis.2001.7871

Gustafsson, J.P., Tiberg, C., Edkymish, A., Kleja, D.B., 2011. Modelling lead (II) sorption to ferrihydrite and soil organic matter. Environ. Chem. 8, 485–492. doi:10.1071/EN11025

Han, P., Wang, X., Cai, L., Tong, M., Kim, H., 2014. Transport and retention behaviors of titanium dioxide nanoparticles in iron oxide-coated quartz sand: Effects of pH, ionic strength, and humic acid. Colloids Surfaces A Physicochem. Eng. Asp. 454,

119–127. doi:10.1016/j.colsurfa.2014.04.020

Hendershot, W., Duquette, M., 1986. A Simple Barium Chloride Method for Determining Cation Exchange Capacity and Exchangeable Cations. Soil Sci. Soc. Am. J. 50, 605–608.

Huang, P., 1995. Environmental Impacts of Soil Component Interactions: Metals, Other Inorganics, and Microbial Activities. CRC Press, Saskatoon.

Hunter, R., 1981. Zeta Potential in Colloid Science: Principles and Applications. Academic Press Inc., London.

Jackson, M.L., 1958. Soil Chemical Analysis. Prentice-Hall Inc., Englewood Cliffs, NJ.

James, R.O., Macnaughton, M.G., 1977. The adsorption of aqueous heavy metals on inorganic minerals. Geochemica Cosmochim. Acta 41, 1549–1555.

Jeppu, G.P., Clement, T.P., 2012. A modified Langmuir-Freundlich isotherm model for simulating pH-dependent adsorption effects. J. Contam. Hydrol. 129–130, 46–53. doi:10.1016/j.jconhyd.2011.12.001

Johnson, P.R., Elimelech, M., 1995. Dynamics of Colloid Deposition in Porous Media : Blocking Based on Random Sequential Adsorption. Langmuir 801–812.

Johnson, P.R., Sun, N., Elimelech, M., 1996. Colloid Transport in Geochemically Heterogeneous Porous Media : Modeling and Measurements Colloid Transport in Geochemically Heterogeneous Porous Media : Modeling and Measurements. Environ. Sci. Technol. 30, 3284–3293. doi:10.1021/es960053

Jung, B., O'Carroll, D., Sleep, B., 2014. The influence of humic acid and clay content on the transport of polymer-coated iron nanoparticles through sand. Sci. Total Environ. 496, 155–64. doi:10.1016/j.scitotenv.2014.06.075

Karamalidis, A., Dzombak, D., 2010. Surface complexation modeling: Gibbsite. Wiley & Sons, New York.

Keller, A., Wang, H., Zhou, D., Lenihan, H., Cherr, G., Cardinale, B., Miller, R., Ji, Z., 2010. Stability and Aggregation of Metal Oxide Nanoparticles in Natural Aqueous Matrices. Environ. Sci. Technol. 44, 1962–1967.

Kinniburgh, D.G., Jackson, M.L., Syers, J.K., 1976. Adsorption of Alkaline Earth, Transition, and Heavy Metal Cations by Hydrous Oxide Gels of Iron and Aluminum. Soil Sci. Soc. Am. J. 40, 796–799.

Kosmulski, M., 2002. The significance of the difference in the point of zero charge between rutile and anatase. Adv. Colloid Interface Sci. 99, 255–264.

Kretzschmar, R., Barmettler, K., Grolimund, D., Yan, Y., Borkovec, M., Sticher, H., 1997. Experimental determination of colloid deposition rates and collision efficiencies in natural porous media. Water Resour. Res. 33, 1129. doi:10.1029/97WR00298

Landner, L., Reuther, R., 2005. Metals in Society and in the Environment. Springer, Dordrecht.

Lewis, J., Sjöstrom, J., 2010. Optimizing the experimental design of soil columns in

saturated and unsaturated transport experiments. J. Contam. Hydrol. 115, 1–13. doi:10.1016/j.jconhyd.2010.04.001

Li, Y., Qu, G., Zhang, L., Wang, T., Sun, Q., Liang, D., Hu, S., 2017. Humic acid removal from micro-polluted source water using gas phase surface discharge plasma at different grounding modes. Sep. Purif. Technol. 180, 36–43. doi:10.1016/j.seppur.2017.02.046

Lin, H.J., Sung, T.I., Chen, C.Y., Guo, H.R., 2013. Arsenic levels in drinking water and mortality of liver cancer in Taiwan. J. Hazard. Mater. 262, 1132–1138. doi:10.1016/j.jhazmat.2012.12.049

Lin, S., Cheng, Y., Bobcombe, Y., L. Jones, K., Liu, J., Wiesner, M.R., 2011. Deposition of silver nanoparticles in geochemically heterogeneous porous media: Predicting affinity from surface composition analysis. Environ. Sci. Technol. 45, 5209–5215. doi:10.1021/es2002327

Liu, D., Johnson, P.R., Elimelech, M., 1995. Colloid Deposition Dynamics in Flow-Through Porous Media: Role of Electrolyte Concentration. Environ. Sci. Technol. 29, 2963–2973. doi:10.1021/es00012a012

Long, T.C., Saleh, N., Tilton, R.D., Gregory, V., 2006. Titanium Dioxide (P25) Produces Reactive Oxygen Species in Implications for Nanoparticle. Environ. Sci. Technol. 40, 4346–4352. doi:10.1021/es060589n

Loosli, F., Le Coustumer, P., Stoll, S., 2015. Effect of electrolyte valency, alginate

concentration and pH on engineered TiO2 nanoparticle stability in aqueous solution. Sci. Total Environ. 535, 1–7. doi:10.1016/j.scitotenv.2015.02.037

Loosli, F., Le Coustumer, P., Stoll, S., 2013. TiO2 nanoparticles aggregation and disaggregation in presence of alginate and Suwannee River humic acids. pH and concentration effects on nanoparticle stability. Water Res. 47, 6052–6063. doi:10.1016/j.watres.2013.07.021

Lumsdon, D.G., 2004. Partitioning of organic carbon, aluminium and cadmium between solid and solution in soils: Application of a mineral-humic particle additivity model. Eur. J. Soil Sci. 55, 271–285. doi:10.1111/j.1365-2389.2004.00599.x

Masciangioli, T., Zhang, W.-X., 2003. Environmental Technologies at the Nanoscale. Environ. Sci. Technol. 37, 102A–108A. doi:10.1021/es0323998

McBride, M., Sauve, S., Hendershot, W., 1997. Solubility control of Cu, Zn, Cd and Pb in contaminated soils. Eur. J. Soil Sci. 48, 337–346. doi:10.1111/j.1365-2389.1997.tb00554.x

McCarthy, J.F., Zachara, J.M., 1989. Subsurface transport of contaminants: binding to mobile and immobile phases in groundwater aquifers. Environ. Sci. Technol. 23, 496–502. doi:10.1021/es00063a001

McKeague, J.A., Day, J.H., 1966. Dithionite- and Oxalate-Extractable Fe and Al as Aids in Differentiating Various Classes Of Soils. Can. J. Soil Sci. 46, 13–22. doi:10.4141/cjss66-003

McKenzie, R.M., 1980. The adsorption of lead and other heavy metals on oxides of manganese and iron. Aust. J. Soil Res. 18, 61–73.

McNeely, R.N., Neimanis, V.P., Dwyer, L., 1979. Water quality sourcebook; a guide to water quality parameters. Ottawa Inland Waters Directorate, Water Quality Branch.

Mehra, O.P., 1958. Iron Oxide Removal from Soils and Clays by a Dithionite-Citrate System Buffered with Sodium Bicarbonate. Clays Clay Miner. 7, 317–327. doi:10.1346/CCMN.1958.0070122

Mikanovic, N., Khayat, K., Pagé, M., Jolicoeur, C., 2006. Aqueous CaCO3 dispersions as reference systems for early-age cementitious materials. Colloids Surfaces A Physicochem. Eng. Asp. 291, 202–211. doi:10.1016/j.colsurfa.2006.06.042

Mizutani, K., Fisher-Power, L.M., Shi, Z., Cheng, T., 2017. Cu and Zn adsorption to a terrestrial sediment: Influence of solid-to-solution ratio. Chemosphere 175, 341–349. doi:10.1016/j.chemosphere.2017.02.069

Morales, V.L., Zhang, W., Gao, B., Lion, L.W., Bisogni, J.J., McDonough, B. a., Steenhuis, T.S., 2011. Impact of dissolved organic matter on colloid transport in the vadose zone: Deterministic approximation of transport deposition coefficients from polymeric coating characteristics. Water Res. 45, 1691–1701. doi:10.1016/j.watres.2010.10.030

Navarro, E., Baun, A., Behra, R., Hartmann, N.B., Filser, J., Miao, A.-J., Quigg, A., Santschi, P.H., Sigg, L., 2008. Environmental behavior and ecotoxicity of

engineered nanoparticles to algae, plants, and fungi. Ecotoxicology 17, 372–386. doi:10.1007/s10646-008-0214-0

Nazemi, S., 2012. Concentration of Heavy Metal in Edible Vegetables Widely Consumed in Shahroud , the North East of Iran. J. Appl. Environ. Biol. Sci 2, 386–391.

Newfoundland and Labrador Regulations, 2003. Environmental Control Water and Sewage Regulations under the Water Resources Act (O.C. 2003-231).

Nowack, B., Bucheli, T.D., 2007. Occurrence , behavior and effects of nanoparticles in the environment. Environ. Pollut. 150, 5–22. doi:10.1016/j.envpol.2007.06.006

Oiffer, A.A.L., Barker, J.F., Gervais, F.M., Mayer, K.U., Ptacek, C.J., Rudolph, D.L., 2009. A detailed field-based evaluation of naphthenic acid mobility in groundwater. J. Contam. Hydrol. 108, 89–106. doi:10.1016/j.jconhyd.2009.06.003

Park, R.M., Bena, J.F., Stayner, L.T., Smith, R.J., Gibb, H.J., Lees, P.S.J., 2004. Hexavalent chromium and lung cancer in the chromate industry: A quantitative risk assessment. Risk Anal. 24, 1099–1108. doi:10.1111/j.0272-4332.2004.00512.x

Parks, A., 1965. The Isoelectric Points of Solid Oxides, Solid Hydroxides, and Aqueous Hydroxo Complex Systems. Chem. Rev. 65, 177–198.

Peng, L., Liu, P., Feng, X., Wang, Z., Cheng, T., Liang, Y., Lin, Z., Shi, Z., 2018. Kinetics of heavy metal adsorption and desorption in soil: Developing a unified model based on chemical speciation. Geochim. Cosmochim. Acta 224, 282–300. doi:10.1016/j.gca.2018.01.014

Pérez-Novo, C., Pateiro-Moure, M., Osorio, F., Nóvoa-Muñoz, J.C., López-Periago, E., Arias-Estévez, M., 2008. Influence of organic matter removal on competitive and noncompetitive adsorption of copper and zinc in acid soils. J. Colloid Interface Sci. 322, 33–40. doi:10.1016/j.jcis.2008.03.002

Philippe, A., Schaumann, G.E., 2014. Interactions of Dissolved Organic Matter with Natural and Engineered Inorganic Colloids : A Review. Environ. Sci. Technol. 48, 8946–8962. doi:dx.doi.org/10.1021/es502342r

Prasanphan, S., Nuntiya, A., 2006. Electrokinetic Properties of Kaolins, Sodium Feldspar and Quartz. Chiang Mai J. Sci. 33, 183–190.

Reeves, J.F., Davies, S.J., Dodd, N.J.F., Jha, A.N., 2008. Hydroxyl radicals (•OH) are associated with titanium dioxide (TiO2) nanoparticle-induced cytotoxicity and oxidative DNA damage in fish cells. Mutat. Res. - Fundam. Mol. Mech. Mutagen. 640, 113–122. doi:10.1016/j.mrfmmm.2007.12.010

Rosenfeldt, R.R., Seitz, F., Schulz, R., Bundschuh, M., 2014. Heavy metal uptake and toxicity in the presence of titanium dioxide nanoparticles: A factorial approach using Daphnia magna. Environ. Sci. Technol. 48, 6965–6972. doi:10.1021/es405396a

Salopek, B., Krasic, D., Filipovic, S., 1992. Measurement and application of zeta-potential. Rud. Zb. 4, 147–151.

Sauve, S., Hendershot, W., Allen, H.E., 2000. Solid-Solution Partitioning of Metals in Contaminated Soils: Dependence on pH, Total Metal Burden, and Organic Matter.

Environ. Sci. Technol. 34, 1125–1131. doi:10.1021/es9907764

Schmidt, J., Vogelsberger, W., 2009. Aqueous long-term solubility of titania nanoparticles and titanium(IV) hydrolysis in a sodium chloride system studied by adsorptive stripping voltammetry. J. Solution Chem. 38, 1267–1282. doi:10.1007/s10953-009-9445-9

Shen, C.Y., Li, B.G., Wang, C., Huang, Y.F., Jin, Y., 2011. Surface Roughness Effect on Deposition of Nano- and Micro-Sized Colloids in Saturated Columns at Different Solution Ionic Strengths. Vadose Zo. J. 10, 1071–1081. doi:Doi 10.2136/Vzj2011.0011

Shi, Z., Allen, H.E., Di Toro, D.M., Lee, S.Z., Flores Meza, D.M., Lofts, S., 2007. Predicting cadmium adsorption on soils using WHAM VI. Chemosphere 69, 605–612. doi:10.1016/j.chemosphere.2007.03.001

Shi, Z., Allen, H.E., Di Toro, D.M., Lee, S.Z., Harsh, J.B., 2013. Predicting PbII adsorption on soils: The roles of soil organic matter, cation competition and iron (hydr)oxides. Environ. Chem. 10, 465–474. doi:10.1071/EN13153

Shuman, L.M., 1977. Adsorption of Zn by Fe and Al Hydrous Oxides as Influenced by Aging and pH. Soil Sci. Soc. Am. J. 41, 703–706.

Singh, R., Gautam, N., Mishra, A., Gupta, R., 2011. Heavy metals and living systems: An overview. Indian J. Pharmacol. 43, 246. doi:10.4103/0253-7613.81505

Solovitch, N., Labille, J., Rose, J., Chaurand, P., Borschneck, D., Wiesner, M.R., Bottero,

J.-Y., 2010. Concurrent Aggregation and Deposition of TiO2 Nanoparticles in a Sandy Porous Media. Environ. Sci. Technol. 44, 4897–4902.

Song, L., Elimelech, M., 1993. Dynamics of colloid deposition in porous media: Modeling the role of retained particles. Colloids Surfaces A Physicochem. Eng. Asp. 73, 49–63. doi:10.1016/0927-7757(93)80006-Z

Sun, H., Zhang, X., Zhang, Z., Chen, Y., Crittenden, J.C., 2009. Influence of titanium dioxide nanoparticles on speciation and bioavailability of arsenite. Environ. Pollut. 157, 1165–1170. doi:10.1016/j.envpol.2008.08.022

Sun, P., Shijirbaatar, A., Fang, J., Owens, G., Lin, D., Zhang, K., 2015. Distinguishable Transport Behavior of Zinc Oxide Nanoparticles in Silica Sand and Soil Columns. Sci. Total Environ. 505, 189–198. doi:10.1016/j.scitotenv.2014.09.095

Tack, F.M., Callewaert, O.W.J.J., Verloo, M.G., 1996. Metal solubility as a function of pH in a contaminated, dredged sediment affected by oxidation. Environ. Pollut. 91, 199–208.

Tang, Y.T., Qiu, R.L., Zeng, X.W., Ying, R.R., Yu, F.M., Zhou, X.Y., 2009. Lead, zinc, cadmium hyperaccumulation and growth stimulation in Arabis paniculata Franch. Environ. Exp. Bot. 66, 126–134. doi:10.1016/j.envexpbot.2008.12.016

Tang, Z., Cheng, T., 2018. Stability and aggregation of nanoscale titanium dioxide particle (nTiO2): Effect of cation valence, humic acid, and clay colloids. Chemosphere 192, 51–58. doi:10.1016/j.chemosphere.2017.10.105

Tipping, E., Rey-Castro, C., Bryan, S.E., Hamilton-Taylor, J., 2002. Al(III) and Fe(III) binding by humic substances in freshwaters, and implications for trace metal speciation. Geochim. Cosmochim. Acta 66, 3211–3224. doi:10.1016/S0016-7037(02)00930-4

Tong, M., Zhu, P., Jiang, X., Kim, H., 2011. Influence of natural organic matter on the deposition kinetics of extracellular polymeric substances (EPS) on silica. Colloids Surfaces B Biointerfaces 87, 151–158. doi:10.1016/j.colsurfb.2011.05.015

Verwey, E., Overbeek, J., 1948. Theory of the stability of lyophobic colloids. Elsevier, Amsterdam.

Vulava, V.M., Kretzschmar, R., Rusch, U., 2000. Cation Competition in a Natural Subsurface Material: Modeling of Sorption Equilibria. Environ. Sci. Technol. 34, 2149–2155. doi:10.1029/2001WR000262

Wang, D., Bradford, S.A., Harvey, R.W., Gao, B., Cang, L., Zhou, D., 2012. Humic acid facilitates the transport of ARS-labeled hydroxyapatite nanoparticles in iron oxyhydroxide-coated sand. Environ. Sci. Technol. 46, 2738–2745. doi:10.1021/es203784u

Wang, D., Paradelo, M., Bradford, S.A., Peijnenburg, W.J.G.M., Chu, L., Zhou, D., 2011. Facilitated transport of Cu with hydroxyapatite nanoparticles in saturated sand: Effects of solution ionic strength and composition. Water Res. 45, 5905–5915. doi:10.1016/j.watres.2011.08.041

Wang, Q., Cheng, T., Wu, Y., 2015. Distinct Roles of Illite Colloid and Humic Acid in Mediating Arsenate Transport in Water-Saturated Sand Columns. Water. Air. Soil Pollut. 226, 1–15. doi:10.1007/s11270-015-2413-7

Wang, S., Mulligan, C.N., 2006. Natural attenuation processes for remediation of arsenic contaminated soils and groundwater. J. Hazard. Mater. 138, 459–470. doi:10.1016/j.jhazmat.2006.09.048

Wang, X., Liu, F., Tan, W., Li, W., Feng, X., Sparks, D.L., 2013. Characteristics of phosphate adsorption-desorption onto ferrihydrite: Comparison with well-crystalline fe (Hydr)oxides. Soil Sci. 178, 1–11. doi:10.1097/SS.0b013e31828683f8

Weir, A., Westerhoff, P., Fabricius, L., Hristovski, K., von Goetz, N., 2012. Titanium dioxide nanoparticles in food and personal care products. Environ. Sci. Technol. 46, 2242–50. doi:10.1021/es204168d

Weng, L., Temminghoff, E.J.M., Van Riemsdijk, W.H., 2001. Contribution of individual sorbents to the control of heavy metal activity in sandy soil. Environ. Sci. Technol. 35, 4436–4443. doi:10.1021/es010085j

Wiesner, M.R., Lowry, G. V, Alvarez, P., Dionysiou, D., Biswas, P., 2006. Assessing the Risks of Manufactured Nanomaterials Assessing the Risks of Manufactured Nanomaterials. Environ. Sci. Technol. 40, 4336–4345. doi:10.1021/es062726m

Williams, L.E., Barnett, M.O., Kramer, T.A., Melville, J.G., 2003. Adsorption and Transport of Arsenic(V) in Experimental Subsurface Systems. J. Environ. Qual. 32,

841–850.

Wu, Y., Cheng, T., 2016. Stability of nTiO2 particles and their attachment to sand : Effects of humic acid at different pH. Sci. Total Environ. 541, 579–589. doi:http://dx.doi.org/10.1016/j.scitotenv.2015.09.116 0048-9697

Xu, C., Guo, L., Dou, F., Ping, C.L., 2009. Potential DOC production from size-fractionated Arctic tundra soils. Cold Reg. Sci. Technol. 55, 141–150. doi:10.1016/j.coldregions.2008.08.001

Xu, R., Zhao, A., Yuan, J., Jiang, J., 2012. pH buffering capacity of acid soils from tropical and subtropical regions of China as influenced by incorporation of crop straw biochars. J. Soils Sediments 12, 494–502. doi:10.1007/s11368-012-0483-3

Yang, Y., Ma, J., Qin, Q., Zhai, X., 2007. Degradation of nitrobenzene by nano-TiO2 catalyzed ozonation. J. Mol. Catal. A Chem. 267, 41–48. doi:10.1016/j.molcata.2006.09.010

Yang, Y., Saiers, J.E., Barnett, M.O., 2013. Impact of interactions between natural organic matter and metal oxides on the desorption kinetics of uranium from heterogeneous colloidal suspensions. Environ. Sci. Technol. 47, 2661–2669. doi:10.1021/es304013r

Zhou, D., Abdel-fattah, A.I., Keller, A. a, 2012. Clay particles destabilize engineered nanoparticles in aqueous environments. Environ. Sci. Technol. 46, 7520–7526.

Zhuang, J., Flury, M., Jin, Y., 2003. Colloid-Facilitated Cs Transport through Water-

Saturated Hanford Sediment and Ottawa Sand. Environ. Sci. Technol. 37, 4905–4911. doi:10.1021/es0264504

Appendices

Appendix 1. Supporting Information for Chapter 2

Sediment treatment procedures

To deplete amorphous metal oxyhydroxides (iron, aluminum, and manganese) from the sediment, a treatment process modified from McKeague and Day's (1966) ammonium oxalate under darkness method (AOD) was used. 40 mL of acidified ammonium oxalate (from stock solution of 8 g of ammonium oxalate and 5.44 g of oxalic acid in 500 mL nanopure water, with pH=3) was added to 10 g of natural sediment in a 50 mL polypropylene centrifuge tube, for 300 g (30 tubes) total. The tubes were capped, placed in a dark box, shaken on a VWR Standard Analog Shaker at 300 rpm for 24 hours, and centrifuged for approximately 5 minutes at 7000 rpm, discarding the supernatant. The procedure was then repeated a second time to remove more amorphous metal oxyhydroxides. To remove excess chemicals introduced the treatment, 40 mL of 0.01 mol /L NaCl was added to each tube and shaken for one hour, centrifuged at 7000 rpm for 5 minutes, and supernatant discarded. The washing procedure was completed thrice, and then the sediment was left to air dry and homogenized.

Organic matter in the sediment was depleted using hydrogen peroxide (H_2O_2), based on a procedure by Jackson (1958). 100 g of sediment was saturated with nanopure water in a 500 mL beaker and placed in a water bath on a hot plate, brought to about 90 °C. H_2O_2 was added to the saturated sediment in 5 mL increments, stirring as the reaction occurred, for a total of 30 mL added H_2O_2. Once nearly all of the liquid evaporated, the

beaker was removed from heat and let cool. The procedure was then completed a second time to remove more organic matter, washed thrice, and homogenized as described previously. The portion of sediment with both organic matter and amorphous metal oxyhydroxides depleted was generated by treating with the AOD procedure first and H_2O_2 procedure second, followed by washing and homogenizing.

Sediment characterizations

Modal mineralogy of crushed sediments was analyzed by Rigaku Ultima IV X-ray diffraction (XRD) system. Amorphous Fe, Al, and Mn oxides were quantified by acid ammonium extraction under darkness (McKeague and Day, 1966), whereas dithionite-citrate-bicarbonate (DCB) extraction (Mehra, 1958) quantified total extractable Fe (amorphous + crystalline). The amount of soil organic carbon (SOC) was found by elemental combustion analysis using a Carlo Erba NA1500 Series II Elemental Analyzer and used to represent SOM. Dissolved organic carbon (DOC) that leached from each sediment at pH 5 and 9 was determined by shaking 1 gram of sediment in 50 mL of 1 mM NaCl for 24 hours, monitoring and adjusting pH as needed, and measuring the supernatant with OI Analytical Aurora 1030 TOC Analyzer, used to represent leached DOM. Sediment pH was found after mixing 1 gram of sediment in 5 mL of nanopure water for 30 minutes. The relative amounts of clay, silt, and sand and grain size distribution were determined by Horiba LA-950 Laser Particle Size Analyzer. ZP of each sediment at pH 5 and 9 was found by mixing 1 g of sediment in 40 mL of 1 mM NaCl for 24 hours, monitoring and adjusting pH as needed, and measuring the supernatant after 1 hour of gravity settling by Malvern Nano ZS Zetasizer.

Table S1. Summary of experimental conditions

Experiment #	pH	Porous Media
1	5	Quartz sand
2	9	
3	5	20% Untreated natural sediment, 80% quartz sand
4	9	
5	5	20% AOD treated sediment, 80% quartz sand
6	9	
7	5	20% H_2O_2 treated sediment, 80% quartz
8	9	
9	5	20% AOD + H_2O_2 treated sediment, 80% quartz sand
10	9	

Table S2. Properties of each sediment used in the column experiments

Property	Natural sediment (untreated)	Metals depleted (AOD treated)	Organics depleted (H_2O_2 treated)	Metals and organics depleted (AOD-H_2O_2 treated)
pH	5.77 ± 0.07	5.74 ± 0.007	5.86 ± 0.04	6.35 ± 0.03
Zeta potential (pH 5; 9)	-27.8 ± 0.28 mV; -40.63 ± 1.88 mV	-43.1 ± 1.83 mV; -54.95 ± 2.05 mV	26.6 ± 1.41 mV; -22.00 ± 6.08 mV	-47.9 ± 1.27 mV; -55.4 ± 0.71 mV
Amorphous Al-Hydroxides	2.0 ± 0.18 mg/g	0.067 ± 0.08 mg/g	1.1 ± 0.1 mg/g	0.072 ± 0.01 mg/g
Amorphous Fe-Oxides	1.5 ± 0.15 mg/g	0.27 ± 0.04 mg/g	0.55 ± 007 mg/g	0.17 ± 0.01 mg/g
Total extractable Fe-Oxides	3.70 ± 0.14 mg/g	0.95 ± 0.1 mg/g	1. 91 ± 0.20 mg/g	0.93 ± 0.02 mg/g
Soil Organic Carbon	7.4 ± 0.4 mg/g	1.6 ± 0.4 mg/g	0.48 ± 0.08 mg/g	0.72 ± 0.3 mg/g
DOC (pH 5, 9)	171.21 ± 43.27 mg/kg; 486.66 ± 147.85 mg/kg	153.64 ± 6.75 mg/kg; 223.39 ± 23.08 mg/kg	37.54 ± 1.31 mg/kg; 142.785 ± 52.43 mg/kg	60.94 ± 0.46 mg/kg; 88.64 ± 22.52 mg/kg
Clay; Silt; Sand	0.51 ± 0.16%; 42.66 ± 5.26%; 56.83 ± 5.38%	0.129 ± .13%; 40.83 ± 8.04%; 59.04 ± 8.09%	0%; 29.51 ± 0.89%; 70.48 ± 0.89%	0%; 37.08 ± 2.40%; 62.92 ± 2.40%
Porosity (in columns with 1:4 parts quartz sand)	0.37 ± 0.015	0.37 ± 0.018	0.36 ± 0.003	0.36 ± 0.011
Bulk density (in columns with 1:4 parts quartz sand)	1.77 ± 0.017 g/cm^3	1.83 ± 0.017 g/cm^3	1.83 ± 0.038 g/cm^3	1.79 ± 0.015 g/cm^3

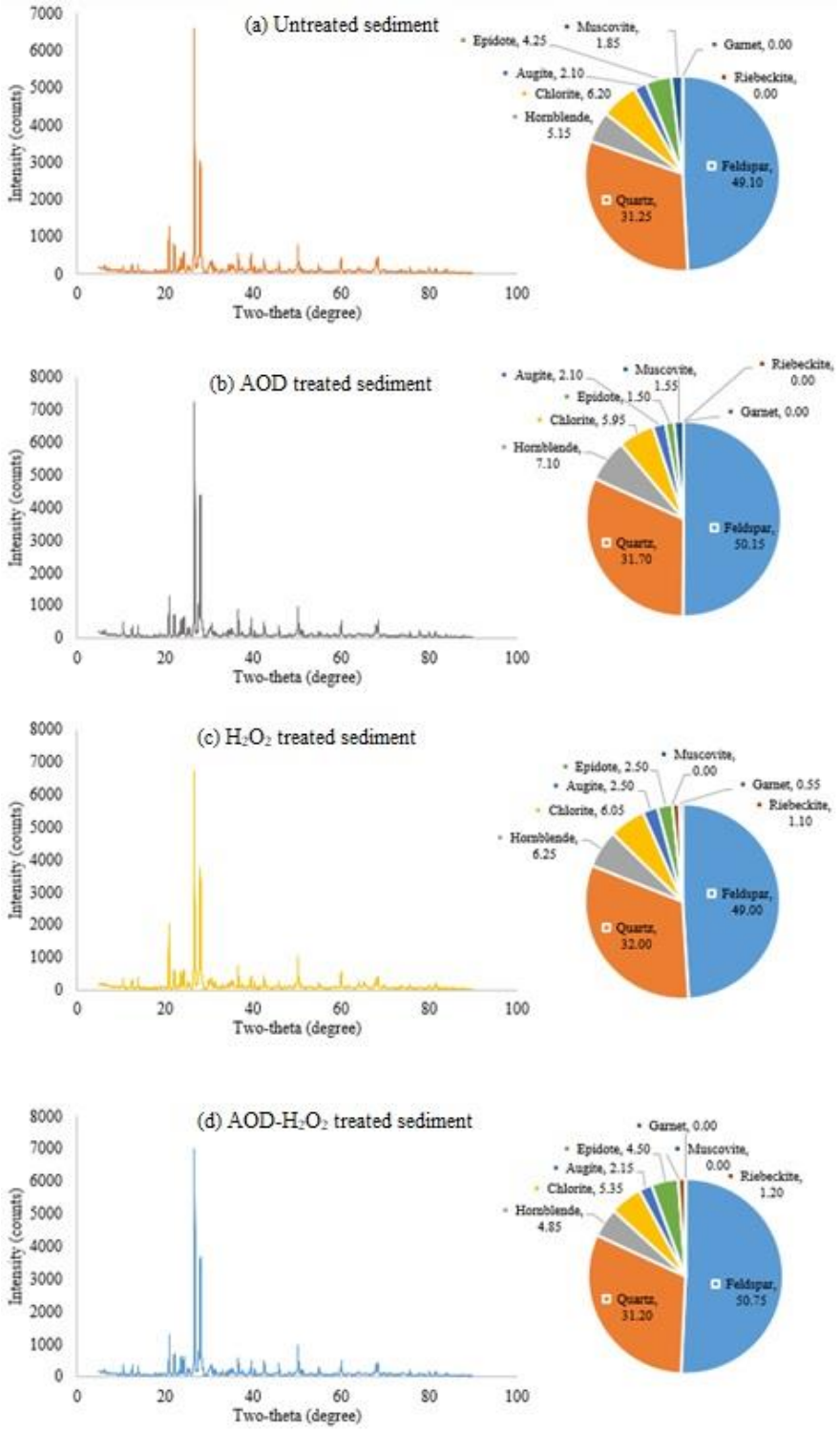

Figure S1. Relative X-ray spectra and corresponding mineralogy of each sediment, measured by XRD and Reitveld refinement.

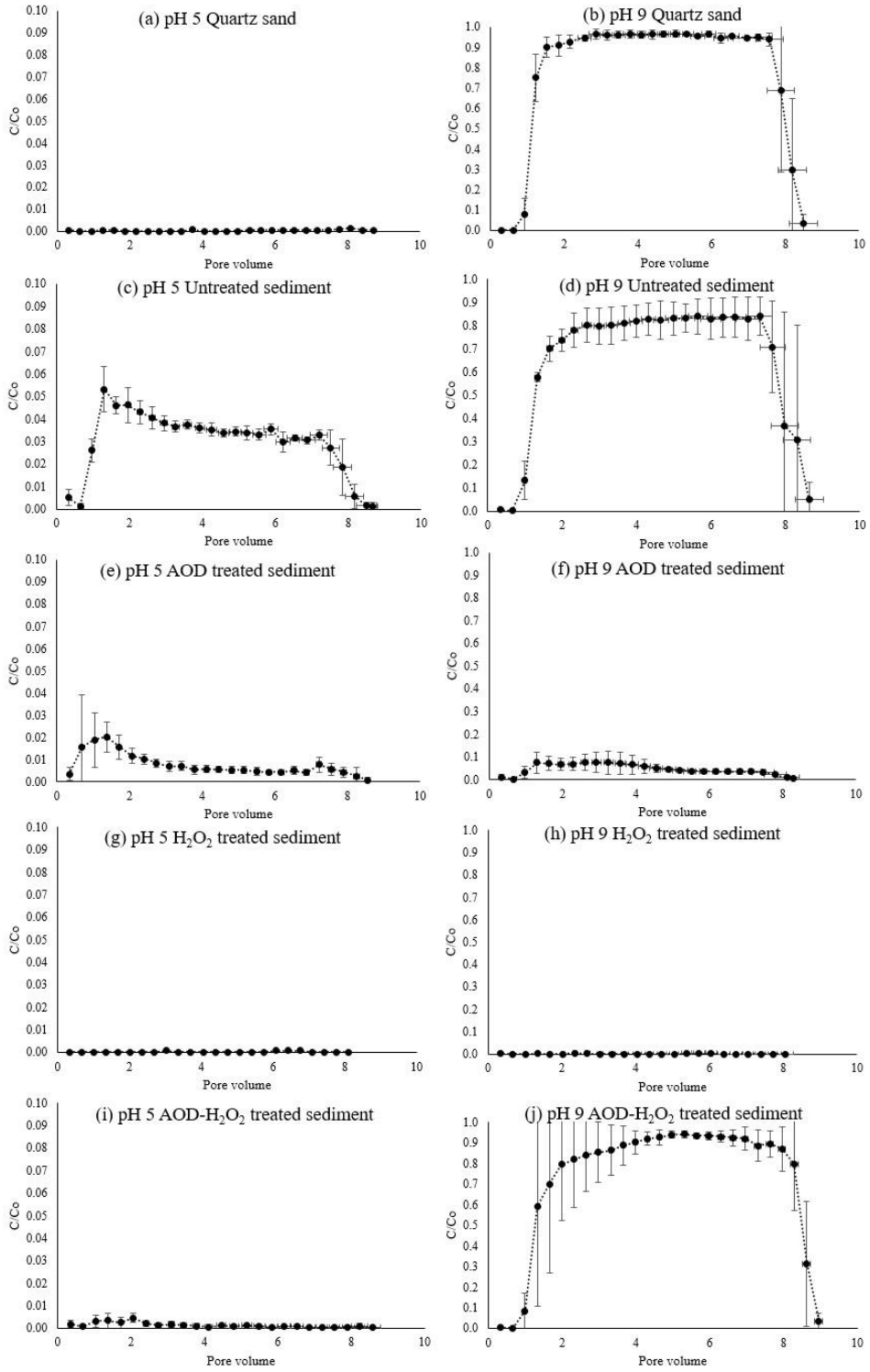

Figure S2. Average of triplicate $nTiO_2$ breakthrough curve experiments with error bars as standard deviation.

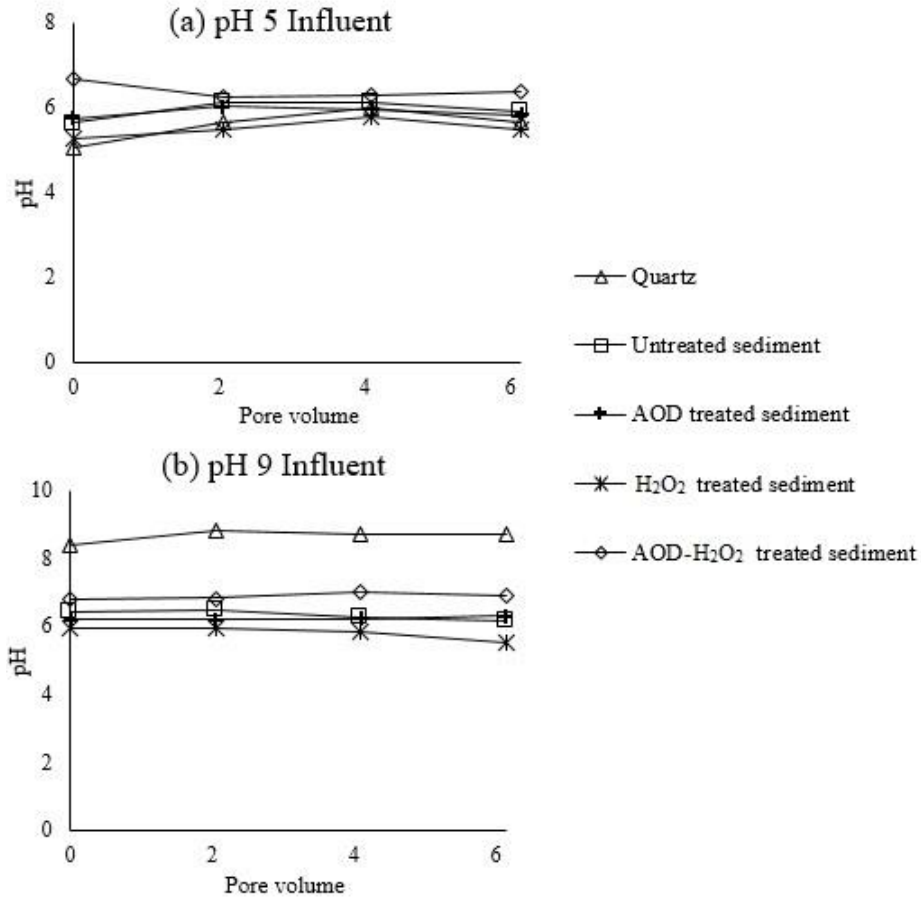

Figure S3. Column effluent pH over time for each column experiment.

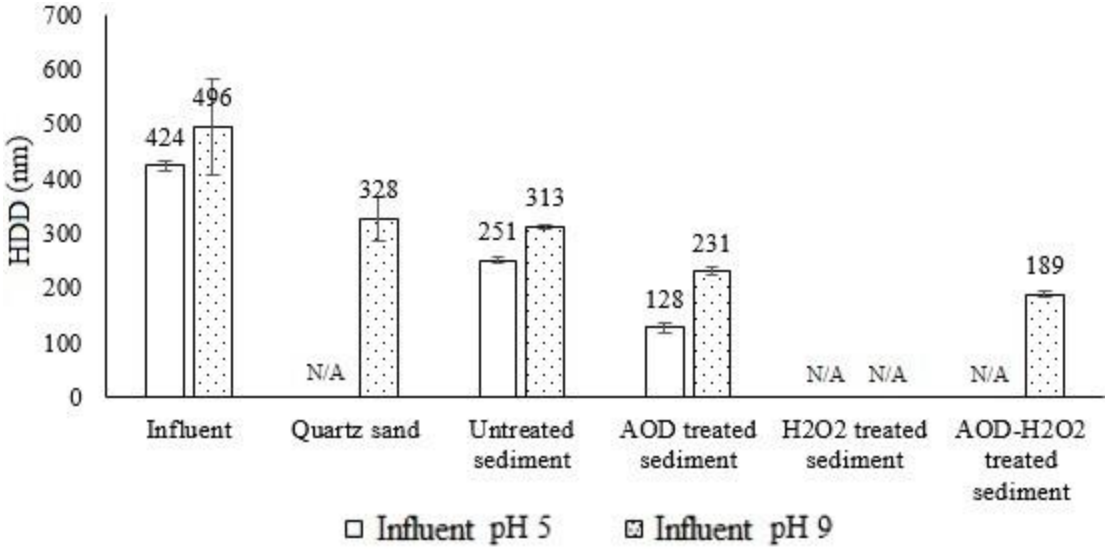

Figure S4. Column effluent HDD for each column experiment.

Appendix 2. Supporting Information for Chapter 3

Sediment treatment procedures

To deplete amorphous metal oxyhydroxides (iron, aluminum, and manganese) from the sediment, a treatment process modified from McKeague and Day's (1966) ammonium oxalate under darkness method (AOD) was used. 40 mL of acidified ammonium oxalate (from stock solution of 8 g of ammonium oxalate and 5.44 g of oxalic acid in 500 mL nanopure water, with pH=3) was added to 10 g of natural sediment in a 50 mL polypropylene centrifuge tube, for 300 g (30 tubes) total. The tubes were capped, placed in a dark box, shaken on a VWR Standard Analog Shaker at 300 rpm for 24 hours, and centrifuged for approximately 5 minutes at 7000 rpm, discarding the supernatant. The procedure was then repeated a second time to remove more amorphous metal oxyhydroxides. To remove excess chemicals introduced the treatment, 40 mL of 0.01 mol /L NaCl was added to each tube and shaken for one hour, centrifuged at 7000 rpm for 5 minutes, and supernatant discarded. The washing procedure was completed thrice, and then the sediment was left to air dry and homogenized.

Organic matter in the sediment was depleted using hydrogen peroxide (H_2O_2), based on a procedure by Jackson (1958). 100 g of sediment was saturated with nanopure water in a 500 mL beaker and placed in a water bath on a hot plate, brought to about 90 °C. H_2O_2 was added to the saturated sediment in 5 mL increments, stirring as the reaction occurred, for a total of 30 mL added H_2O_2. Once nearly all of the liquid evaporated, the beaker was removed from heat and let cool. The procedure was then completed a second time to remove more organic matter, washed thrice, and homogenized as described

previously. The portion of sediment with both organic matter and amorphous metal oxyhydroxides depleted was generated by treating with the AOD procedure first and H_2O_2 procedure second, followed by washing and homogenizing.

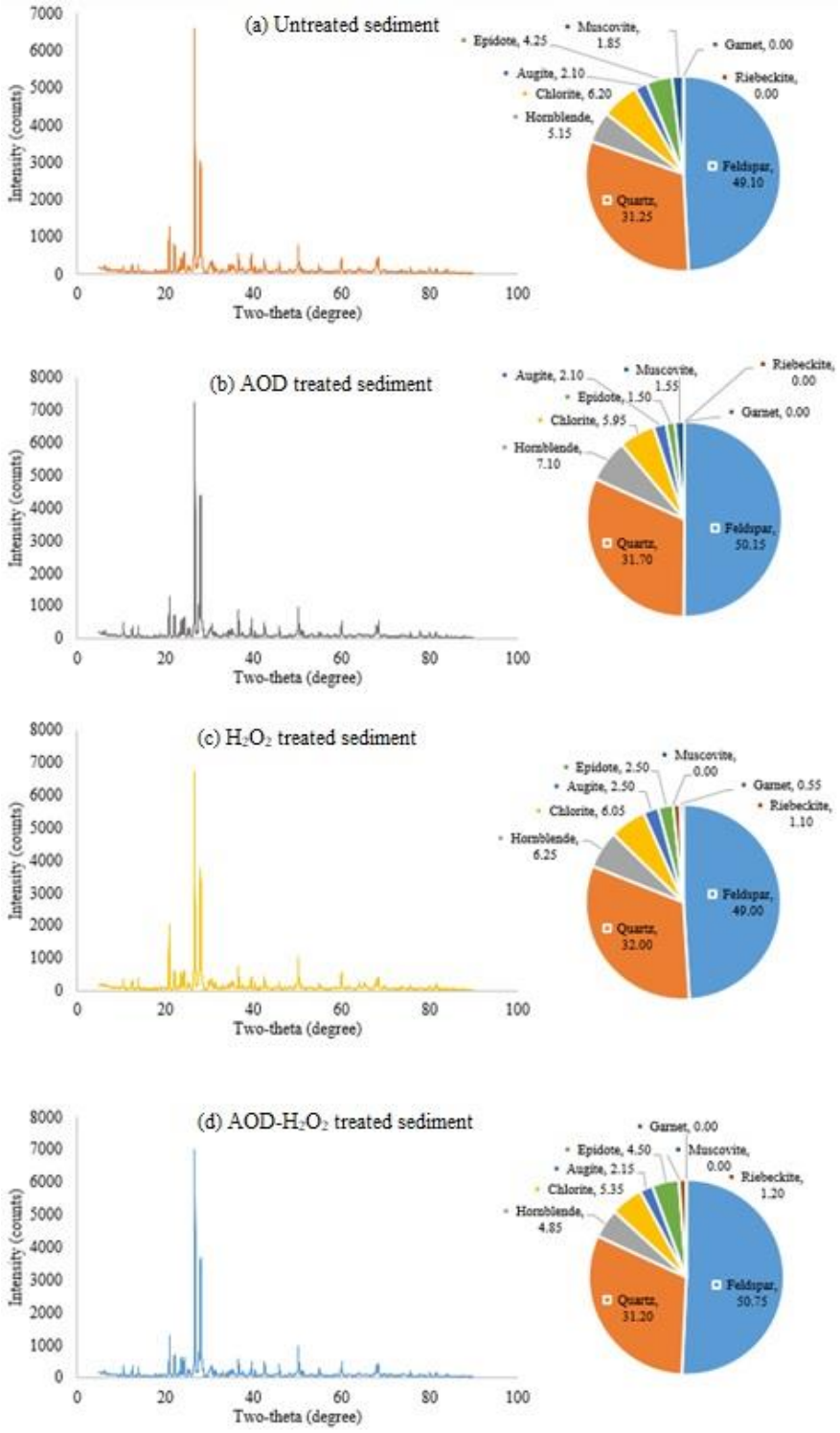

Figure S5. Relative X-ray spectra and corresponding mineralogy of each sediment, measured by XRD and Reitveld refinement.

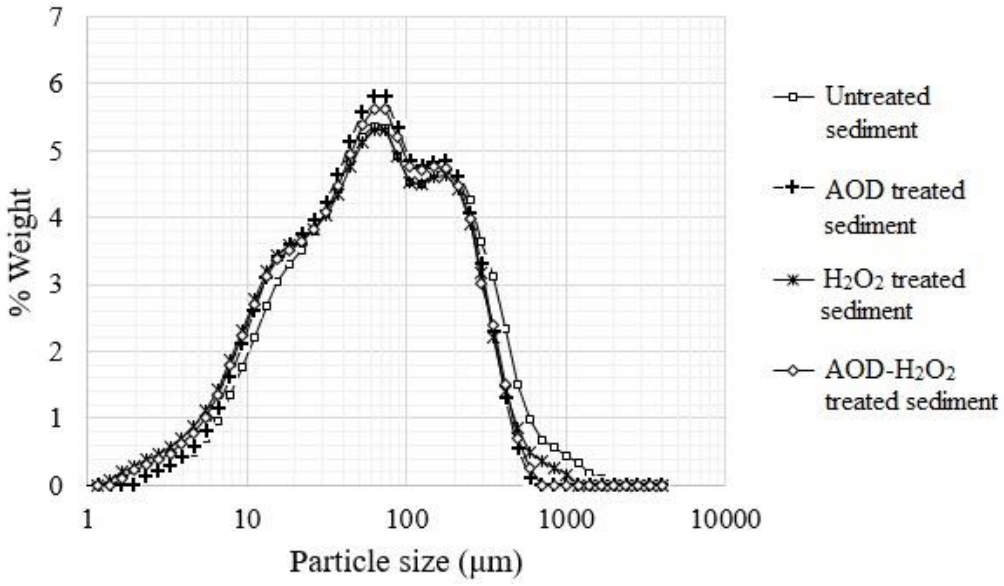

Figure S6. Grain size distribution of each type of sediment as determined by Horiba LA-950 Laser Particle Size Analyzer.

Table S3. Properties of each sediment used in the adsorption experiments.

Property	Natural sediment (untreated)	Metals depleted (AOD treated)	Organics depleted (H_2O_2 treated)	Metals and organics depleted (AOD + H_2O_2 treated)
Amorphous Fe-Oxides	0.15 ± 0.015%	0.040 ± 0.0045%	0.18 ± 0.028%	0.034 ± 0.0050%
Total extractable Fe-Oxides	0.37 ± 0.014%	0.15 ± 0.017%	0.39 ± 0.005%	0.14 ± 0.001%
Amorphous Al-Hydroxides	0.20 ± 0.018%	0.0099 ± 0.0010%	0.13 ± 0.00048%	0.011 ± 0.000088%
Soil Organic Carbon	0.74 ± 0.04%	0.29 ± 0.05%	0.12 ± 0.002%	0.065 ± 0.01%
pH	5.77 ± 0.07	6.14 ± 0.13	5.07 ± 0.021	6.30 ± 0.014
Clay; Silt; Sand	0.51 ± 0.16%; 42.66 ± 5.26%; 56.83 ± 5.38%	0.67 ± 0.20%; 46.80 ± 1.38%; 52.53 ± 1.36%	1.98 ± 0.10%; 46.98 ± 4.11%; 51.03 ± 4.21%	1.51 ± 0.21%; 46.79 ± 7.22%; 51.70 ± 7.39%
Exchangeable Ca	280 ± 0.62 mg/kg	363 ± 0.74 mg/kg	393 ± 19.45 mg/kg	245 ± 14.39 mg/kg
Exchangeable Mg	13 ± 0.63 mg/kg	41 ± 0.81 mg/kg	3.57 ± 0.23 mg/kg	23.57 ± 0.58 mg/kg
Originally adsorbed Cu	3.00 ± 0.62 mg/kg	Less than detection	6.28 ± 0.39 mg/kg	Less than detection
Originally adsorbed Zn	1.65 ± 0.12 mg/kg	3.04 ± 0.10 mg/kg	3.03 ± 0.17 mg/kg	2.53 ± 0.13 mg/kg

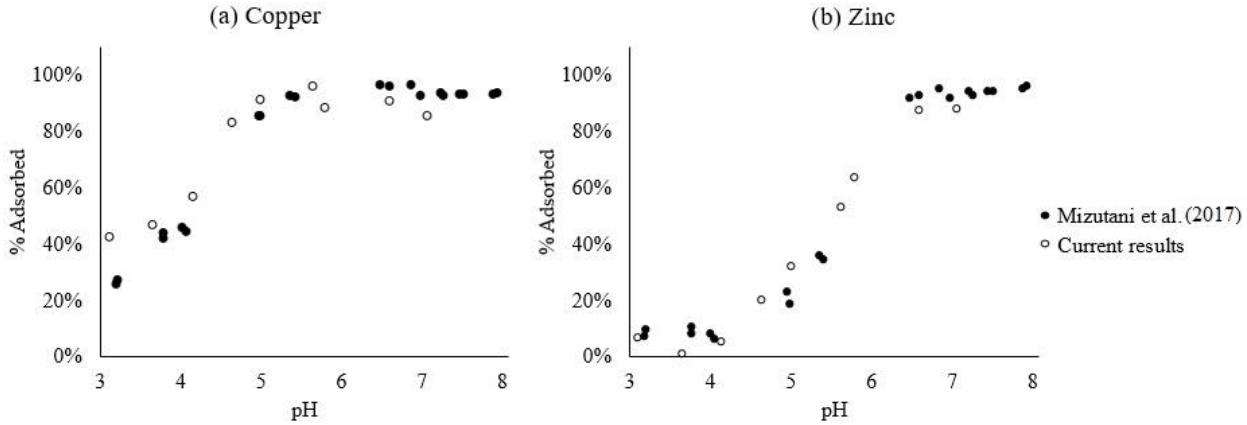

Figure S7. Comparison of identical adsorption experiments for Cu and Zn using the untreated sediment in this study and in earlier work (Mizutani et al., 2017).